FACULTAD DE CIENCIAS

DEPARTAMENTO DE BIOLOGIA MOLECULAR

METABOLIC GENES IN HEPATOCELLULAR CARCINOMA DEVELOPMENT

Elisa Manieri

Madrid, 2016

DEPARTAMENTO DE BIOLOGIA MOLECULAR

FACULTAD DE CIENCIAS

UNIVERSIDAD AUTONOMA DE MADRID

METABOLIC GENES IN HEPATOCELLULAR CARCINOMA DEVELOPMENT

PhD Thesis submitted by

ELISA MANIERI

Degree in Biotechnology by Univesitá degli Studi Milano-Bicocca

Master Degree in Medical Biotechnology by

Universitá degli studi Milano-Bicocca

PhD Director: Dr. Guadalupe Sabio-Buzo

Laboratory “Stress kinases in Diabetes, Cancer and Cardiovascular Disease”

Myocardial Pathophysiology Area

Centro Nacional de Investigaciones Cardiovasculares Carlos III (CNIC-Carlos III)

MADRID, 2016

Dra. Guadalupe Sabio Buzo, Jefa del Grupo “Papel de las quinasas activadas por el estrés en el desarrollo de enfermedades cardiovasculares, diabetes y cáncer”, Área de Fisiopatología del Miocardio, CNIC-Carlos III, como Directora

Dr. Federico Mayor Menendez, Catedrático de la Universidad Autónoma de Madrid y Jefe del Grupo “Receptores acoplados a proteínas G: redes de señalización e implicaciones fisiopatológicas”, Departamento de Biología Celular e Inmunología, CBM Severo Ochoa CSIC-UAM, como Tutor

CERTIFICAN

Que la Tesis Doctoral titulada “Metabolic genes in hepatocellular carcinoma development” ha sido realizada en el Centro Nacional de Investigaciones Cardiovasculares (CNIC) y tutelada por el Departamento de Biología Molecular de la Universidad Autónoma de Madrid.

El trabajo realizado por **Doña Elisa Manieri** reúne todas las condiciones requeridas por la legislación vigente, así como la originalidad y calidad científica para poder ser presentada y defendida ante el Tribunal Calificador con el fin de optar al grado de Doctor.

Y para que conste se extiende el presente certificado

Madrid, Mayo 2016

VºBº Directora

Dra. Guadalupe Sabio Buzo

VºBº Tutor

Dr. Federico Mayor Menendez

This PhD Thesis has been carried out by Elisa Manieri at the “Stress kinases in Diabetes, Cancer and Cardiovascular Disease” laboratory from the Myocardial Pathophysiology Area, Centro Nacional de Investigaciones Cardiovasculares Carlos III (CNIC-Carlos III) in Madrid, and partially at Centro Nacional de Biotecnología CSIC, under the supervision of Dr. Guadalupe Sabio Buzo.

The support received from the following Grants and Fellowships has permitted to develop this PhD work:

- La Caixa International PhD Fellowship Program, 2010 Call. Recipient: Elisa Manieri (2010-2014).

- Role of p38MAPK family and microRNA in obesity, chronic inflammation and development of hepatocellular carcinoma. Principal Investigator: Guadalupe Sabio. European Foundation for the Study of Diabetes (EFSD 0203); 01/09/2010 – 30/09/2012

- Role of obesity in the development of hepatocellular carcinoma. Principal Investigator: Guadalupe Sabio. European Commission. European Research Council Starting Independent Researcher Grant (ERC-StG-260464). 2010-2015

- Quinasas del estrés en el cáncer y las enfermedades metabólicas. Principal Investigator: Guadalupe Sabio. SAF2013-43506-R Ministerio de Economía y Competitividad; 2014 -2016

- Inmunidad tumoral e inmunoterapia del cáncer. Principal Investigator: Guadalupe Sabio. Comunidad de Madrid (S2010/BMD-2326); 2012 – 2017

- Papel de la obesidad en el desarrollo del cáncer hepático. Principal Investigator: Guadalupe Sabio. Ministerio de Ciencia e Innovación (SAF2010-19347); 2011 – 2013

ABSTRACT

Hepatocellular carcinoma (HCC) is the second leading cause of death for cancer worldwide. Several studies on hepatocellular carcinoma epidemiology linked this malignancy with obesity and metabolic disorders. However, little is known about the molecular mechanisms responsible for this connection. The main purpose of this thesis is to elucidate the role of *Jnk1* and *Ppara*, two important metabolic genes, in hepatocellular carcinoma development.

Adipose tissue is the most important organ for lipid storage; during obesity it undergoes to a substantial remodeling. JNK1 is known to control IL-6 production in the adipose tissue during obesity and its depletion in adipocyte protects against liver steatosis, a predisposing factor for HCC development. We demonstrate that adipose tissue JNK1 in normal diet can trigger hepatocellular carcinoma development. In fact, the deletion of JNK1 in adipose tissue increases circulating levels of adiponectin, which in turn activates AMPKα and p38α in hepatocytes, protecting against chemical-induced tumor development. Our results highlight the relevance of adipose tissue in liver cancer development and the central role that JNK1 plays in this crosstalk.

PPARα is a nuclear receptor of fatty acids. It is highly expressed in the liver and obesity induces its activation. However, PPARα role in liver carcinogenesis is controversial. Here we show that PPARα activation promotes obesity-associated hepatic cancer. Mice lacking PPARα are protected against chemical-induced hepatocellular carcinoma when fed a high fat diet. Additionally, bone marrow transplantation experiments reveal no significant contribution of inflammatory cells, suggesting a cell-autonomous function of PPARα in hepatocytes. Hepatic PPARα activation, induced by *Jnk1* and *Jnk2* deletion, is sufficient to cause spontaneous liver cancer, confirming a central role of PPARα activation in liver tumorigenesis. Our results provide a molecular mechanism linking metabolic disorders with liver cancer, emphasizing a central role for PPARα in the connection.

PRESENTACIÓN

El carcinoma hepatocelular es la segunda causa de muerte por cáncer en el mundo. Estudios epidemiológicos relacionan el carcinoma hepatocelular con la obesidad y los trastornos metabólicos. Sin embargo los mecanismos moleculares que controlan esta conexión no están del todo aclarados. El objetivo principal de esta tesis es determinar el papel de *Jnk1* y *Ppara*, dos importantes genes metabólicos, en el desarrollo del carcinoma hepatocelular.

El tejido adiposo es el órgano más importante para el almacenamiento de los lípidos, sufriendo una considerable remodelación durante la obesidad. JNK1 es una proteína quinasa activada por estrés que controla la producción de IL-6 por parte del tejido adiposo durante la obesidad. Nuestros resultados demuestran que JNK1 en el tejido adiposo puede facilitar el desarrollo del carcinoma hepático en animales alimentados con dieta no grasa. De hecho, la eliminación de JNK1 en el tejido adiposo induce el aumento de los niveles circulantes de adiponectina. Esta adipoquina activa AMPKα y p38α en los hepatocitos, protegiendo del desarrollo del tumor hepático inducido por compuestos químicos carcinógenos. Nuestros resultados destacan la importancia del tejido adiposo en el desarrollo del carcinoma hepatocelular y el papel central que JNK1 ejerce en la comunicación entre el tejido adiposo y el hepatocito.

PPARα es un receptor nuclear de ácidos grasos. Está altamente expresado en el hígado, y la obesidad induce su activación. Sin embargo, no se conoce en la actualidad el papel de PPARα en la carcinogénesis hepática. En esta tesis demostramos que la activación de PPARα facilita el desarrollo del cáncer hepático en animales alimentados con dieta grasa. Ratones carentes en PPARα están protegidos frente al desarrollo del carcinoma hepatocelular inducido por carcinógenos químicos cuando son alimentados con dieta grasa. Además, experimentos de trasplante de medula ósea revelan que la contribución de las células inflamatoria no es significativa, sugiriendo que la función de PPARα es propia del hepatocito. La activación hepática de PPARα inducida por la supresión de *Jnk1* y *Jnk2*, es suficiente para causar cáncer hepático espontáneamente, confirmando el papel central de la activación de PPARα en el desarrollo del carcinoma hepático. Nuestros resultados aportan un mecanismo molecular que conecta los trastornos metabólicos con el cáncer hepático, resaltando un papel central de PPARα en esta relación.

INDEX

LIST OF CONTENTS

LIST OF FIGURES AND TABLES

ABBREVIATIONS

A

Acc1	Acetyl-coenzyme A carboxylase 1 gene
Acox1	Peroxisomal acyl-coenzyme A oxidase 1
Adipoq	Adiponectin gene
AdipoR1	Adiponectin receptor 1
AdipoR2	Adiponectin receptor 2
AKT	Protein kinase B
Alb	Albumin
ALT	Alanine aminotransferase
AMDIS	Automated mass spectrometry deconvolution and identification system
AMP	Adenosine monophosphate
AMPK	AMP-activated protein kinase
ANOVA	Analysis of variance
AP-1	Activator protein 1
APO-CIII	Apolipoprotein C3
AST	Aspartate aminotransferase
ATM	Adipose Tissue Macrophages

B

BM	Bone marrow
BMI	Body mass index
BSTFA	*N*,*O*-Bis(trimethylsilyl)trifluoroacetamide

C

cAMP	Cyclic AMP
Cas9	Crispr-associated protein 9
CBP/p300	CREB-binding protein
CCL2	Chemokine (C-C motif) ligand 2

CCL3	Chemokine (C-C motif) ligand 3
Ccna1	Cyclin A1 gene
Cdc25c	M-phase inducer phosphatase 3 gene
CD-HFD	Choline deficient-high fat diet
Cdk2	Cyclin-dependent kinase 2 gene
c-Fos	Cellular Fos
c-Jun	Cellular Jun
c-Myc	Cellular Myc
Cpt-I	Carnitine palmitoyltransferase I
Cpt-II	Carnitine palmitoyltransferase II
CREB	cAMP response element binding
CRISPR	Clustered regularly interspaced short palindromic repeats
CXCL2	Chemokine (C-X-C motif) ligand 2

D

DEN	Diethylnitrosamine
DMEM	Dulbecco's modified Eagle's medium
DNA	Deoxyribonucleic acid
DNAse	Deoxyribonuclease

E

EDTA	Ethylenediaminetetraacetic acid
EGTA	Ethylene glycol-bis(β-aminoethyl ether)-N,N,N',N'-tetraacetic acid
Ehhadh	Peroxisomal bifunctional enzyme gene
Elane	Elastase gene
ELISA	Enzyme-linked immunosorbent assay
Emr1	f4/80 gene
ER	Endoplasmic reticulum

ERKs	Epithelial signal-regulated kinases
ESI	Electrospray ionization

F

FA	Fatty acids
FABP	Fatty acid-binding protein
Fabp4	Fatty acid binding protein 4
Fas	Fatty acids synthase gene
FBS	Fetal bovine serum
FFA	Free Fatty Acids
Fgf21	Fibroblast growth factor 21
F^{KO}	$Fabp4Cre^{+}Jnk1^{f/-}$
FLICE	FADD-like IL-1β-converting enzyme
FLIP	FLICE-inhibitory protein
Foxm1	Forkhead box protein M1 gene
F^{WT}	$Fabp4Cre^{+}Jnk1^{+/-}$

G

Gapdh	Glyceraldehyde 3-phosphate dehydrogenase
GC-MS	Gas chromatography-mass spectrometry

H

HBV	Hepatitis B Virus
HCC	Hepatocellular carcinoma
HCV	Hepatitis C Virus
HFD	High fat diet
Hif1α	Hypoxia-inducible factor 1-alpha gene
HMW	High molecular weight

I

i.d.	Internal diameter
i.p.	Intraperitoneal
IFNγ	Interferon γ
IL-10	Interleukin 10
IL-12	Interleukin 12
IL-1β	Interleukin 1 β
IL-6	Interleukin 6
iNos	Inducible nitric oxide synthase
IRS	Insulin receptor substrate
IS	Internal standard
i.v.	Intravenous

J

JAK	Janus Kinase
JNK	c-Jun N-terminal kinase
JNK1	c-Jun N-terminal kinase 1
JNK2	c-Jun N-terminal kinase 2
JNK3	c-Jun N-terminal kinase 3

L

Lcad	Long-chain acyl-CoA dehydrogenase
LC-MS	Liquid chromatography-Mass spectrometry
L-FABP	Liver-type fatty acid-binding protein
LMW	Low molecular weight
LoxP	Locus of X-over P1
LPL	Lipoprotein lipase
LPS	Lipopolysaccharide

LTB_4	Leukotriene B_4
Lyz2	Lysozyme gene

M

MAPK	Mitogen-activated protein kinases
Mcad	Medium-chain acyl-CoA dehydrogenase
MEK	MAPK/ERK kinase
MKK4	MAP kinase kinase 4
MKK7	MAP kinase kinase 7
M-MLV	Moloney Murine Leukemia Virus
mRNA	Messenger RNA
MS	Mass spectrometry
MSD	Macromolecular structure database
mTOR	Mammalian target of rapamycin
mTORC1	Mammalian target of rapamycin complex 1

N

NAFLD	Non-alcoholic fatty liver disease
NASH	Non-alcoholic steatohepatitis
NCoR/SMRT	Nuclear receptor co-repressor/silencing mediator for retinoid and thyroid hormone receptors
ND	Normal chow diet
NF-κB	Nuclear Factor kappa-light-chain-enhancer of activated B cells
NO	Nitric Oxide
Nos2	Inducible nitric oxide synthase gene
ns	No statistically significant difference

O

OPLS-DA	Orthogonal partial least squares discriminant analysis

P

PBS	Phosphate-buffered saline
PCA	Principal components analysis
PCNA	Proliferating cell nuclear antigen
PCR	Polymerase chain reaction
PHx	Partial hepatectomy
Plin	Perilipin gene
PMSF	Phenylmethylsulfonyl fluoride
PPAR	Peroxisome proliferator-activated receptor
PPARα	Peroxisome proliferator-activated receptor α
PPARβ/δ	Peroxisome proliferator-activated receptor β/δ
PPARγ	Peroxisome proliferator-activated receptor γ
PPREs	Peroxisome proliferator response elements

Q

QC	Quality control
qRT-PCR	Quantitative real time polymerase chain reaction
QTOF	Quadrupole time of flight

R

RAF	Rapidly accelerated fibrosarcoma
RAS	Rat sarcoma protein
Rasal2	Ras GTPase activating protein-like 2 gene
RI	Retention index
RIP1	Receptor interacting protein1

RNA	Ribonucleic acid
RNA-seq	RNA sequencing
ROS	Reactive oxygen species
RT	Retention time
RTL	Retention time locked

S

SAPK	Stress-activated protein kinases
Scd1	Stearoyl-CoA desaturase 1 gene
SDS-PAGE	Sodium dodecyl sulfate polyacrylamide gel electrophoresis
SEM	Standard error of the mean
Serpine1	Serpin peptidase inhibitor clade E gene
SRC1	Steroid receptor co-activator 1
SREBP1	Sterol regulatory element-binding protein 1
STAT3	Signal Transducer and Activator of Transcription 3

T

T-BARS	Thiobarbituric acid reactive substances
TICs	Total ion chromatograms
TMCS	Trimethylsilyl chloride
Tnfa	TNFα gene
Tnfsf10	Tumor necrosis factor super family 10
TNFα	Tumor necrosis factor alpha
TRAIL	TNF-related apoptosis-inducing ligand
Tris	Tris(hydroxymethyl)aminomethane
Trp53	p53 gene

U

UHPLC	Ultra-high performance liquid chromatography

V

VEGF	Vascular Endothelial Growth Factor
VIP	Variance importance in projection values
Vlcad	Very long-chain acyl-CoA dehydrogenase

W

WAT	White adipose tissue
WHO	World Health Organization
WT	Wild type

INTRODUCTION

World Health Organization (WHO) defines *cancer* as the uncontrolled growth and spread of cells that can affect almost any part of the body. One major feature of cancer is the rapid insurgence of abnormal cells that grow beyond their usual boundaries, with the capability to invade adjoining parts of the body and spread to other organs. Cancer is one of the most important leading causes for morbidity and mortality worldwide with approximately 14 million new cases and 8.2 million cancer related deaths in 2012 (Figure I1). Moreover, the number of new cases is expected to rise about 70% in the next two decades (data from World Cancer Report 2014). These data remark the urgency to understand in-depth cancer development and find new therapies.

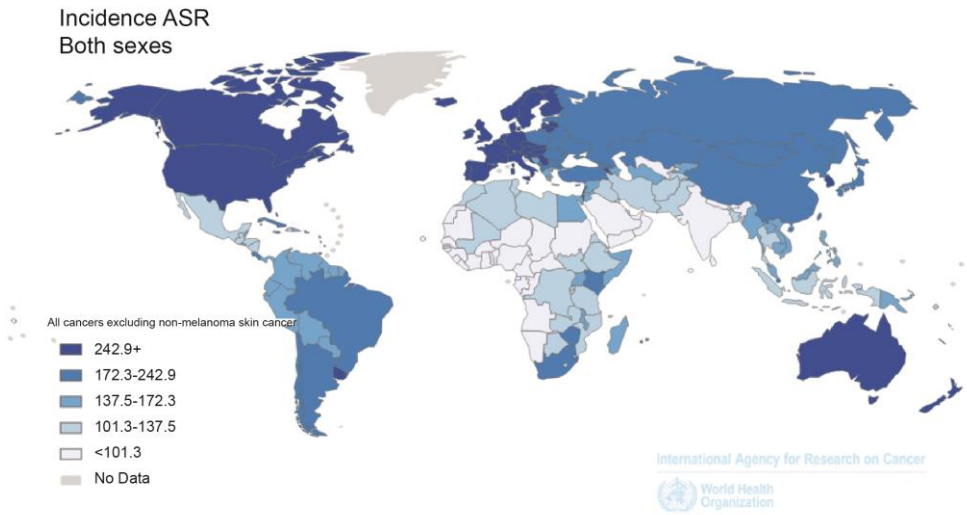

Figure I1. Cancer Incidence Age-Standardized Rate in both sexes.
Data source: GLOBOCAN 2012, Map production: IARC, World Health Organization.

1. INFLAMMATION AND CANCER

Research along the last two decades elucidated the link between chronic inflammation and cancer. In fact, inflammation plays a pivotal role across all stages of cancer: initiation, promotion and progression. Tumor initiation requires the accumulation of DNA mutations (Hanahan and Weinberg, 2011). During chronic inflammation, activated inflammatory cells produce cytokines, such as tumor necrosis factor α (TNFα), which in turn induce reactive oxygen species (ROS) production and accumulation in target cells (Corda et al., 2001, Meier et al., 1989). Moreover, inflammatory cells can produce peroxynitrate (ONOO-) and nitrate (NO) that diffuse cell membrane and act on neighboring epithelial

cells (Hussain et al., 2003). Free radicals induce DNA damage as well as protein structural and functional modification, both being a driving factor in cell malignant transformation (Hussain et al., 2003). Inflammation is triggered by different kind of injuries, in order to eliminate the cause of damage; furthermore, inflammation also stimulates tissue regeneration by promoting the secretion of cytokines and growth factors. Those molecules can also induce tumor progression, as they stimulate proliferation or cell survival as a secondary effect (Grivennikov et al., 2010). For example, interleukin 6 (IL-6), a well-known pro-inflammatory cytokine, induces activation of the pro-survival signaling pathway JAK/STAT3 (Catlett-Falcone et al., 1999, Bollrath et al., 2009, Grivennikov et al., 2009, Zhong et al., 1994). Moreover, activated inflammatory cells produce factors that stimulate neoangiogenesis, such as vascular endothelial growth factor (VEGF). Sustained angiogenesis is a hallmark of tumors, fundamental in tumor progression; blood nutrients are in fact required to sustain the high proliferative rate of malignant cells (Hanahan and Weinberg, 2011). Finally, inflammation plays a role in tumor invasion. Cancer cells invasion requires extracellular matrix proteolysis. Inflammatory cells are the main source of proteases and metalloproteinases, thus supporting tumor invasion and metastasis (Kessenbrock et al., 2010).

1.1 Obesity, metabolic syndrome and cancer

Several inflammation-inducing *stimuli*, such as virus infection or chronic exposure to irritants, can prompt cancer development through the activation of the immune system. In particular, evidences supporting a link between obesity, inflammation and cancer have been collected during the last decade. Obesity is considered a new global pandemic, being the most common metabolic disorder worldwide (WHO). Obesity, clinically defined as a body mass index (BMI) higher than 30, is a major cause of morbidity and mortality and it is associated with increased risk of type 2 diabetes mellitus, heart disease, metabolic syndrome, hypertension, stroke but also different forms of cancer (Haslam and James, 2005). Epidemiological studies indicate that being overweight or obese is associated with increased cancer-mortality risk of 1.5 fold in men and 1.6 fold in women (Calle et al., 2003). Obesity promotes cancer initiation and progression by different mechanisms. Adipose tissue is the most important organ for lipid

storage. In the obese state, adipocyte enlargement induces cellular and metabolic changes that can affect whole-body metabolic homeostasis. In fact, adipocytes expansion induces hypoxia, adipocytes cell death, lipolysis with free fatty acids (FFA) release from adipocytes. Moreover, cytokines and chemokines production in adipose tissue is also increased (Sun et al., 2011). All these events are potent inducers of macrophages recruitment. Macrophages that are activated by pro-inflammatory *stimuli* and that express typical inflammation markers, such as IL-6, TNFα, NO production, are called *classically activated* or M1 macrophages. In contrast, *alternatively activated* or M2 macrophages produce anti-inflammatory cytokines, such as IL-10, and express typical anti-inflammatory markers, such as arginase (Mantovani et al., 2004). Normal adipose tissue macrophages (ATM) have predominantly a M2-phenotype, while obesity induces a phenotypic switch in their polarization towards M1 phenotype (Lumeng et al., 2007). Notably, M1-infiltrated macrophages produce pro-inflammatory cytokines, as IL-6, TNFα, IL-1β, inducing a generalized low-grade inflammation associated with obesity. IL-6 and TNFα are important cancer promoters, by inducing STAT3 and NF-κB/JNK pathways increasing cell survival, proliferation, angiogenesis and metastasis (Pikarsky et al., 2004, Zhong et al., 1994). Besides their role in lipid storage, adipocytes are important secretory cells; they maintain body metabolic homeostasis through adipokines production and secretion (Gavrilova et al., 2000). Adipose tissue remodeling during obesity does not involve changes in ATM phenotype only, but also in the adipokines profile; in fact, obesity is associated with an increase in the pro-inflammatory cytokines production (Hotamisligil et al., 1993), a reduction in adiponectin circulating levels (Asayama et al., 2003), an increase in leptin plasma levels (Considine et al., 1996) and a dysregulation of other adipokines (Antuna-Puente et al., 2008). Among all adipokines, leptin and adiponectin dysregulation are involved in tumor progression. Leptin is a well-studied adipokine that has an important role in appetite regulation. During obesity, high amount of circulating leptin can result in hypothalamic leptin-resistance (El-Haschimi et al., 2000). Moreover, leptin has been described as a pro-tumorigenic adipokine that enhances angiogenesis and induces cell survival through JAK/STAT3 pathway (Uddin et al., 2011). Adiponectin is one of the most abundant transcripts in adipose tissue (Maeda et al., 1996). It is

synthesized as a monomeric form that undergoes to oligomerization to form trimers (low molecular weight, LMW), that can associate into hexamers (medium molecular weight) and, finally, into multimers (high molecular weight, HMW) before secretion (Wang et al., 2006b). Adiponectin circulating levels are reduced in obesity and malignancies (Arita et al., 1999, Kelesidis et al., 2006). In fact, it acts as an anti-tumor molecule, by activating AMP-activated protein kinase (AMPK), inhibiting mTOR signaling pathway along with other pro-tumorigenic signaling pathways, such as NF-κB/STAT3, and by enhancing p21 and p53 activity (Dalamaga et al., 2012). Adipose tissue remodeling has an effect on other tissues. For example, increased-lipid efflux from adipose tissue is absorbed by other organs, in particular liver, pancreas and muscle. Excess of circulating FFA and TNFα induces insulin resistance through the inhibitory phosphorylation of insulin receptor substrate 1 and 2 in Serine and Threonine (IRS1 and IRS2) (Aguirre et al., 2002, Solinas et al., 2006, Hirosumi et al., 2002). Insulin resistance increases circulating levels of glucose and insulin. Notably, hyperinsulinemia and hyperglycemia are two important tumor promoters: on one hand, glucose can facilitate cancer cells metabolic switch to glycolysis -a mechanism known as Warburg effect (Warburg, 1956)- and can increase cell survival under hypoxic conditions, through the induction of Hif1α expression (Catrina et al., 2004). On the other hand, insulin is an important growth factor and hyperinsulinemia *per se* can promote transformed cells proliferation (Hill and Milner, 1985).

2. LIVER CANCER

Liver cellularity includes two major cells types: parenchymal and non-parenchymal cells. Parenchymal hepatocytes comprise about 80% of liver volume. Non-parenchymal cells include the sinusoidal endothelial cells, Kupffer cells, bile duct cells, hepatic stellate cells and oval cells. The most common primary liver cancer is hepatocellular carcinoma (HCC), which accounts for 85-90% of liver cancers (El-Serag and Rudolph, 2007). HCC is generated by hepatocytes uncontrolled proliferation. Other types of liver cancers are cholangiocarcinoma, which originates from hyperproliferation of bile duct cells, and a rare malignancy named angiosarcoma, whose etiology is the proliferation of endothelial cells.

2.1 Hepatocellular carcinoma

Hepatocellular carcinoma (HCC) is the second most common cause of death for cancer worldwide. Recent data estimate that HCC has been responsible for nearly 746,000 deaths in 2012 (9.1% of total deaths) (GLOBOCAN 2012). Patients diagnosed with HCC have poor prognosis and overall ratio of mortality to incidence is 0.95 (GLOBOCAN 2012). In fact the geographical pattern of incidence and mortality of HCC are quiet similar (Figure I2A and I2B). Typically, HCC is asymptomatic at an early stage, resulting in frequent late diagnosis. Together with lack of effective therapies, advance-stage disease at diagnosis explains the high mortality ratio observed in HCC patients (Stotz et al., 2015). In fact, the gold-standard therapy is considered liver transplant or partial hepatectomy; however, only a minority of patients is eligible for surgery due to the late-stage of the pathology at diagnosis (Llovet et al., 2003).

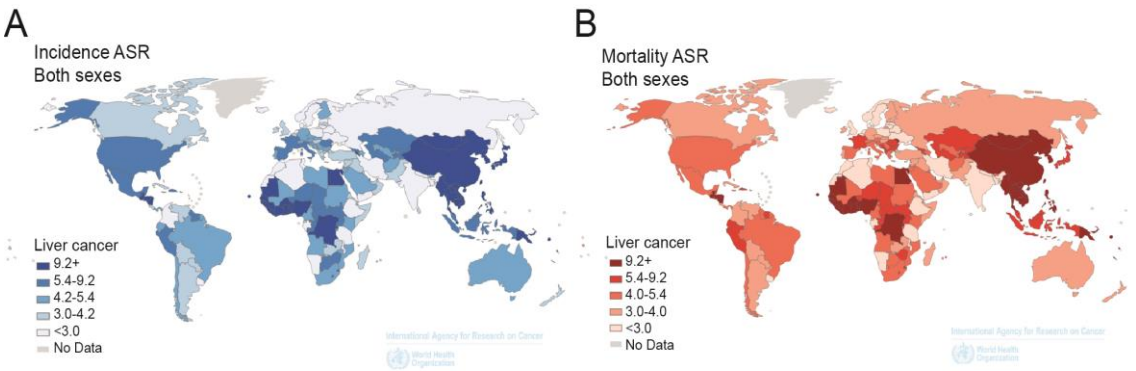

Figure I2. Liver Cancer Incidence and Mortality.
Liver cancer Incidence (A) and mortality (B). Age Standardized Rates (ASR). Data source: GLOBOCAN 2012, Map production: IARC, World Health Organization.

The majority of patients are treated with Sorafenib, a multi-kinase inhibitor targeting tyrosine kinase receptors (e.g. vascular endothelial growth factor receptors and platelet-derived growth factor receptor-beta) and downstream intracellular serine/threonine kinases (e.g. Raf-1, wild-type B-Raf and mutant B-Raf). All these kinases control cell proliferation and tumor angiogenesis (Keating and Santoro, 2009). Sorafenib has several secondary effects (diarrhea, hand-foot skin reaction, weight loss) and can increase the overall survival only about 3 months (Llovet et al., 2008). Therefore, there is an evident

and urgent need to understand the molecular mechanism underlying HCC, in order to develop more specific and effective therapies.

2.2 Obesity, inflammation and HCC

Several malignant *stimuli* have been demonstrated to act as driving forces in HCC development (HBV and HCV infection, alcohol, aflatoxin B). Among them hepatitis B and C virus infection account for more than 50% of all cases of HCC (El-Serag, 2011). HBV or HCV infection leads to chronic liver inflammation that can degenerate in fibrosis, cirrhosis and, ultimately, HCC development (Freeman et al., 2001, Yang et al., 2011). However, several studies conducted in Western countries showed that 30-40% of patients with HCC does not present HBV or HCV infection, which indicates the presence of other drivers in HCC development (El-Serag, 2011). Epidemiological studies have highlighted a strong relation between obesity and HCC; in fact, increased BMI rises the relative risk of death by HCC of 4.52 and 1.68, in men and women respectively (Calle et al., 2003) (Figure I3).

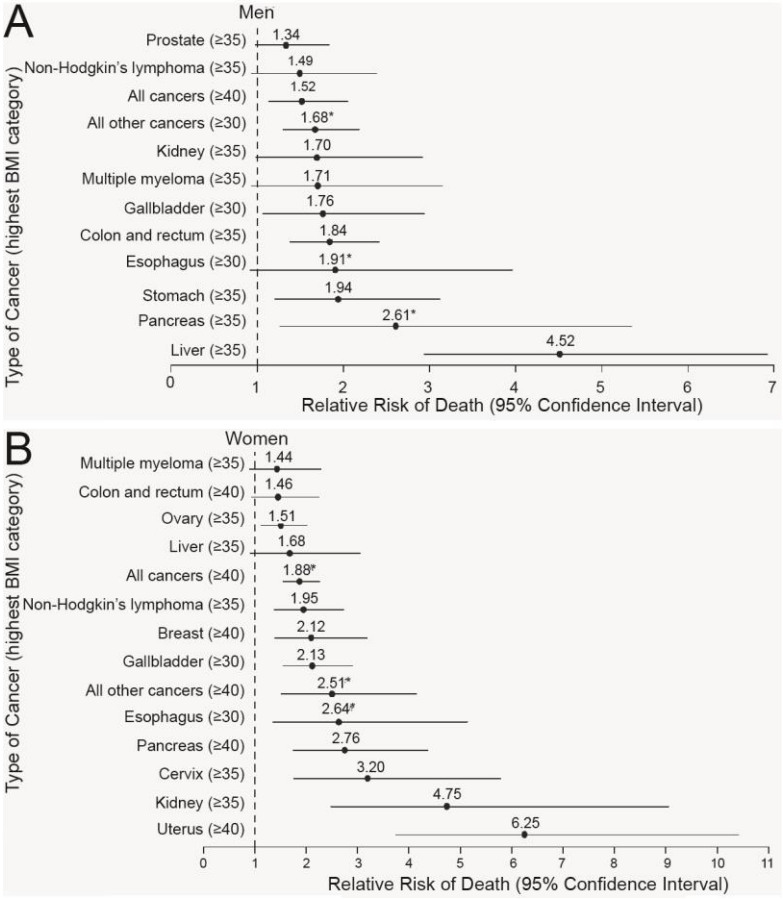

Figure I3. Mortality from Cancer According to Body-Mass Index for U.S. Men and Women in the Cancer Prevention Study II, 1982 through 1998.
A) Men and B) Women graphical representation of cancer risk. For each relative risk the comparison was between subjects in the highest BMI category (in parentheses) and subjects in the reference category (BMI 18.5 to 24.9). Asterisks indicate relative risks for subjects who never smoked. Results of the linear test for trend were significant ($p \leq 0.05$) for all cancer sites. Adapted from Calle *et al.*, 2003.

Non-alcoholic fatty liver disease (NAFLD), the liver manifestation of obesity and type 2 diabetes (Abdelmalek and Diehl, 2007), can degenerate in the more severe non-alcoholic steatohepatitis (NASH) and cirrhosis, which is the major risk factor for HCC development (Starley et al., 2010) (Figure I4).

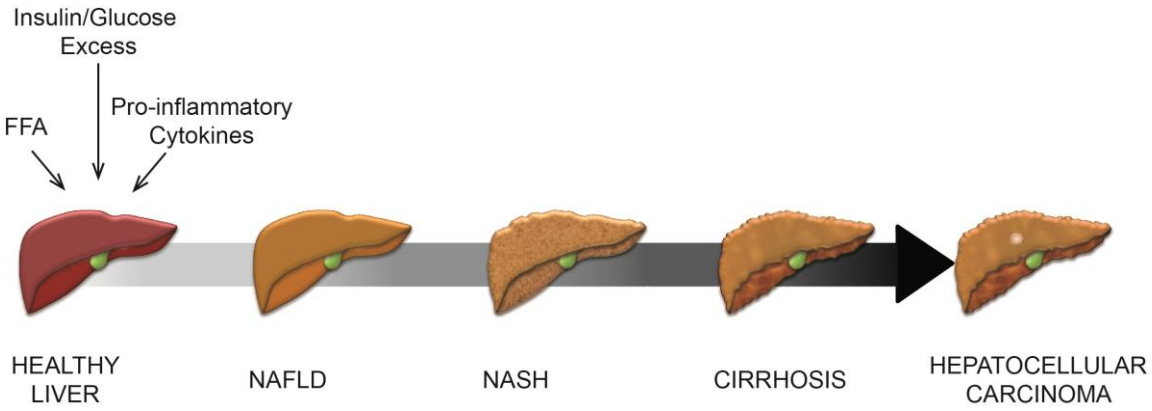

Figure I4. Progression from Healthy Liver to Hepatocellular Carcinoma.
Different *stimuli*, such as FFA, pro-inflammatory cytokines, insulin or glucose excess, induce non-alcoholic fatty liver disease (NAFLD). This can degenerate in the more severe non-alcoholic steatohepatitis (NASH) and cirrhosis, which is irreversible and is considered one of the main predisposing factors for hepatocellular carcinoma (HCC) development.

The mechanistic model of HCC insurgence consists in a severe hepatocellular damage that induces massive hepatocytes cell death and consequent compensatory proliferation. Sustained cycles of hepatocytes destruction-compensatory proliferation lead to accumulation of mutations in proliferative hepatocytes (Baffy et al., 2012, Fujimoto et al., 2016). Several mechanisms of hepatocellular damage take place during obesity and other associated metabolic disorders. The most remarkable feature of NAFLD is FFA accumulation in hepatocytes that leads to hepatic lipotoxicity. Excess of nutrients activates mammalian target of rapamycin complex 1 (mTORC1), which in turn, stimulates lipogenesis through the induction of the sterol regulatory element-binding protein 1 (SREBP1) (Han et al., 2015), enhancing lipid accumulation. Moreover, mTORC1 activation inhibits cell autophagy (Kim et al., 2011). Hypernutrition also inhibits AMPK activation, an important inducer of autophagy (Kim et al., 2011). Reduced autophagy results in aberrant proteins and mitochondria accumulation, which increase endoplasmic reticulum (ER) stress and ROS production, respectively (Wang et al., 2006a, Takamura et al.,

2011), causing hepatocytes cell death. Sustained hepatocytes necrosis and apoptosis activate Kupffer cells, increasing IL-6 and TNFα secretion. These two molecules are able to activate JAK/STAT3 and NF-κB pathways, providing both pro-survival and anti-apoptotic stimuli to mutated hepatocytes (Park et al., 2010), thus enhancing tumor progression. Taking together these data, a clear link between obesity induced-NAFLD and HCC emerges. However, further investigation on the role of metabolic genes in HCC development is needed, in order to elucidate the mechanisms underlying such correlation.

3. METABOLIC GENES

3.1 Stress-activated protein kinases

Mitogen-activated protein kinases (MAPK) is a family of protein kinases that transduce a variety of extracellular signals, regulating cellular responses (Sabio and Davis, 2014). Three groups of MAPKs have been identified: the epithelial signal-regulated kinases (ERKs), the p38 MAPKs, and the c-Jun N-terminal kinases (JNKs). While ERKs are mainly activated by mitogens and differentiation signals, JNKs and p38 MAPKs are activated by stress stimuli and are collectively known as stress-activated protein kinases (SAPKs) (Manieri and Sabio, 2015). The SAPK family is composed of the four isoforms of p38 (p38α, β, γ, δ) and the three isoforms of JNK (JNK1, 2, and 3) (Paul et al., 1997).

3.1.1 c-Jun N-terminal kinases

JNKs isoforms are encoded by three genes, located in different chromosomes and conserved among species: *Jnk1* and *Jnk2* are ubiquitously expressed, while *Jnk3* is specifically expressed in brain, testis and heart (Davis, 2000, Chang and Karin, 2001). Several splice variants have been described for each JNK member, and they can be separated in two groups based on their size: the short forms of about 46 kDa (JNK1a1, JNK1b1, JNK2a1 JNK2b1 JNK3a1) and the long forms of about 54 kDa (JNK1a2, JNK1b2, JNK2a2 JNK2b2 JNK3a2) (Gupta et al., 1996). JNK1 short isoforms predominate over JNK2 short variants in the majority of cell types, while the reverse pattern is observed for the long forms (Gupta et al., 1996). The function and the exact modulation of each of these splice variants is still unsolved. A wide range of *stimuli* induces JNKs activation, such as environmental stresses (hypoxia, U.V., ionizing radiation), toxins, drugs, TNFα and IL-6 and metabolic changes, including hyperlipidemia.

These *stimuli* induce a phosphorylation cascade that culminates with the activation of JNKs, which induces the proper response to a specific *stimulus*, characterized by apoptosis, cell proliferation, differentiation or cell migration. JNKs activation is mediated by a dual phosphorylation on tyrosine and threonine in the conserved Thr-Pro-Tyr motif in their activation loop. Two MAP kinase kinases, MKK4 and MKK7 mediate such phosphorylation events (Paul et al., 1997). More than fifty proteins have been identified as JNKs substrates. These include c-Jun, which once phosphorylated can dimerize with JunB, JunD or c-Fos to form the transcription factor activator protein-1 (AP-1) (Hotamisligil et al., 1996). Other important substrates are insulin receptor substrate 1 (IRS1) (Lee et al., 2003); c-MYC; p53, and numerous transcription factors (Davis, 2000, Chang and Karin, 2001).

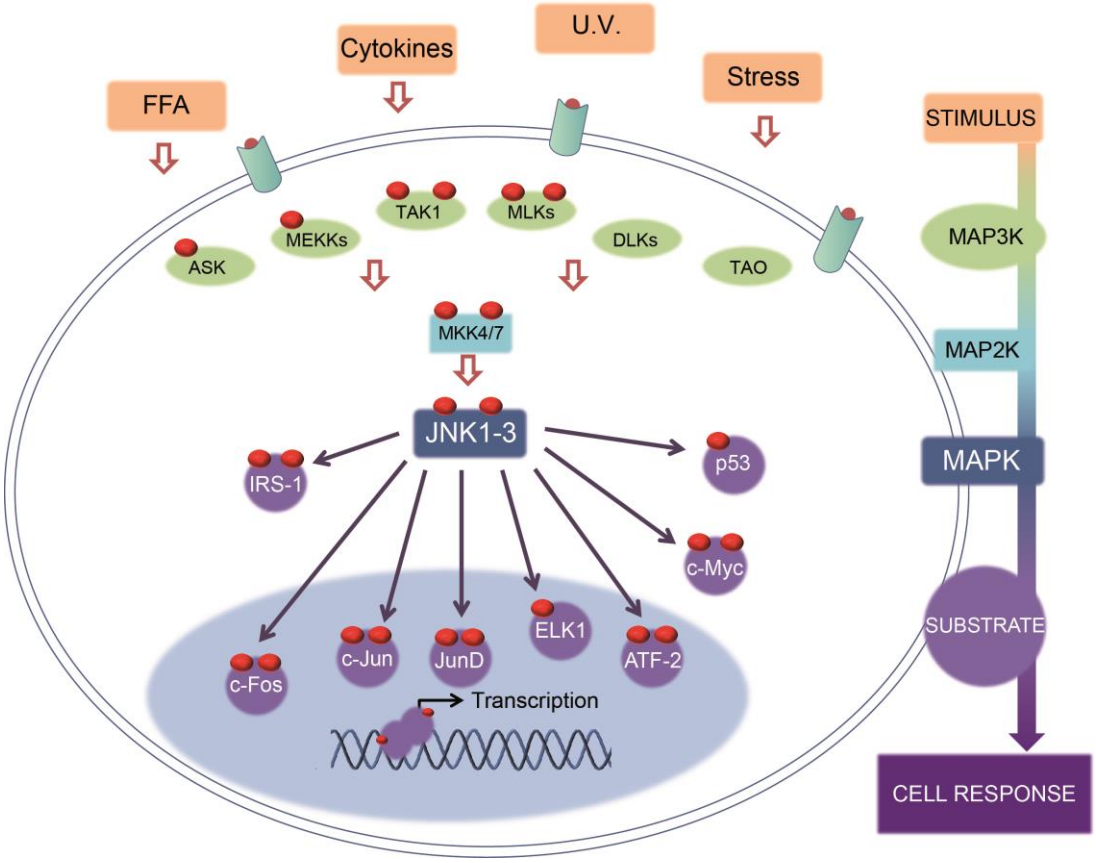

Figure I5. Schematic representation of JNKs pathways.
Cellular stress *stimuli*, such as cytokines, FFA and U.V., activate a phosphorylation cascade, which culminates with JNKs activation. JNKs phosphorylate their substrates inducing a *stimulus*-specific cell response.

3.1.2 JNKs in HCC

JNKs play a central role in cell response to stress *stimuli*, and they are able to induce apoptosis or cell proliferation depending on the *stimulus* nature and of its intensity. For this reason, their role has been studied in tumor development, highlighting isoform-specific, cell-specific and tumor-specific influence of JNK family members in cancer (Wagner and Nebreda, 2009). In addition, sequencing analyses of human cancer specimens have identified somatic mutations at *JNK1* and *JNK2* and upstream kinase *MKK7*, suggesting their importance in tumor development (Greenman et al., 2007, Jones et al., 2008). C-Jun, a downstream effector of JNKs pathway, has been shown to have a promoting function through suppression of p53 pathway in liver cancer (Eferl et al., 2003). Moreover, JNK1 activation is increased in p38α knock out hepatocytes, promoting tumorigenesis (Hui et al., 2007). JNK1, but not JNK2, constitutive knock out mice are protected against chemical-induced HCC development, due to p21 up-regulation and c-MYC down-regulation (Hui et al., 2008). Furthermore, it has been described a differential role for JNK1 and JNK2 in hepatocytes and liver non-parenchymal cells (Das et al., 2011). Das and colleagues demonstrated that deficiency of JNK1 and JNK2, specifically in hepatocytes, enhance tumor growth. In contrast, their depletion in both hepatocytes and non-parenchymal cells strongly suppress tumor growth (Das et al., 2011). They observed p21 up-regulation in both systems, but c-MYC downregulation only in the latter one, indicating a potential role for JNK in c-MYC expression during HCC development. Compensatory proliferation plays a major role in HCC development (Grivennikov et al., 2010), and it could be stimulated by cytokines produced by hepatic immune cells (Naugler et al., 2007, Park et al., 2010). Das and colleagues demonstrated a reduction in cytokines production in the context of JNK depletion in both, parenchymal and non-parenchymal cells, followed by a reduction in cell death and compensatory proliferation (Das et al., 2011). Together these results support a pro-inflammatory and pro-tumorigenic role of JNK1 and 2 in non-parenchymal cells, causing cytokines expression and compensatory proliferation, while hepatocytes JNKs expression appears to decrease cell death and compensatory proliferation during HCC (Das et al., 2011).

3.1.3 JNK in metabolism

A part from their role in tumor development, JNK-SAPK family has a major role in obesity and metabolic disorders. In fact, JNK3 has been recently described as a key player in regulating feeding behavior under HFD *stimulus* (Vernia et al., 2016), while a large body of literature indicates JNK1 and JNK2 isoforms as important regulators of obesity-induced inflammation and metabolic disorders (Tuncman et al., 2006, Singh et al., 2009, Han et al., 2013). JNK pathway is strongly activated in liver, adipose tissue and muscle during dietary and genetically induced obesity, and mice knockout for JNK1, but not JNK2, are protected against obesity and insulin resistance (Hirosumi et al., 2002). For this reason the majority of research carried out on JNKs and metabolic disorders is especially focused on JNK1 and its tissue-specific role in metabolism (Sabio et al., 2009, Sabio et al., 2008, Solinas et al., 2007, Sabio et al., 2010). These studies took advantage of JNK1 tissue-specific knock out models, and highlighted a double influence of JNK1 in metabolism: on the one hand, JNK1 induces a cell-autonomous effect, influencing the response of the cell to obesity; on the other hand, JNK1 influences the crosstalk between different organs, modifying their response to obesity-associated effects. Of particular interest for this Thesis is the role that JNK1 exerts in adipose tissue. JNK1 deletion in adipocytes does not influence HFD-induced weight gain, but protects adipose tissue against obesity-induced insulin resistance. Moreover in absence of JNK1, adipose tissue IL-6 production is reduced, protecting liver from steatosis and insulin resistance development (Sabio et al., 2008). As mentioned before, liver steatosis can degenerate in NAFLD and the more severe NASH, which are predisposing factors for HCC development (Starley et al., 2010). Despite the pivotal role played by JNK1 in inflammation, metabolism and HCC, its involvement in organs crosstalk and liver carcinogenesis has not been well studied.

3.2 Peroxisome proliferator-activated receptors

Peroxisome proliferator-activated receptors (PPARs) are ligand-activated receptors that belong to the nuclear hormone receptor superfamily. In mammals there are three PPAR isoforms: PPARα (encoded by *Nr1c1* gene), PPARβ/δ (*Nr1c2*) and PPARγ (*Nr1c3*) (Issemann and Green, 1990, Kliewer et al., 1994). Each isoform is encoded by a different gene and has a tissue-specific

expression depending of their functions. Expression of PPARα is highest in tissues with high levels of β-oxidation, as liver, brown adipose tissue, hearth, kidney and immune cells (Mandard et al., 2004); PPARγ is mainly expressed in adipose tissue and intestine, (Fajas et al., 1997), whereas PPARβ/δ is ubiquitously expressed (Girroir et al., 2008). PPARs are lipid sensors, and they are activated by dietary fatty acids and their metabolic derivatives. PPARs are present in the nucleus associated with retinoid X receptors (RXRs) and the nuclear receptor co-repressor/silencing mediator for retinoid and thyroid hormone receptors (NCoR/SMRT). PPARδ is the only isoform that can bind to DNA while is associated with NCoR/SMRT co-repressor. After ligand binding, PPARs can move apart from the co-repressor and bind to DNA sequences named peroxisome proliferation response elements (PPREs) in the promoter of their target genes and to co-activator complexes such as steroid receptor co-activator 1 (SRC1) and cAMP response element binding (CREB)-binding protein (CBP/p300) (Daynes and Jones, 2002). PPREs contain repeats of the sequence AGGTCA separated by one or two nucleotides (named DR1 and DR2 respectively) and are located in the promoter region of target genes (Tugwood et al., 1992, Mascaro et al., 1999, Green and Wahli, 1994, A et al., 1997). Each PPAR isoform responds to different types of ligands, exerting a different function (Kliewer et al., 1994).

3.2.1 PPARα

PPARα is highly expressed in liver and it is a major regulator of hepatic lipid metabolism. Endogenous ligand of PPARα include fatty acids (FA), in particular omega-3 fatty acids, such as arachidonic acid, linoleic acid, docosahexaenoic acid, eicosapentaenoic acid, eicosanoids derivatives as leukotriene B4 (Krey et al., 1997); synthetic ligands include principally fibrates and pirinix acid (WY14,643) (Briguglio et al., 2010). Ligand binding induces expression of genes involved in lipid metabolism, in particular fatty acid oxidation, ketogenesis, lipid transport and gluconeogenesis (Pawlak et al., 2015). In addition to its role in metabolism, PPARα exerts also an anti-inflammatory function (Devchand et al., 1996, Staels et al., 1998).

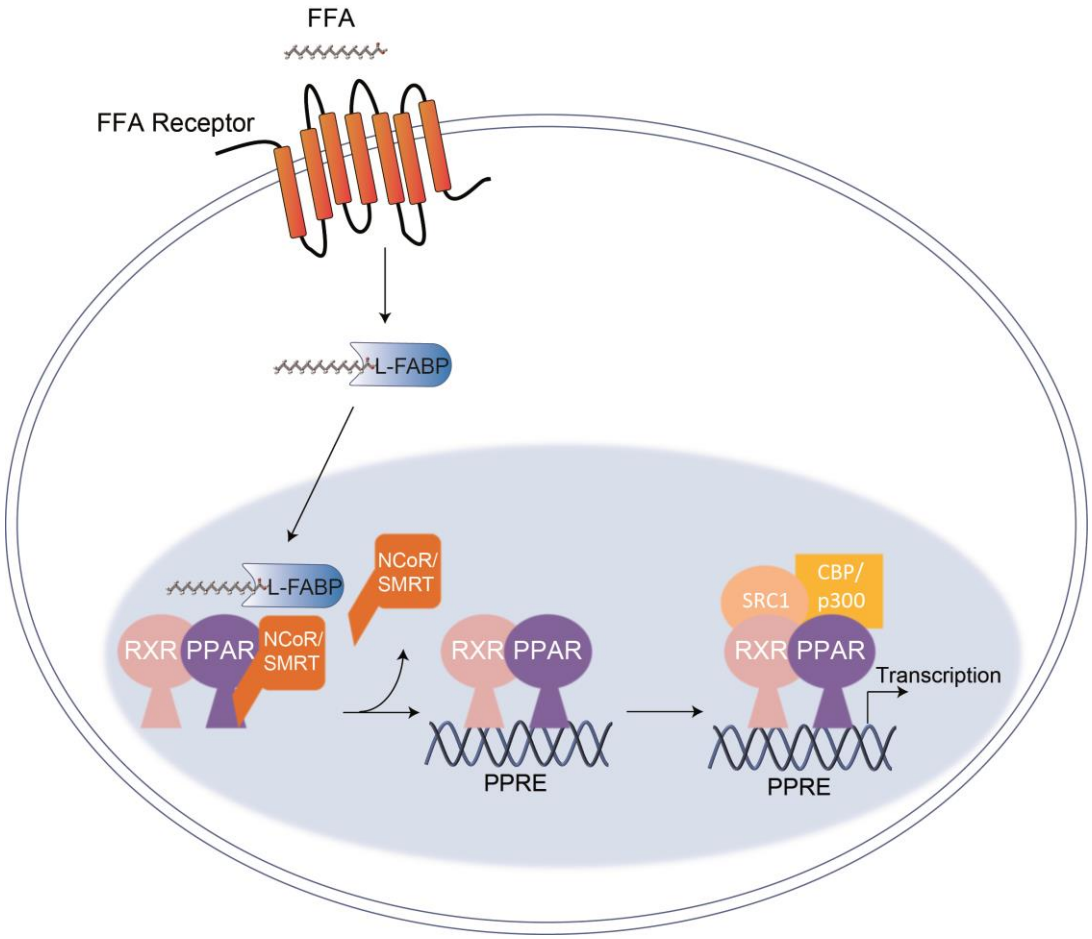

Figure I6. Schematic representation of PPARs activation.
Free fatty acids (FFA) and their derivatives are internalized by FFA receptor. They are recognized by cytosolic L-FABP, which brings them to the inhibited complex RXR-PPAR-NCoR/SMRT. Ligand binding induces co-repressor NCoR/SMRT separation from the complex and RXR-PPAR. After dissociation from co-repressor, RXR-PPAR complex can bind to PPRE DNA sequences. PPARs can bind co-activator complexes, such as SRC1 and CBP/p300, activating gene transcription.

3.2.2 PPARα in metabolism

Fatty acids (FA) are transported in the cell by membrane-associated fatty acid transport proteins (FABPs) (Schaffer and Lodish, 1994). Genes encoding for some FABPs are direct targets of PPARα, indicating that activation of PPARα enhances FA entrance in the cell (Martin et al., 1997). Among them *L-Fabp* gene have been described to present PPREs sequence and protein binding between PPARα and L-FABP has been reported, suggesting that L-FABP may channel PPARα ligands to the receptor (Helledie et al., 2002). A part from genes controlling FA trafficking, PPARα is an important transcription factor for rate-limiting enzymes of peroxisomal β-oxidation, as *Acox1* (Peroxisomal Acyl-

CoA Oxidase 1) and *Ehhadh* (Peroxisomal bifunctional enzyme) (Dreyer et al., 1992); *Cpt-I* and *Cpt-II* that trigger FA transport through mitochondria membrane (Mascaro et al., 1998); and medium, long and very long-chain acyl-CoA dehydrogenase genes (*Mcad*, *Lcad*, *Vlcad*) (Gulick et al., 1994, Aoyama et al., 1998). Moreover, hepatic PPARα activity is enhanced in fasting conditions, because of the increase in fatty acids oxidation due to ketogenesis. In this context, PPARα induces expression of genes involved in ketogenesis and fatty acid oxidation, in particular *Fgf21* that is a key mediator of these processes (Badman et al., 2007). In addition PPARα induces lipoprotein lipase (LPL) gene expression and inhibits mRNA production of a LPL inhibitor (APO-CIII), increasing the hydrolysis of lipoprotein triglyceride in FFA (Schoonjans et al., 1996a, Hertz et al., 1995). Finally PPARα controls hepatic lipogenesis enhancing *Srebp1c* transcription in humans and SREBP1c target genes in mice (*Fas*, *Acc1* and *Scd*-1) (Fernandez-Alvarez et al., 2011, Patel et al., 2001). Taking into account all the functions of PPARα in controlling hepatic metabolism, it is clear its role as a sensor and regulator of liver energy balance.

3.2.3 PPARα in inflammation

Beyond its fundamental role in hepatic metabolism, PPARα has a prominent role in inflammation. Using *Ppara*$^{-/-}$ mouse model and fibrates, different groups showed its role as anti-inflammatory protein. In fact, *Ppara*$^{-/-}$ mice suffered prolonged inflammatory response when treated with leukotriene B4 (LTB_4) in the ear-swelling test (Devchand et al., 1996). LTB_4 is a pro-inflammatory eicosanoid that binds PPARα inducing the transcription of ω and β-oxidation genes, which lead to its catabolism (Devchand et al., 1996). In addition, splenocytes from *Ppara*$^{-/-}$ mice respond to lipopolysaccharide (LPS) stimulation producing two to three times more pro-inflammatory cytokines as IL-6 and IL-12 than WT cells (Poynter and Daynes, 1998). Furthermore, PPARα ligands inhibit IL-1-induced IL-6 production and cyclooxygenase-2 expression in smooth-muscle cells (Staels et al., 1998). PPARα also acts through the repression of NF-κB signaling to reduce prostaglandin production (Staels et al., 1998). These data underlie a protective role of PPARα against inflammation.

3.2.4 PPARα and HCC development

PPARα has a pivotal role in protect liver from steatosis and obesity-induced hepatic inflammation (Stienstra et al., 2007, Ip et al., 2003) and use of PPARα agonists, as fibrates, seem to have a promising activity contrasting obesity effects (Forman et al., 1997, Schoonjans et al., 1996b). However, its role in hepatocellular carcinoma development is less clear. It has been shown that mice lacking PPARα are more prone to chemical-induced HCC development, due to increased activation of NF-κB pathway and consequent escape from apoptosis (Zhang et al., 2014). In addition, *in vitro* studies on HCC cell lines demonstrate growth inhibitory effect of PPARα agonists (Panigrahy et al., 2008, Maggiora et al., 2010). Conversely, studies with PPARα agonists as Wy14-643 showed increase HCC development in WT mice, due to increased DNA in synthesis, while Wy14-643-treated *Ppara*$^{-/-}$ mice were refractory to HCC, suggesting a PPARα promoting effect (Peters et al., 1997). Moreover, PPARα activation has been described to be essential in the HCV-induced liver steatosis and HCC development (Tanaka et al., 2008). Tanaka and colleagues demonstrated that *Ppara*$^{-/-}$ mice expressing HCV core protein are protected against HCC development, while increasing activation of PPARα in heterozygous mice with clofibrate enhances liver tumorigenesis (Tanaka et al., 2008).

Concluding, PPARα has a fundamental role in hepatic metabolism and inflammation. Thus, elucidate its function in HCC development in physiological conditions that enhance its activation, as obese state, would be helpful to find new therapies for this malignancy.

OBJECTIVES

Hepatocellular carcinoma is the second cause of cancer-related death. Epidemiological studies suggest an association of liver cancer with obesity and metabolic disorders. However the mechanisms underlying this correlation and the link between adipose tissue and liver cancer are poorly understood. The aim of this Thesis is to study two metabolic genes, JNK1 and PPARα, to understand how their function as metabolic controllers could affect hepatocellular carcinoma development.

1. Study the role of adipose tissue JNK1 in hepatocellular carcinoma development

1.1 Evaluate the effect of adipose tissue JNK1 on chemical-induced liver tumorigenesis in normal chow diet and high fat diet conditions

1.2 Analyze the consequences of JNK1 ablation in adipose tissue

1.3 Unveil the molecular mechanism through which adiponectin inhibits hepatic tumorigenesis

1.4 Identify other possible target of JNK1 that can have a role in adipose tissue to liver crosstalk during hepatocellular carcinoma development

2. Elucidate the role of PPARα in liver cancer development during obesity

2.1 Study the effect of PPARα on chemical-induced liver tumorigenesis in normal chow diet and high fat diet conditions

2.2 Define in which cellular compartment PPARα is important for liver tumorigenesis

2.3 Elucidate the molecular mechanism through which PPARα controls this process

2.4 Verify the importance of PPARα in liver cancer using another model to induce its activation

MATERIALS AND METHODS

1. ROLE OF JNK1 IN ADIPOSE TISSUE-LIVER CROSSTALK IN HCC DEVELOPMENT

Animals

Experimental model was generated as previously described (Sabio et al., 2008). Briefly, mice in which JNK1 gene was flanked by *LoxP* sequences (*Jnk1*$^{f/f}$) (generated in Roger J. Davis' laboratory) were crossed with mice expressing *Cre* recombinase under the control of adipose tissue specific *Fabp4* promoter (*Fabp4-Cre*) (He et al., 2003). To reduce the *LoxP* sequence recombination and achieve a better depletion of *Jnk1* gene, we crossed these mice with full knock out *Jnk1* mice (Jackson Laboratories; B6.129S1-*Mapk8*^{tm1Flv}/J, here called *Jnk1*$^{-/-}$), obtaining *Fabp4-Cre*$^{+}$*Jnk1*$^{f/-}$ mice (F^{KO} mice). Littermates without conditional *Jnk1* allele (*Fabp4-Cre*$^{+}$*Jnk1*$^{+/-}$) were used as control mice (F^{WT}) (Figure M1).

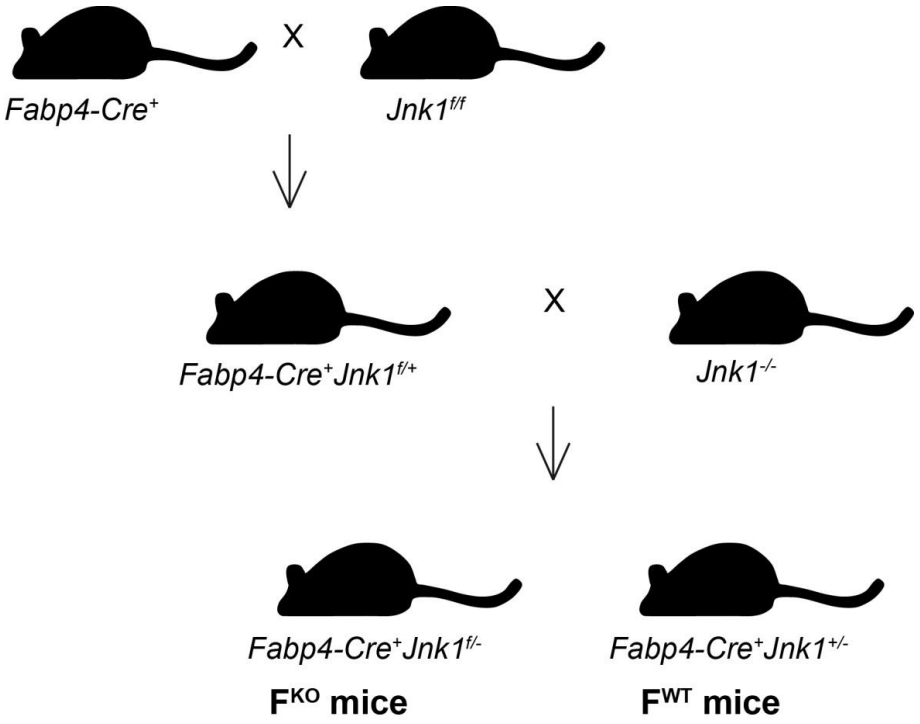

Figure M1. Schematic representation of mouse lines crossing to generate F^{WT} and F^{KO} mice.

Fabp4-Cre^{+} mice were crossed with *Jnk1*$^{f/f}$ to obtain *Fabp4-Cre*$^{+}$*Jnk1*$^{f/+}$ mice. These mice were crossed with *Jnk1*$^{-/-}$ mice generating *Fabp4-Cre*$^{+}$*Jnk1*$^{+/-}$ (F^{WT}) and adipose tissue JNK1 specific knock out *Fabp4-Cre*$^{+}$*Jnk1*$^{f/-}$ (F^{KO}) mice.

Adiponectin knock out mice were purchased from Jackson Laboratories (B6;129-*Adipoq*^{tm1Chan}/J, here called *Adipoq*$^{-/-}$). These mice were crossed with *Fabp4-Cre*$^{+}$*Jnk1*$^{f/f}$ mice and *Jnk1*$^{-/-}$ mice as represented in Figure M2, to generate F^{KO}*Adipoq*$^{-/-}$ and F^{WT}*Adipoq*$^{-/-}$ models (Figure M2).

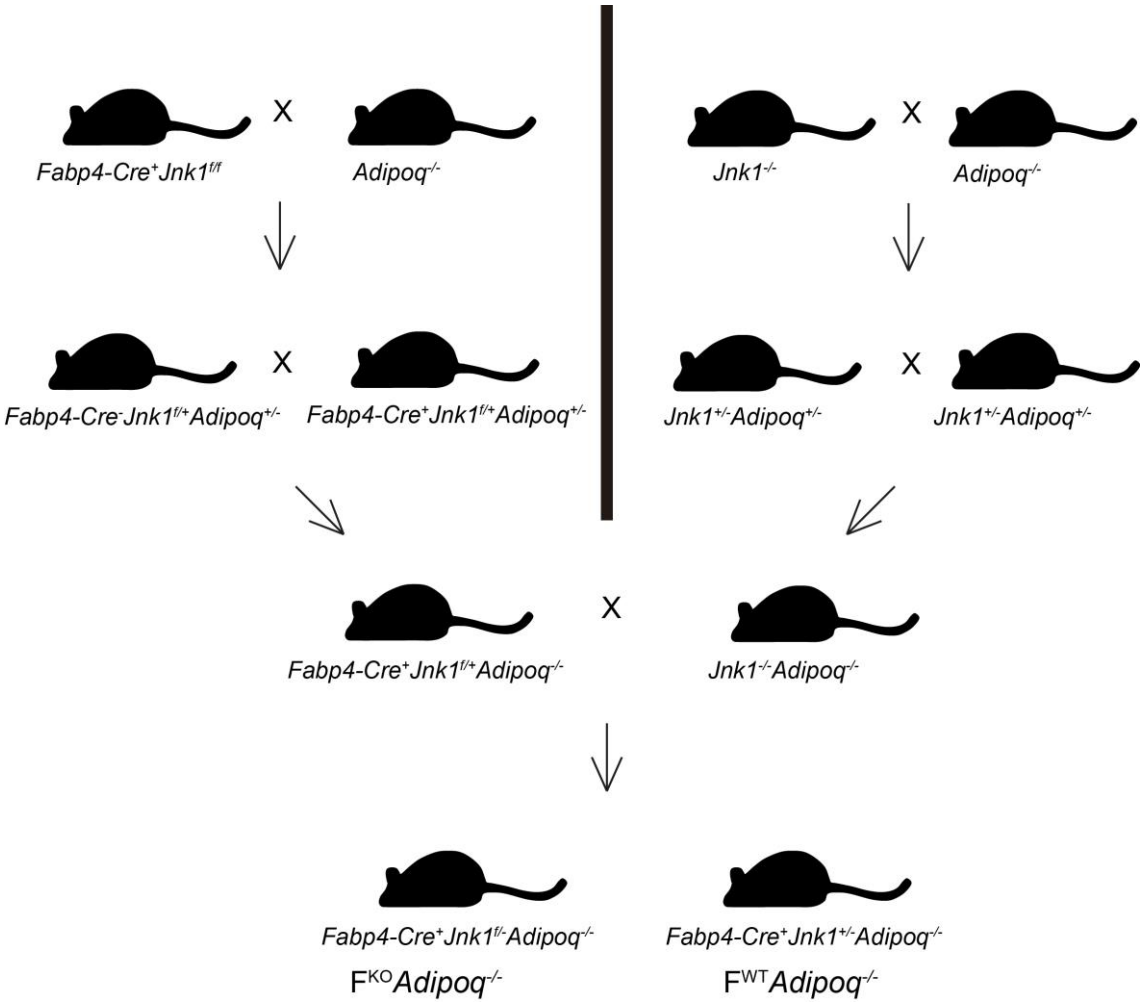

Figure M2. Schematic representation of mouse lines crossing to generate F^{WT}*Adipoq*$^{-/-}$ and F^{KO} *Adipoq*$^{-/-}$ mice.

Representation of mouse lines crossing to generate control F^{WT}*Adipoq*$^{-/-}$ and adipose tissue JNK1 specific knock out F^{KO}*Adipoq*$^{-/-}$ mice. On one side *Fabp4-Cre*$^{+}$*Jnk*$^{f/f}$ mice were crossed with adiponectin knock out (*Adipoq*$^{-/-}$) mice to obtain *Fabp4-Cre*$^{+}$*Jnk1*$^{f/+}$*Adipoq*$^{-/-}$ mice. On the other side *Jnk1*$^{-/-}$ mice were crossed with *Adipoq*$^{-/-}$ to obtain *Jnk1*$^{-/-}$*Adipoq*$^{-/-}$ mice. Finally, *Fabp4-Cre*$^{+}$*Jnk1*$^{f/+}$*Adipoq*$^{-/-}$ mice were crossed with *Jnk1*$^{-/-}$*Adipoq*$^{-/-}$ mice to obtain *Fabp4-Cre*$^{+}$*Jnk1*$^{+/-}$*Adipoq*$^{-/-}$ (F^{WT}*Adipoq*$^{-/-}$) and *Fabp4-Cre*$^{+}$*Jnk1*$^{f/-}$*Adipoq*$^{-/-}$ (F^{KO} *Adipoq*$^{-/-}$) mice

Genotypes were identified by PCR analysis of genomic DNA isolated from mouse-tails. All experiments were performed in male mice. For tumor studies, mice on postnatal day 14 received a single i.p. injection of 50 mg/kg body

weight diethylnitrosamine (DEN, Sigma-Aldrich) dissolved in saline. Six weeks after DEN treatment, mice were fed a high-fat diet (HFD, Research Diet Inc.) or standard chow diet *ad libitum* until sacrifice 8 months after DEN injection. Tumors were measured with an analogical caliber. Before sacrifice, body weight was measured and blood samples were taken for metabolomics and cytokines analysis. For time course studies mice were sacrificed 15 days and 1 month after DEN injection. In all cases, mice were euthanized after overnight starvation.

For partial hepatectomy (PHx) experiments adult mice (8-12-week-old), were anesthetized using a mixture of isoflurane and oxygen. Two-thirds of the liver was excised according to Mitchell and Willenbring (Mitchell and Willenbring, 2008), medial and left lateral lobes were removed. Mice were sacrificed 48 hours or 15 days after PHx and their liver was weighted to analyze hepatic mass regeneration.

Mice were housed in a pathogen-free animal facility and kept on a 12-hour light/dark cycle at constant temperature and humidity. All animal experiments conformed to EU Directive 2010/63EU and Recommendation 2007/526/EC, enforced in Spanish law under Real Decreto 53/2013

Cell culture

Hep53.4 cell line was purchased from CLS-Cell Lines Service GmbH. It is an established cell line generated from DEN-induced HCC in C57BL/6J mice as previously described (Kress et al., 1992). Hep53.4 cells were cultured in DMEM supplemented with 10% FBS, L-glutamine and penicillin/streptomycin.

Retrovirus production

Retrovirus expressing p38α D176A/F327S was produced in HEK-293 Phoenix-ECO cell line, which is stably transfected to express Moloney Murine Leukemia Virus (M-MLV) viral packaging proteins. Transient calcium phosphate co-transfection of HEK-293 Phoenix-ECO cells was done with 20 µg of pBABE.p38αD176A/F327S (courtesy of Dr. Ángel Nebreda's laboratory) or pBABE EMPTY VECTOR together with 2.5 µg of packaging virus DNA. The supernatants containing the retrovirus particles were collected 48 and 72 hours after removal of the calcium phosphate precipitate and were filtered with 0.45

µm filter. Virus has been concentrated by ultracentrifugation for 90 minutes 49,000 x *g* at 4 °C (Ultraclear Tubes, Beckman Coulter; Optima XPN-100 Ultracentrifuge Beckman, SW28 rotor).

Xenograft

For xenograft experiments 5 x 10^4 Hep53.4 cells were mixed 1:1 with Corning® Matrigel® Matrix (Corning) and subcutaneously injected in each flank of anesthetized mice. Tumor growth was monitored measuring length and width every 3-4 days with a digital caliber. At final point mice were sacrificed and tumors were extracted. Length, width and thickness were measured to established tumor volume.

In AMPKα activation by metformin experiment mice were treated with metformin dissolved in drinking water (300 mg/day/Kg) starting one week before xenograft injection and changing water every day. Mice body weight was measured every week.

Metabolomics

Metabolomics analysis was carried out by the Advanced Imaging Unit at CNIC. Serum samples from F^{WT} and F^{KO} mice 8 months after DEN-treatment were analyzed.

Metabolite extraction and derivatization.

Plasma samples were prepared for gas chromatography-mass spectrometry (GC−MS) analysis as previously described (Garcia and Barbas, 2011). Proteins were precipitated with acetonitrile and separated by centrifugation (15,400 x *g*). After deproteinization step supernatant was transferred to another glass vial and then evaporated to dryness in a Speedvac Concentrator (Thermo Fisher Scientific, Waltham, MA, USA). Derivatization was achieved in different stages: O-methoxyamine hydrochloride in pyridine and methoxymation was carried out overnight. *N*,*O*-Bis(trimethylsilyl)trifluoroacetamide (BSTFA) with 1% Trimethylsilyl chloride (TMCS) was then added, and after silylation, sample was dissolved in heptane with C18:0 methyl ester (IS).

Quality Control (QC)

For quality checking, electropherograms from serum samples and quality controls (QCs) were tested. QC samples were prepared by combining equal

volumes of serum from each sample. Five samples were independently prepared from this pool of samples, by following the same procedure as for the other samples. QC samples were analyzed throughout the run to provide a measure of the system's stability, performance and reproducibility of the sample-treatment procedure.

GC-MS analysis

GC−MS analyses were performed by a 7890A gas chromatography instrument (Agilent Technologies, Santa Clara, CA, USA) interfaced to inert macromolecular structure database (MSD) with Quadrupole (Agilent Technologies 5975). 2 µl of previously derivatized samples was injected in split mode using an Agilent Technologies 7693 autosampler onto a GC column DB5-MS (30 m length, 0.25 mm i.d., 0.25 µm film 95% dimethyl/5% diphenylpolysiloxane) with an integrated pre-column (10 m J&W) from Agilent Technologies. Carrier gas (He) flow rate was set at 1 ml/min and injector temperature at 250 °C. Split ratio was fixed from 1:5 to 1:10 with 3 to 10 ml/min He split flow into a Restek 20782 (Bellefonte, PA, USA) deactivated glass-wool split liner. Temperature gradient was programmed: initial oven temperature was set at 60 °C (held for 1 minute), then increased to 325 °C at 10 °C/min, and finally a cool-down period was applied for 10 minutes before the next injection. Total analysis time was 37.5 minutes. Detector transfer line, filament source, and quadrupole temperatures were set at 290 °C, 230 °C, and 150 °C, respectively. Serum samples from F^{WT} and F^{KO} mice 8 months after DEN-treatment were analyzed by means of a metabolic fingerprinting approach using liquid chromatography-mass spectrometry (LC−MS) platform. To remove phospholipids and proteins, 225 µl of serum and 10 µl of methionine sulfone, internal standard (IS), were vortex-mixed with 300 µl of methanol-ammonium foremate (1:1, v/v) and then passed through a Supelco HybridSPE Phospholipid Ultra cartridge (Supelco, Sigma Aldrich). The extracts were then dried at 35 ºC by use of a speedvac and dissolved in 100 µl of 0.1 mol/l of formic acid. After centrifugation (16,000 x g, 4 ºC, 20 minutes) supernatant was transferred directly to a vial (Chromacol, UK) ready for injection.

Samples were analyzed by an Ultra-high performance liquid chromatography (UHPLC) system (1290 Infinity series, Agilent Technologies, Waldbronn,

Germany) consisting of a degasser, two binary pumps, and thermostated autosampler connected to an Agilent Technologies QTOF (6550) mass spectrometry detector. Electrospray ionization (ESI) was used as an ion source. Samples (0.5 µl) were injected onto a reversed-phase column (Zorbax Extend C18, 2.1 × 5.0 mm, 1.8 µm, Agilent Technologies) thermostated at 60 °C. The system was operated in positive and negative mode at 0.6 ml/min flow rate with solvent A, water with 0.1% of formic acid, and solvent B, acetonitrile with 0.1% of formic acid. Gradient started from 5% of solvent B for the first minute, then to 80% in minute 7, then to 100% in minute 11.5, and returned to starting conditions in 0.5 minutes, keeping the re-equilibration until minute 15.

Data were collected in positive and negative ESI ion modes in separate runs. The detector operated in full scan mode from 50 to 1,000 m/z for positive mode and from 50 to 1,100 m/z for negative mode with a scan rate of 1 scan per second. Accurate mass measurements were obtained by means of an automated calibrant delivery system using ESI source with Jet Stream technology that continuously introduced a calibration solution, with reference masses at m/z 121.0509 (protonated purine) and m/z 922.0098 [protonated hexakis(1H,1H,3H- tetrafluoropropoxy)phosphazine or HP-921] in positive ion mode; and m/z 112.9856 (TFA anion) and m/z 1033.9881 [hexakis(1H,1H,3H-tetrafluoropropoxy)phosphazine or HP- 0921] in negative ion mode. The capillary voltage was set to 3,000 V for both positive and negative ionization modes, and the nebulizer gas flow rate was 12 l/min. Randomized samples were analyzed in two separate runs (first for positive and second for negative mode).

GC-MS and LC-MS data treatment and metabolite identification

Data were acquired using the Agilent MSD ChemStation Software. Total ion chromatograms (TICs) were inspected according to quality of chromatograms and internal standard signal. Peak detection and deconvolution were automatically performed with Automated Mass Spectrometry Deconvolution and Identification System (AMDIS, www.amdis.net). Then, deconvoluted compounds were identified according to retention time (RT), retention index (RI), and mass spectrum. RI calculation relies on conversion of RT into constants, which are independent of system variability.

RI for each compound was obtained by normalization of its RT by the RT and RI of the closest eluting n-alkane, presented in the mix of fatty acid methyl esters, which was injected before the samples. Based on mass spectrum and RI comparison with those from the Fiehn RTL library, the list of identified compounds was created. Additionally, mass spectra of possible compounds, which have not been found in the Fiehn RTL library, were searched through the NIST mass spectral library. According to this information, the in-house target library was created with RT and target m/z data. Multialignment was performed by MassProfiler Professional B.02.02 software (Agilent Technologies). Subsequently, filtering on frequency, sum of the derivatives, and normalization to IS were performed before statistical analysis.

Statistical analysis

An unsupervised multivariate analysis, Principal components analysis (PCA), was applied to check trends, outliers, and the quality of the analysis. Supervised multivariate analysis, such as orthogonal partial least squares discriminant analysis (OPLS-DA), was required to select metabolites that contributed most to separation and discrimination between groups. Statistically significant metabolites were selected based on the Jack-knife confidence interval (p<0.05) and variable importance into projection Variance Importance in Projection values (VIP). Compounds detected by LC-MS were first putatively identified using public available databases. The identity of compounds found in the databases was confirmed by LC−MS/MS analyses. For GC-MS, metabolites found to be statistically significant were identified based on comparison of their retention time, retention index and mass spectra with Fiehn RTL library, in-house target plasma library or NIST library.

Validation of the PLS-DA model

To avoid the risk of overfitting for a PLS-DA model used for selection of statistically significant metabolites according to Jack-knifed confidence intervals, the model was validated by use of a cross-validation tool, using one third out approach.

Histology

Adipose tissue was fixed with 10% formalin and embedded in paraffin. Sections were cut (4 µm) and stained with hematoxylin and eosin (American Master Tech Scientific) for histopathological examination.

Real Time qPCR

Total RNA was isolated from liver, tumor and adipose tissues using the RNeasy Mini Kit (Qiagen) with on-column DNase I-digestion. Complementary DNA was synthesized with the High-Capacity Complementary DNA Reverse Transcription Kit (Applied Biosystems). Sequences of primers used for quantitative real-time-polymerase chain reaction (qRT-PCR) are provided in Table I. Expression levels were normalized to *Gapdh* mRNA. qRT-PCR was performed using Fast SYBR Green system (Applied Biosystems) in a 7900HT Fast Real-time PCR thermal cycler (Applied Biosystems). A dissociation curve program was employed after each reaction to verify primers specificity.

Luminex

Serum cytokine concentrations were measured by multiplexed ELISA with a Luminex 200 analyzer (Millipore).

Biochemical analysis

Total proteins were extracted in lysis buffer (50 mM Tris-HCl pH 7.5, 1 mM EGTA, 1 mM EDTA pH 8.0, 50 mM NaF, 1 mM sodium glycerophosphate, 5 mM pyrophosphate, 0.27 M sucrose, 1% Triton X-100, 0.1 mM PMSF, 0.1% 2-mercaptoethanol, 1 mM sodium-ortovanadate, 1 µg/ml leupeptin, 1 µg/ml aprotinin). Extracts were separated by SDS–PAGE and transferred to 0.2 µm pore size nitrocellulose membranes (Bio Rad). Blots were probed with primary antibodies to JNK (#9252); phospho AMPKα (#2531); AMPKα (#26035); FLIP (#3210); phospho p38α (#9211) from Cell Signaling Technology; p38α (sc-535) from Santa Cruz Biotechnology, Inc.; Vinculin (V4505) from Sigma-Aldrich. All antibodies were used at 1:1000 dilution. After washes, membranes were incubated with an appropriate horseradish peroxidase-conjugated secondary antibody (GE Healthcare), and signal was detected using an enhanced chemiluminescent substrate for the detection of horseradish peroxidase (Clarity Western ECL substrate; Biorad). Protein levels were analyzed by optical density with ImageJ. For adiponectin detection, plasma samples were run in native

conditions. Samples were diluted in PBS (1:10) and with Native Tris-Glycine Sample Buffer 2X (Invitrogen). Diluted samples were loaded on pre-cast native gels to preserve adiponectin multimers (NativePAGE™ Bis-Tris gel system, Thermo Fisher Scientific) and run with Novex Tris-Glycine Native Running Buffer (Invitrogen). After transference membrane was blocked with milk prepared in PBS without detergents. Blot was probed with primary antibody to Adiponectin (PA1-054) from Thermo Fisher Scientific, 1:500 dilution. After washes, membranes were incubated with a fluorescent secondary antibody (Goat anti rabbit 680nm 926-32221, Odyssey). Signal was detected and analyzed by Odyssey LI-COR.

RNA-sequencing

RNA-sequencing was done in collaboration with Genomics Unit, CNIC.

Total RNA was isolated from adipose tissue using the RNeasy Mini Kit (Qiagen) with on-column DNase I-digestion. Samples were pooled two by two to obtain 1 µg of total RNA (500 ng from each pooled-sample). Total RNA was processed with TruSeq RNA Sample Preparation to create a cDNA library from each pool. Libraries were sequencing with Illumina Genome Analyzer IIx Sequencing System. Total RNA processing with TruSeq RNA Sample Preparation and sequencing were performed by Genomic Unit at CNIC.

Data obtained from RNA sequencing were analyzed using Ingenuity® Pathway Analysis (IPA).

Statistical analysis

Differences between groups were examined for statistical significance using 2-tailed Student's *t* test or ANOVA coupled to Bonferroni's post-test.

TABLE I – qRT-PCR primers

GENE	Forward Primer	Reverse Primer
Plin	ACAGCAGAATATGCCGCCAA	GGCTGACTCCTTGTCTGGTG
Nos2	GTTCTCAGCCCAACAATACAA	GTGGACGGGTCGATGTCAC
Tnfsf10	ATGGTGATTTGCATAGTGCTCC	GCAAGCAGGGTCTGTTCAAGA
Rasal2	ATGGAGCTGTCTCCGTCGT	GCCTTTTACATCGAACACCCG
Serpine1	TTCAGCCCTTGCTTGCCTC	ACACTTTTACTCCGAAGTCGGT
Lyz2	ATGGAATGGCTGGCTACTATGG	ACCAGTATCGGCTATTGATCTGA
Emr1	CCCCAGTGTCCTTACAGAGTG	GTGCCCAGAGTGGATGTCT
Il6	TAGTCCTTCCTACCCCAATTTCC	TTGGTCCTTAGCCACTCCTTC
Il1b	GCAACTGTTCCTGAATCAACT	ATCTTTTGGGGTCCGTCAACT
Tnfa	CCCTCACACTCAGATCATCTTCT	GCTACGACGTGGGCTACAG
Gapdh	TGAAGCAGGCATCTGAGGG	CGAAGGTGGAAGAGTGGGA

2. ROLE OF PPARα ACTIVATION IN LIVER CANCER

Animals

PPARα knock out mice (B6;129S4-Ppara^{tm1Gonz}/J, here called *Ppara*$^{-/-}$) and Albumin Cre-recombinase mice (B6.Cg-Tg(Alb-cre)^{21Mgn}/J, here called LWT) were purchased from Jackson Laboratory. Mice with compound JNK1/2 deficiency in hepatocytes (LDKO) have been described (Das et al., 2011, Das et al., 2009). Genotypes were identified by PCR analysis of genomic DNA isolated from mouse-tails. All experiments were performed in male mice. For tumor studies, *Ppara*$^{-/-}$ and WT mice on postnatal day 14 received a single i.p. injection of 50 mg/kg body weight diethylnitrosamine (DEN, Sigma-Aldrich) dissolved in saline. Six weeks after DEN treatment, mice were put on a high-fat diet (HFD, Research Diet Inc.) or standard chow diet *ad libitum* until sacrifice 8 months after DEN injection. One group of HFD-fed mice was used for Kaplan-Meier analysis. For acute response studies, 6-week-old *Ppara*$^{-/-}$ and WT mice were fed a HFD for 13 weeks, given a single 100 mg/kg body weight i.p. injection of DEN, and sacrificed after 48 hours. Radiation chimeras were generated by exposing 2-month-old DEN-injected recipient mice to 2 x 650 Gy ionizing radiation and reconstituting with $2x10^7$ cells from donor bone marrow by tail vein injection. Two weeks after bone marrow transplant, mice were fed a HFD *ad libitum* until sacrifice 8 months after DEN injection. Before sacrifice, body weight was measured and blood samples were taken for analysis of ALT/AST and cytokines. In all cases, mice were euthanized after overnight starvation. Mice were housed in a pathogen-free animal facility and kept on a 12-hour light/dark cycle at constant temperature and humidity.

For partial hepatectomy (PHx) experiments 6-week-old mice were HFD-fed during 6 weeks. Mice were anesthetized using a mixture of isoflurane and oxygen. Two-thirds of the liver was excised according to Mitchell and Willenbring (Mitchell and Willenbring, 2008), medial and left lateral lobes were removed. Mice were sacrificed 48 hours or 15 days after PHx and their liver was weighted to analyzed hepatic mass regeneration.

All animal experiments conformed to EU Directive 2010/63EU and Recommendation 2007/526/EC, enforced in Spanish law under Real Decreto

53/2013 and the Institutional Animal Care and Use Committee (IACUC) of the University of Massachusetts Medical School approved all studies using animals.

Serum analysis

Serum activities of ALT and AST were assessed with the ALT and AST Reagent Kit (Biosystems Reagents) using a Benchmark Plus Microplate Spectrophotometer (Biorad). Serum cytokine concentrations were measured by multiplexed ELISA with a Luminex 200 analyzer (Millipore).

Biochemical analysis

Total liver proteins were extracted in lysis buffer (50 mM Tris-HCl pH 7.5, 1 mM EGTA, 1 mM EDTA pH 8.0, 50 mM NaF, 1 mM sodium glycerophosphate, 5 mM pyrophosphate, 0.27 M sucrose, 1% Triton X-100, 0.1 mM PMSF, 0.1% 2-mercaptoethanol, 1 mM sodium-ortovanadate, 1 µg/ml leupeptin, 1 µg/ml aprotinin). Extracts were separated by SDS–PAGE and transferred to 0.2 µm pore size nitrocellulose membranes (Bio Rad). Blots were probed with primary antibodies to caspase-3 (#9662), cleaved caspase-3 (#9661), phospho ERK (#9101), ERK (#9102), phospho JNK (#9255), JNK (#9252), phospho STAT3 (#9145), phospho Akt T308 (#9275), phospho Akt S473 (#9271), Akt (#9272), all from Cell Signaling Technology; PCNA (ab1897, Abcam); p53 (sc-99, Santa Cruz Biotechnology); and Vinculin (V4505, Sigma). All antibodies were used at 1:1000 dilution except for anti-p53, which was diluted 1:500. After washes, membranes were incubated with an appropriate horseradish peroxidase-conjugated secondary antibody (GE Healthcare), and signal was detected using an enhanced chemiluminescent substrate for the detection of horseradish peroxidase (Clarity Western ECL substrate; Biorad).

Histochemistry

Liver and tumor tissues were fixed with 10% formalin and embedded in paraffin. Sections were cut (4 µm) and stained with hematoxylin and eosin (American Master Tech Scientific) for histopathological examination. Sections were also incubated with Bouin's fluid overnight, counter-stained with hematoxylin (Sigma), and then stained with Masson-Trichrome stain (American Master Tech Scientific). Cell proliferation was assessed by immunohistochemical staining for PCNA (ab1897, Abcam) according to the manufacturer's instructions.

Real time q-PCR

Total RNA was isolated from liver and tumor tissue using the RNeasy Mini Kit (Qiagen) with on-column DNase I-digestion. Complementary DNA was synthesized with the High-Capacity Complementary DNA Reverse Transcription Kit (Applied Biosystems). Sequences of primers used for quantitative real-time-polymerase chain reaction (qRT-PCR) are provided in Table II. Expression levels were normalized to *Gapdh* mRNA. qRT-PCR was performed using the Fast SYBR Green system (Applied Biosystems) in a 7900HT Fast Real-time PCR thermal cycler (Applied Biosystems). A dissociation curve program was employed after each reaction to verify purity of the PCR products.

Statistical analysis

Differences between groups were examined for statistical significance using 2-tailed Student's *t*-test or ANOVA coupled to Bonferroni's post-test. Kaplan-Meier analysis was performed using the log-rank test.

TABLE II – qRT-PCR primers

GENE	Forward Primer	Reverse Primer
Cdk2	CCTGCTCATTAATGCAGAGGG	GTGCTGGGTACACACTAGGTG
CcnA1	GCCTTCACCATTCATGTGGAT	TTGCTGCGGGTAAAGAGACAGAG
Foxm1	CTGATTCTCAAAAGACGGAGGC	TTGATAATCTTGATTCCGGCTGG
Cdc25c	ATGTCTACAGGACCTATCCCAC	ACCTAAAACTGGGTGCTGAAAC
Trp53	CTCTCCCCCGCAAAAGAAAAA	CGGAACATCTCGAAGCGTTTA
p21	CCTGGTGATGTCCGACCTG	CCATGAGCGCATCGCAATC
p57	CGAGGAGCAGGACGAGAATC	GAAGAAGTCGTTCGCATTGGC
p19	CTGAACCGCTTTGGCAAGAC	GCCCTCTCTTATCGCCAGAT
Lyz2	ATGGAATGGCTGGCTACTATGG	ACCAGTATCGGCTATTGATCTGA
Elane	AGCAGTCCATTGTGTGAACGG	CACAGCCTCCTCGGATGAAG
Emr1	CCCCAGTGTCCTTACAGAGTG	GTGCCCAGAGTGGATGTCT
Il6	TAGTCCTTCCTACCCCAATTTCC	TTGGTCCTTAGCCACTCCTTC
Il1b	GCAACTGTTCCTGAATCAACT	ATCTTTTGGGGTCCGTCAACT
Tnfa	CCCTCACACTCAGATCATCTTCT	GCTACGACGTGGGCTACAG
Il10	GCTCTTACTGACTGGCATGAG	CGCAGCTCTAGGAGCATGTG
Ccl2	TTAAAAACCTGGATCGGAACCAA	GCATTAGCTTCAGATTTACGGGT
Ccl3	TTCTCTGTACCATGACACTCTGC	CGTGGAATCTTCCGGCTGTAG
Gapdh	TGAAGCAGGCATCTGAGGG	CGAAGGTGGAAGAGTGGGA

RESULTS

1. ROLE OF JNK1 IN ADIPOSE TISSUE-LIVER CROSSTALK IN HCC DEVELOPMENT

Epidemiological studies have established a strong association between excess of body adiposity and increased cancer risk (Renehan et al., 2008). Obesity induces the activation of the stress-activated protein kinase JNK1 (Hirosumi et al., 2002). JNK1 activation in the adipose tissue of HFD-fed mice promotes liver insulin resistance and steatosis by increasing the circulating levels of the inflammatory cytokine IL-6 (Sabio et al., 2008). Inflammation is a well-known driver of cancer, and hepatocellular carcinoma (HCC) is a classical model of inflammation-linked malignancy (Maeda et al., 2005). Thus, we evaluated the role of adipose tissue JNK1 in the development of HCC. To pursue this goal we took advantage of a mouse model with specific *Jnk1* deficiency in the adipose tissue (Sabio et al., 2008). The experimental mouse model was generated by crossing mice in which JNK1 gene was flanked by *LoxP* sequence (*Jnk1*$^{f/f}$) with mice expressing *Cre* recombinase under the control of adipose tissue specific *Fabp4* promoter (*Fabp4-Cre*) (He et al., 2003). To increase the *LoxP* sequence recombination and achieve a better depletion of *Jnk1* gene, we crossed these mice with full knock out *Jnk1* mice (*Jnk1*$^{-/-}$) obtaining one depleted allele and the other with *LoxP* sequence (*Fabp4-Cre*$^{+}$*Jnk1*$^{f/-}$, F^{KO} mice). Littermates without conditional *Jnk1* allele (*Fabp4-Cre*$^{+}$ *Jnk1*$^{+/-}$) were used as control mice (F^{WT}). The specificity of *Cre*-mediated gene inactivation largely depends on the regulatory sequences used to control its expression. However, in some cases, unspecific recombination have been observed in tissues (Schmidt-Supprian and Rajewsky, 2007). Therefore, we systematically analyzed JNK1 expression at protein level in order to validate our genetic model. Lysates from several tissues of F^{KO}, F^{WT} and control of depletion *Jnk1*$^{-/-}$ mice were analyzed by western blot. JNK1 levels were decreased in adipose tissue from F^{KO} in comparison with F^{WT} indicating a partial depletion of JNK1 in F^{KO} mice in adipocytes (Figure R1A), while the expression of JNK1 in other tissues was maintained (Figure R1B). These results confirmed that the depletion of JNK1 is partial but tissue-specific. This residual expression of JNK1 in adipose tissue of F^{KO} mice could be due to the presence of other non-adipocyte cells.

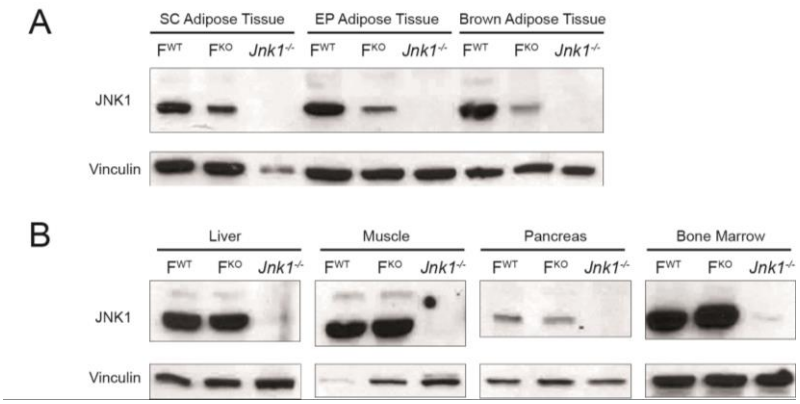

Figure R1. JNK1 expression analysis in organs from F^{WT} and F^{KO} mice.
JNK1 expression was assessed by western blot in several tissues from control (F^{WT}) and adipose tissue specific JNK1 deficient (F^{KO}) mice. *Jnk1*$^{-/-}$full body knock out organs were used as control of depletion. A) Immunoblot analysis of JNK1 in samples of subcutaneous (SC), epididymal (EP) and brown adipose tissue from F^{WT}, F^{KO} and *Jnk1*$^{-/-}$ mice. Vinculin protein expression was monitored as a loading control. B) Immunoblot analysis of JNK1 in samples of liver, muscle, pancreas and bone marrow from F^{WT}, F^{KO} and *Jnk1*$^{-/-}$ mice. Vinculin protein expression was monitored as a loading control.

1.1 JNK1 deficiency in adipose tissue does not protect against HCC in HFD

To evaluate whether depletion of JNK1 in the adipose tissue could affect the development of HCC, 14 days-old F^{KO} and F^{WT} control mice were injected with the carcinogenic compound diethylnitrosamine (DEN). DEN is a chemical compound able to induce tumors specifically in liver; in fact, it is metabolized by hepatocytes inducing cell death and compensatory proliferation, as well as mutations in hepatocytes (Bakiri and Wagner, 2013). Gene expression profiling of DEN-derived HCC showed strong similarities to that of human HCC (Lee et al., 2004). For this reason it has been extensively used as a model to study HCC development in rodents. Six weeks after DEN injection, mice were separated in two groups, one fed a normal chow diet (ND) and the other fed a high fat diet (HFD), in which 60% of calories were fat-derived. HFD feeding is a well-known procedure to induce obesity, diabetes and insulin resistance in mice (Park et al., 2010). Mice were sacrificed eight months after DEN injection and livers were examined for HCC development (Figure R2A). No changes in body weight were observed between HFD-F^{KO} and HFD-F^{WT} mice (Figure R2B). No differences between genotypes were appreciated in tumor generation between

HFD-fed F^{KO} and HFD-F^{WT} mice (Figure R2C). Moreover, no significant changes in tumor number or tumor size were detected (Figure R2D, E). These data demonstrate that under HFD condition, lack of JNK1 in adipose tissue does not affect liver cancer development. It has been shown that obesity induces IL-6 production in adipose tissue (Fried et al., 1998) and JNK1 depletion in this tissue reduces the expression of IL-6 in HFD (Sabio et al., 2008). However, our data suggest that IL-6 produced by adipose tissue during obesity is not relevant in chemical-induced HCC development.

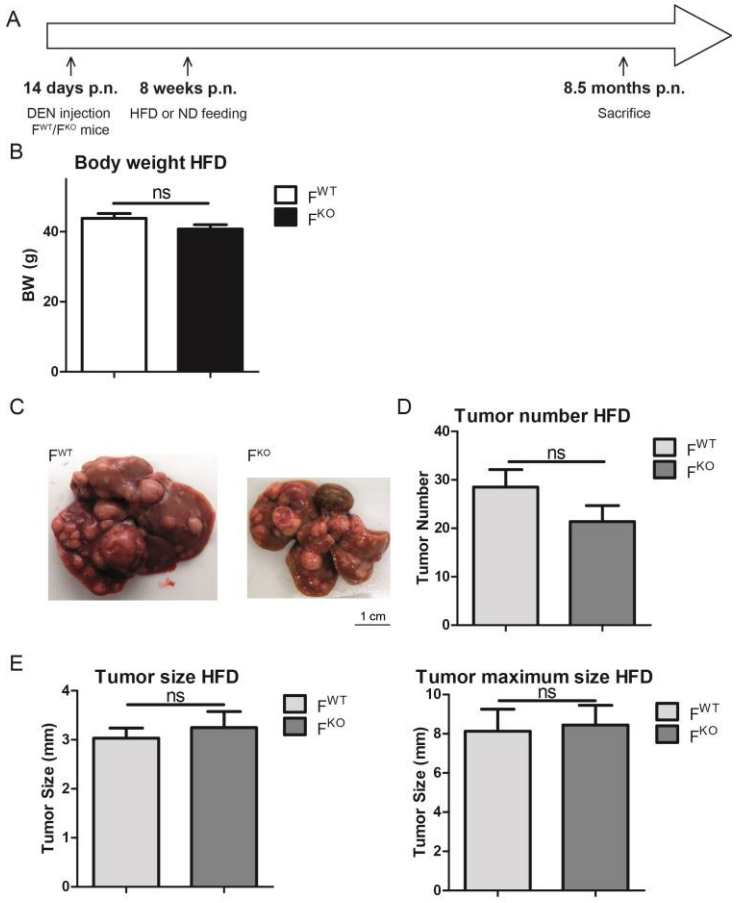

Figure R2. Effect of adipose tissue JNK1 deficiency on HCC in HFD-fed mice.
A) Control (F^{WT}) and adipose tissue JNK1 knock out (F^{KO}) mice were injected i.p. with diethylnitrosamine (DEN; 50 mg/kg) on postnatal day 14 and put on a high-fat diet (HFD) 6 weeks later. B) Body weight (BW) of HFD-fed F^{WT} and F^{KO} mice was measured 8 months after DEN injection. C) DEN-induced HCC in HFD-fed control mice (F^{WT}) and adipose tissue JNK1-deficient mice (F^{KO}) at 8.5 months of age. D, E) Quantification of tumor number (C) and size (D) in HFD-fed DEN-injected F^{WT} and F^{KO} mice. D) The maximum diameter of individual tumor nodules (right panel) and the mean width of tumor nodules (left panel) are presented. Data are shown as means ± SEM; Student's *t*-test; ns= No statistically significant difference; n=15-18

1.2 JNK1 deficiency in adipose tissue protects against HCC in normal diet

We next evaluated the effect of JNK1 deficiency in the adipose tissue in control condition, under chow diet (ND). As expected, the incidence and the size of tumors were reduced in ND-fed F^{WT} mice compared with HFD-fed animals (Figure R2C and R3A). These data correlate with previous report that demonstrated that obesity enhances tumor growth (Park et al., 2010). Interestingly, ND-fed F^{KO} mice were protected against HCC development compared with ND-fed F^{WT} control mice (Figure R3A). In fact, ND-fed F^{KO} presented a smaller number of tumors (Figure R3B) and developed smaller lesions than F^{WT} counterparts (Figure R3C). These results indicate that the absence of JNK1 in the adipose tissue induces protection against DEN-induced HCC development in normal diet condition, but not during HFD.

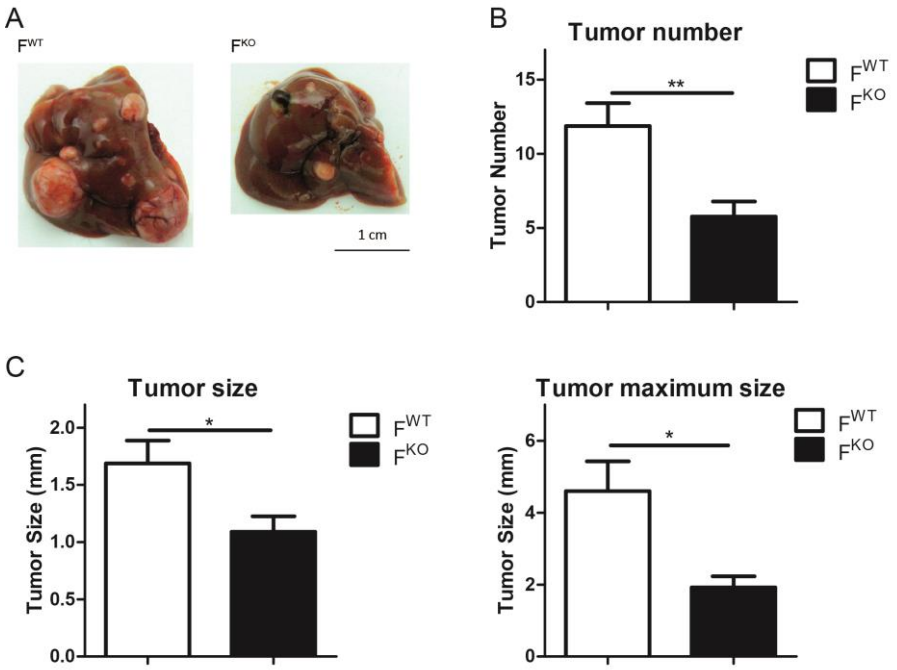

Figure R3. Effect of adipose tissue JNK1 deficiency on HCC in ND-fed mice.
Control (F^{WT}) and adipose tissue JNK1 knock out (F^{KO}) mice were injected i.p. with diethylnitrosamine (DEN; 50 mg/kg) on postnatal day 14 and fed with normal chow diet (ND). Mice were sacrificed 8 months after DEN injection. A) DEN-induced HCC in HFD-fed F^{WT} and F^{KO} at 8.5 months of age. B, C) Quantification of tumor number (B) and size (C) in ND-fed DEN-injected F^{WT} and F^{KO} mice. C) The maximum diameter of individual tumor nodules (right panel) and the mean width of tumor nodules (left panel) are presented. Data are shown as means ± SEM; * $p<0.05$, ** $p<0.005$; Student's *t*-test; n=15-18

1.3 Different metabolites profile in F^{WT} and F^{KO} blood

Cancer cells are proliferative cells that grow continuously. For this reason a cancer cell energy requirement is different from that of a non-tumor cell. In fact, transformed cells undergo to metabolic reprogramming in order to effectively support neoplastic proliferation (Warburg, 1956, Hanahan and Weinberg, 2011). Metabolic changes in tumor cells are reflected in circulating metabolites (Holmes et al., 2008, Odunsi et al., 2005, Asiago et al., 2010). Thus, to further characterize the differences between F^{KO} and F^{WT} mice after chronic-DEN treatment, we analyzed serum metabolomics from both genotypes by mass spectrometry (MS). Interestingly, serum from F^{WT} and F^{KO} showed dramatic differences in their metabolites profiles, indicating alternative tumor metabolism between the two genotypes (Figure R4).

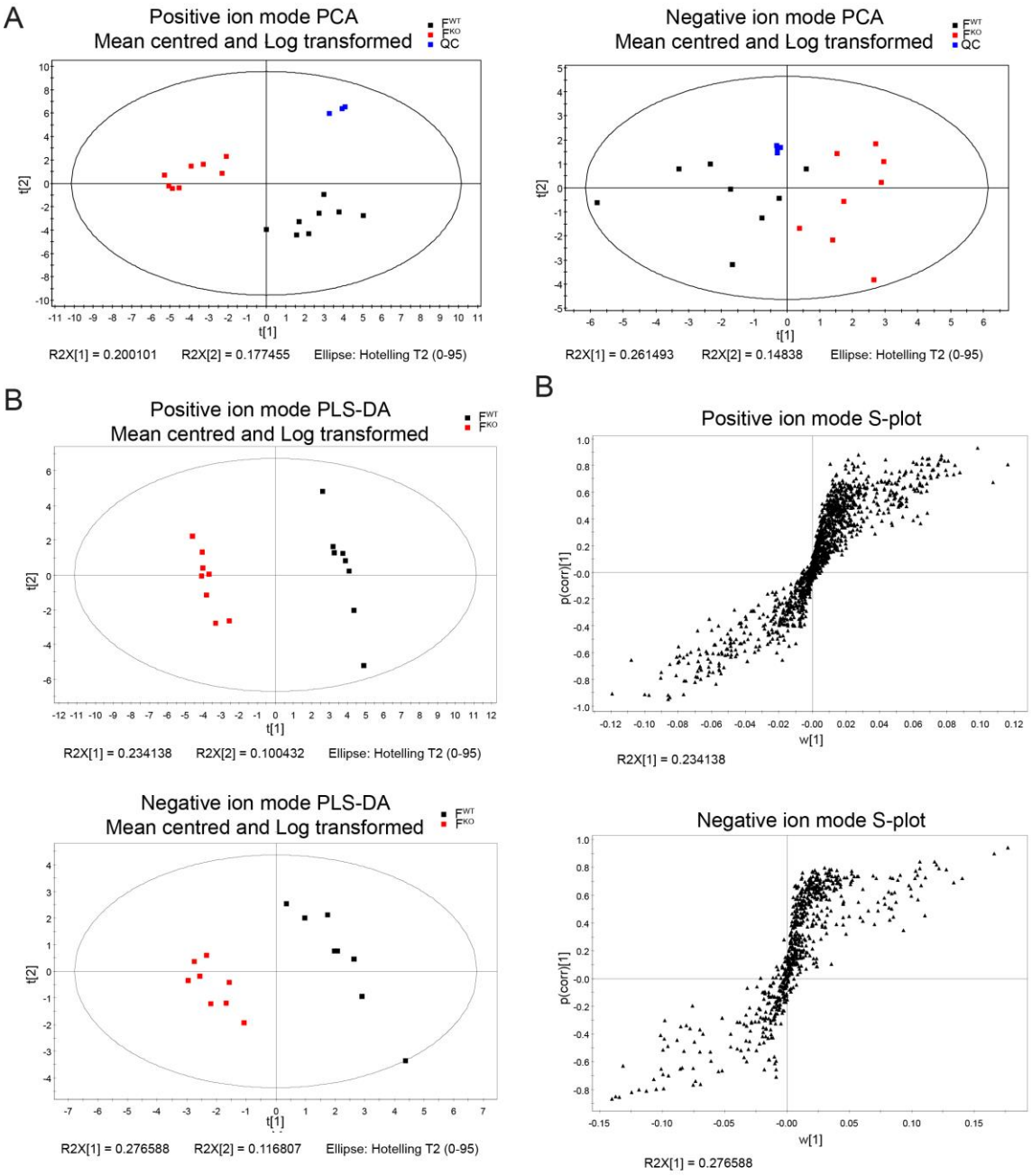

Figure R4. Metabolomics analysis of serum from DEN-treated F^{WT} and F^{KO} mice.
ND-fed control mice (F^{WT}) and adipose tissue JNK1-deficient mice (F^{KO}) were injected with diethylnitrosamine (DEN; 50 mg/kg) on postnatal day 14 and sacrificed 8 months later. Serum metabolites from these mice were analyzed by mass spectrometry. A) Score plot for principal components analysis (PCA) model built with the whole data set and with prediction for quality controls (QCs) for the metabolites found with positive (right panel) and negative (left panel) ionization modes of serum samples from ND-fed F^{WT} (in black) and F^{KO} (in red) mice. B) Orthogonal partial least squares-discriminant analysis (OPLS-DA) score plot with positive (upper panels) and negative (bottom panels) ionization modes of serum samples from ND-fed F^{WT} (in black) and F^{KO} (in red) mice. VIP of OPLS-DA panels are shown in the right part of the figure. n=8.

1.4 JNK1 deficiency in adipose tissue protects against xenograft tumor development

In order to further assay the role of adipose tissue in cancer development we performed a xenograft experiment in ND-fed F^{KO} and ND-fed F^{WT} mice. For this purpose we used a murine hepatocellular cell line (Hep53.4), derived from DEN-induced HCC in C57BL/6J mice (Kress et al., 1992). We subcutaneously injected 5 x 10^4 Hep53.4 cells in each flank of F^{WT} and F^{KO} mice. Tumor growth was monitored over time and at sacrifice. Time-course measurement of tumor growth showed that tumor implanted in F^{KO} mice grew with a slower kinetic than the ones implanted in F^{WT} mice (Figure 5A). This was also corroborated at final point, 5 weeks after cells injection (Figure R5B). These results are consistent with the role of JNK1 in adipose tissue observed previously, and suggest that JNK1 in adipose tissue controls the production or secretion of circulating molecules that could protect against tumor development.

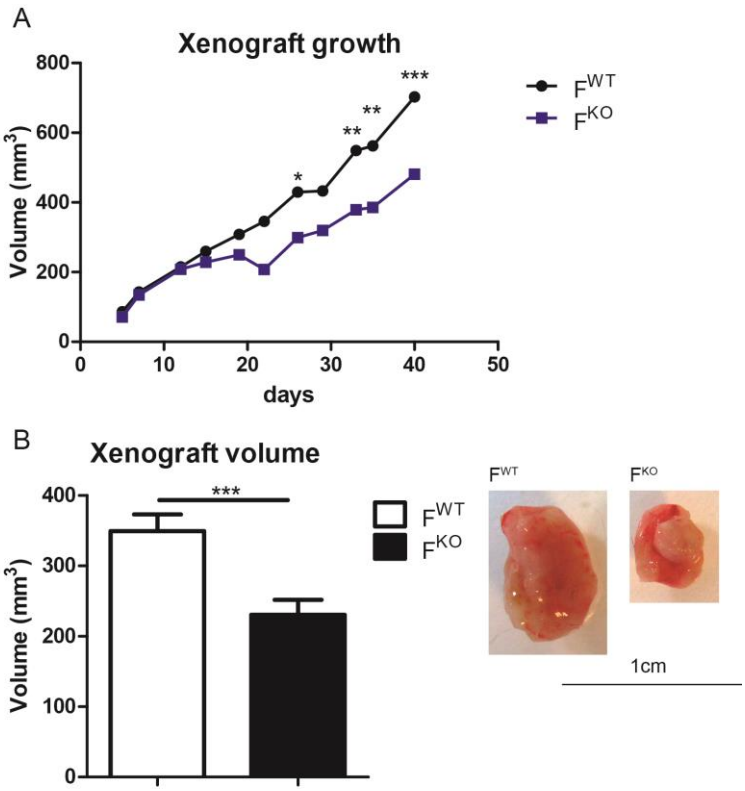

Figure R5. Hep53.4 cells xenograft in ND-fed F^{WT} and F^{KO} mice.
ND-fed control (F^{WT}) and adipose tissue JNK1 deficient (F^{KO}) mice were subcutaneously injected with 5 x 10^4 Hep53.4 cells in each flank and sacrificed 5 weeks later. A) Tumor volume was measured every 3-4 days and tumor volume is represented. B) Mean of tumor volumes at sacrifice is represented. Data are shown as means ± SEM; *** $p<0.001$; Student's *t*-test; n=18 tumors (9 mice for each genotype).

1.5 *Jnk1* deletion in adipose tissue does not influence liver regeneration

To understand the mechanism by which deficiency of JNK1 in adipose tissue protects against liver cancer development, we tested its role in hepatocyte proliferation. Two-thirds partial hepatectomy (PHx) is an established model to assess liver proliferation capability. After partial hepatectomy, the liver is able to restore the loss mass through a complex and well-orchestrated response. In fact, PHx triggers a sequence of organized events leading to cell proliferation and liver regeneration, beginning with the entrance of differentiated hepatocytes in cell cycle (Michalopoulos, 2007). To verify if loss of JNK1 in the adipose tissue influences hepatic regeneration, control F^{WT} and F^{KO} mice were examined 48 hours or 15 days after PHx. Measurement of liver mass did not show any difference between F^{WT} and F^{KO} mice in liver regeneration; in fact, F^{KO} mice have the same ability as F^{WT} mice to restore liver size 48 hours (Figure R6A) as well as 15 days after PHx (Figure R6B). These data indicated that adipose tissue JNK1 depletion does not influence liver proliferation after partial hepatectomy.

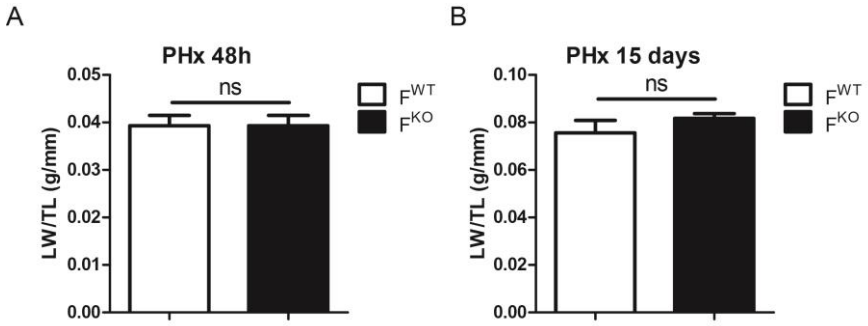

Figure R6. Liver regeneration after partial hepatectomy in ND-fed F^{WT} and F^{KO} mice.
10-12-week-old ND-fed control (F^{WT}) and adipose tissue JNK1 knock out (F^{KO}) mice underwent to partial hepatectomy (PHx). Liver mass was analyzed 48 hours (A) and 15 days (B) after PHx. Ratio between liver weight (LW) and tibia length (TL) is represented. Data are shown as means ± SEM; ns= No statistically significant difference; Student's *t*-test; n=6.

1.6 Adipose tissue lacking JNK1 is functional and presents normal infiltration levels

Adipose tissue is the main organ for fat storage and it has a high capacity to expand in a non-transformed state. To further characterize the mouse model we

measured body weight in ND-fed mice. No significant differences in body weight were observed between ND-fed F^{KO} and F^{WT} mice (Figure R7A). The same fat deposition correlates with similar adipocyte size analyzed by microscopy in white adipose tissue samples stained with hematoxylin and eosin (H&E) (Figure R7B). Hence, protection from HCC was not due to differences in fat accumulation. We hypothesized that lack of JNK1 in the adipose tissue may affect adipokines production or fat functionality. *Plin* is the gene coding for perilipin, which is an important regulator of lipid storage. It coats and protects lipid droplets from lipases (Tansey et al., 2001); decrease in perilipin expression in adipose tissue would indicate increased lipolysis (Tansey et al., 2001). Thus, we checked *Plin* mRNA levels to test white adipose tissue (WAT) functionality. F^{KO} mice showed normal levels of *Plin* transcript (Figure R7C), indicating a normal phenotype of WAT and no changes in lipolysis compared with control mice.

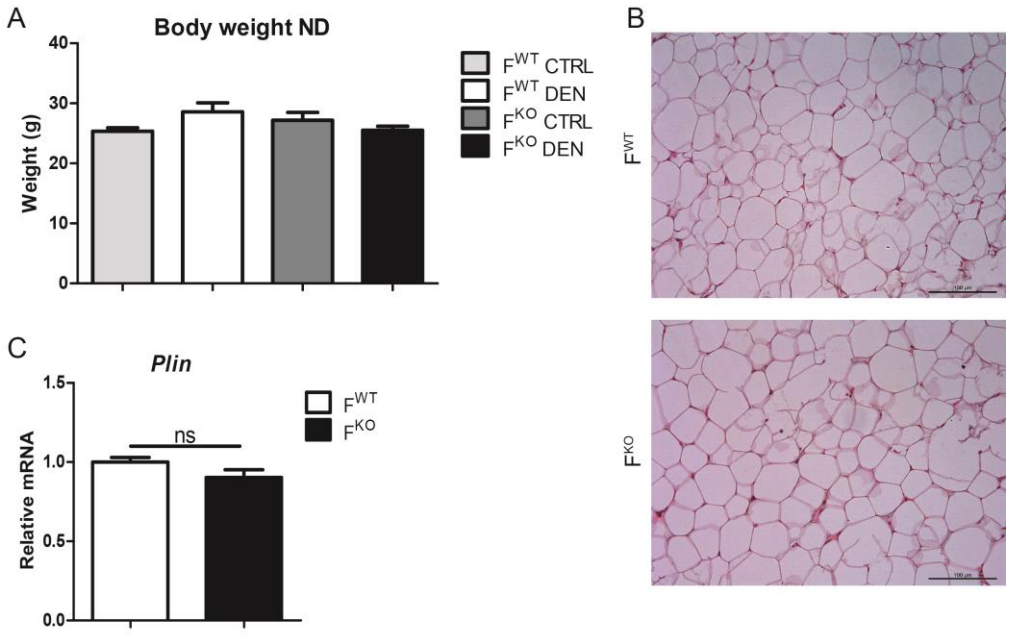

Figure R7. Body weight and white adipose tissue analysis of ND-fed F^{WT} and F^{KO} mice. ND-fed control (F^{WT}) and adipose tissue JNK1 knock out (F^{KO}) mice were i.p. injected with diethylnitrosamine (DEN; 50 mg/kg) at postnatal day 14 and sacrificed 8 months later. A) Body weight of ND-fed F^{WT} and F^{KO} mice chronically treated (DEN) or not treated (CTRL) with DEN. B) Representative white adipose tissue sections stained with hematoxylin and eosin from ND-fed F^{WT} and F^{KO} mice 8 months after DEN injection. Scale bar=100µm C) qRT-PCR analysis of perilipin expression in white adipose tissue from ND-fed F^{WT} and F^{KO} mice 8 months after DEN injection. mRNA expression was normalized to *Gapdh.* Data are shown as means ±SEM; ns= No statistically significant difference. Student's *t*-test; n=8.

Inflammation has been shown to be an important risk factor for different types of cancer (Balkwill and Mantovani, 2001). Macrophage infiltration in adipose tissue produces a low-grade inflammatory environment that could favor tumor growth (Mayi et al., 2012, Wagner et al., 2012). Hence, we checked WAT infiltration in ND-fed F^{KO} and F^{WT} mice. No differences in mRNA levels of three distinct macrophage markers, *Lyz2*, *Emr1* and *Nos2*, were appreciated, indicating normal macrophage infiltration levels in ND-fed F^{KO} WAT (Figure R8A). Adipocytes and infiltrated macrophages induce inflammation secreting pro-inflammatory cytokines, such as IL-6, IL-1β and TNFα, molecules that have been shown to promote liver tumor (Maeda et al., 2005). Moreover, JNK1 is a key regulator of the expression of several cytokines (Das et al., 2009). To analyze whether lack of JNK1 could affect adipose tissue production of cytokines we measure by qRT-PCR the expression levels of *Il1b*, *Tnfa* and *Il6*. F^{KO} mice showed decreased expression of *Il1b* and *Tnfa* mRNA compared with F^{WT} counterparts (Figure R8B). However, this reduction in gene expression was not reflected in blood circulating levels of these cytokines (Figure R8C), suggesting that these transcriptional changes could not be responsible of the protection observed in F^{KO} mice.

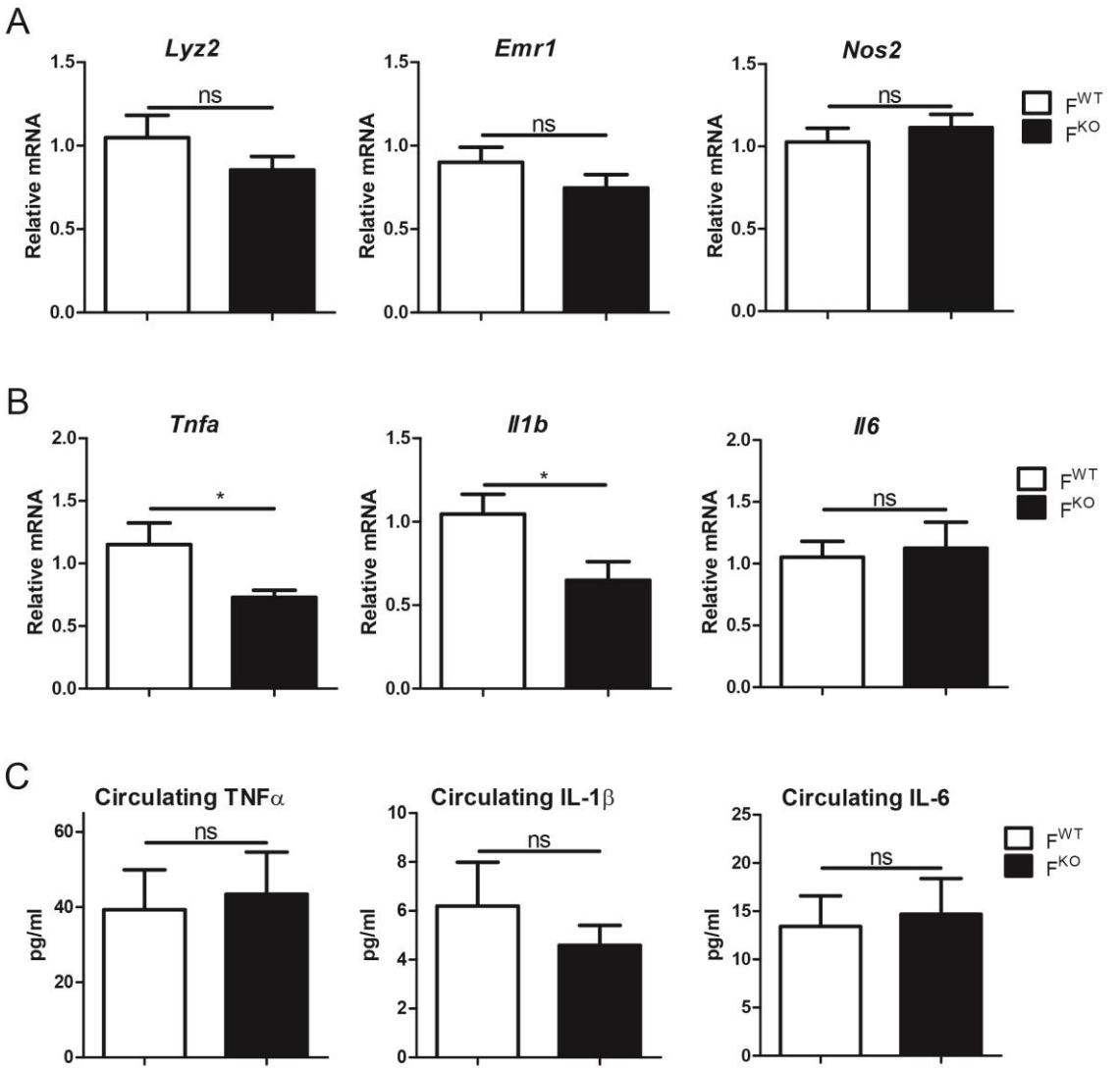

Figure R8. Macrophage infiltration in white adipose tissue and circulating cytokines analysis in ND-fed F^{WT} and F^{KO} mice.

ND-fed control (F^{WT}) and adipose tissue JNK1 knock out (F^{KO}) mice were i.p. injected with diethylnitrosamine (DEN; 50 mg/kg) at postnatal day 14 and sacrificed 8 months later. A) White adipose tissue qRT-PCR analysis of macrophage infiltration markers expression, *Lyz2*, *Emr1* and *Nos2*. B) White adipose tissue qRT-PCR analysis of cytokines expression, *Tnfa*, *Il1b* and *Il6*. mRNA expression was normalized to *Gapdh*. Data are shown as means ±SEM; * $p<0.05$, ns= No statistically significant difference; Student's t-test; n=8. C) Luminex analysis of circulating TNFα, IL-1β and IL-6. Data are shown as means ±SEM; * $p<0.05$, ns= No statistically significant difference; Student's t-test; n=17-20.

1.7 Increased circulating adiponectin in F^{KO} mice

The adipose tissue is an important secreting organ; it produces and releases a variety of circulating molecules known as adipokines to the blood stream (Gavrilova et al., 2000). Among them, adiponectin is one of the most important

adipose tissue-secreted molecules (Maeda et al., 1996). JNK1 full-body knock out animals present higher circulating levels of adiponectin (Hirosumi et al., 2002). Furthermore, circulating adiponectin is reduced in obesity (Arita et al., 1999), a well-known risk factor for HCC development (Calle et al., 2003). Thus, we analyzed whether lack of JNK1 in adipose tissue results in increased adiponectin levels. Measurement of adiponectin levels in serum indicated that 8 months DEN-injected F^{KO} mice had higher circulating levels of this adipokine than F^{WT} counterparts (Figure R9A). In particular, low molecular weight (LMW) adiponectin was increased in blood from F^{KO} mice in comparison to F^{WT} serum (Figure R9B), pointing out the possible role of adiponectin in the observed phenotype.

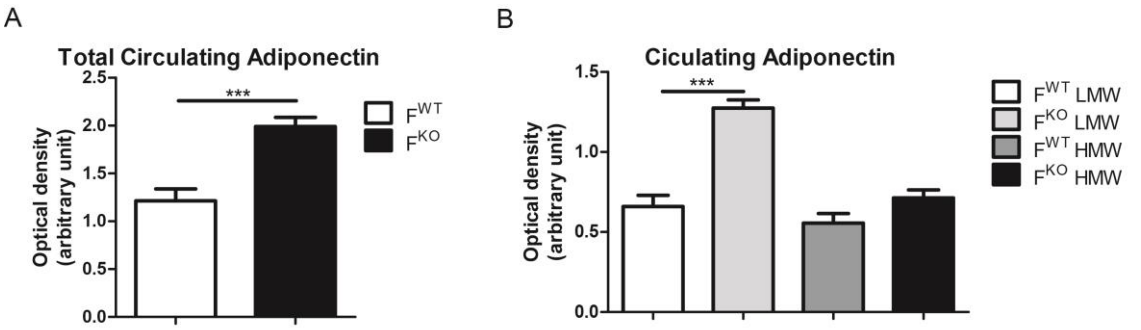

Figure R9. Circulating adiponectin levels in ND-fed F^{WT} and F^{KO} mice.
ND-fed control (F^{WT}) and adipose tissue JNK1 knock out (F^{KO}) mice were i.p. injected with diethylnitrosamine (DEN; 50 mg/kg) at postnatal day 14 and sacrificed 8 months later. Serum from F^{WT} and F^{KO} mice were analyzed for adiponectin levels. A) Immunoblot quantification of total circulating adiponectin in ND-fed F^{WT} and F^{KO} mice. Data are shown as means ±SEM; *** $p<0.001$; Student's *t*-test; n=9-12. B) Immunoblot quantification of low molecular weight (LMW) and high molecular weight (HMW) adiponectin in ND-fed F^{WT} and F^{KO} mice. Data are shown as means ±SEM; *** $p<0.001$; One-way ANOVA coupled to Bonferroni's post-test; n=9-11.

1.8 Adiponectin depletion reverts the phenotype of F^{KO} mice.

To evaluate whether higher adiponectin levels were sufficient to protect F^{KO} mice from HCC development, we abolished adiponectin production in F^{KO} and F^{WT} mice genetically, by crossing them with adiponectin full-body knock out mice (*Adipoq*$^{-/-}$). We analyzed tumor growth in xenograft experiments in adult F^{KO}*Adipoq*$^{-/-}$ (*Fabp4-Cre*$^{+}$*Jnk1*$^{f7-}$*Adipoq*$^{-/-}$) and control F^{WT}*Adipoq*$^{-/-}$ (*Fabp4-Cre*$^{+}$*Jnk1*$^{+/-}$*Adipoq*$^{-/-}$) mice. Tumor growth was monitored over time and at

sacrifice. Measurement of tumor size showed a comparable xenograft pace of growth in $F^{WT}Adipoq^{-/-}$ and $F^{KO}Adipoq^{-/-}$. This was corroborated 5 weeks after Hep53.4 cells injection, when we observed indistinguishable tumor sizes in $F^{KO}Adipoq^{-/-}$ and $F^{WT}Adipoq^{-/-}$ (Figure R10). In conclusion, ablation of adiponectin was sufficient to revert the protection observed in F^{KO} mice. This result suggests that adiponectin is a key player in the protection observed in F^{KO} mice.

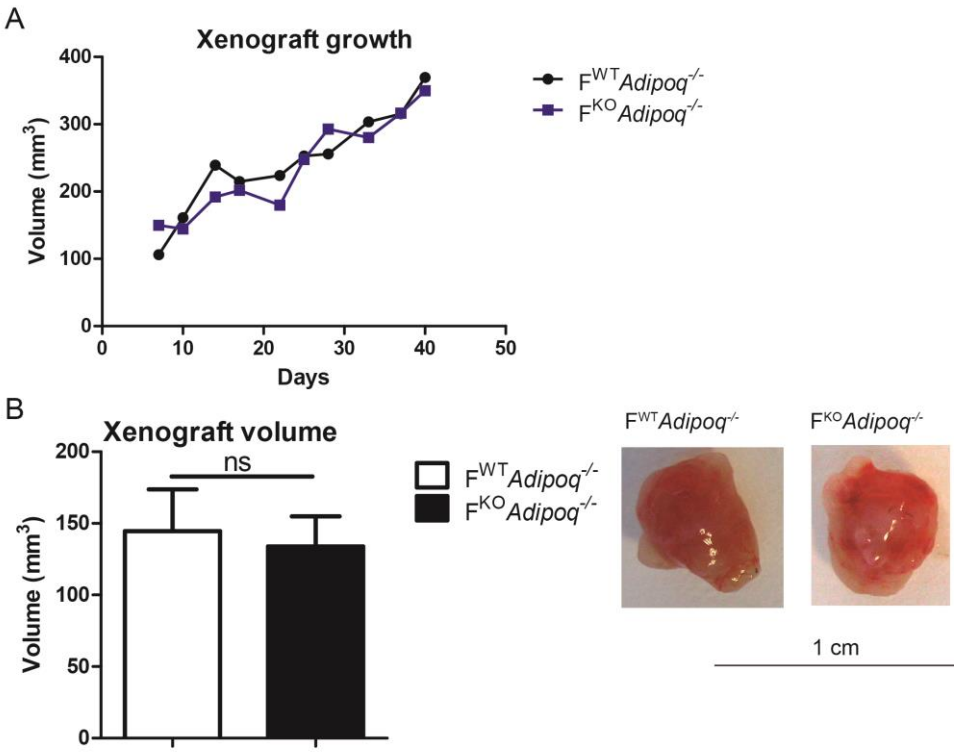

Figure R10. Hep53.4 cells xenograft in $F^{WT}Adipoq^{-/-}$ and $F^{KO}Adipoq^{-/-}$ mice.
Adiponectin knock out mice were crossed with adipose tissue JNK1 deficient mice and control mice to obtain $F^{WT}Adipoq^{-/-}$ and $F^{KO}Adipoq^{-/-}$ mice. $F^{WT}Adipoq^{-/-}$ and $F^{KO}Adipoq^{-/-}$ mice were subcutaneously injected with 5 x 10^4 Hep53.4 cells in each flank and sacrifice 5 weeks later. A) Tumors were measured every 3-4 days and tumor volume is represented. B) Means of tumor volume at sacrifice are represented. Pictures from representative tumor are presented. Data are shown as means ± SEM; ns= No statistically significant difference; Student's t-test; n=18-20 tumors (9-10 mice for each genotype).

To further verify that high adiponectin levels in F^{KO} animals were necessary to protect F^{KO} mice against chemical-induced HCC, 14 days old $F^{KO}Adipoq^{-/-}$ mice and $F^{WT}Adipoq^{-/-}$ littermates were DEN-treated and sacrificed 8 months after injection. Tumor analysis revealed that adiponectin deficiency induced a

complete rescue of F^{KO} phenotype. Indeed, F^{KO}*Adipoq*$^{-/-}$ mice showed similar susceptibility to DEN-induced HCC development to F^{WT}*Adipoq*$^{-/-}$ mice (Figure R11A). Number and size of tumors lesions was not statistically different between genotypes (Figures R11B and R11C). These results strongly indicate that adiponectin is the circulating molecule responsible of the protection against HCC development observed in F^{KO}.

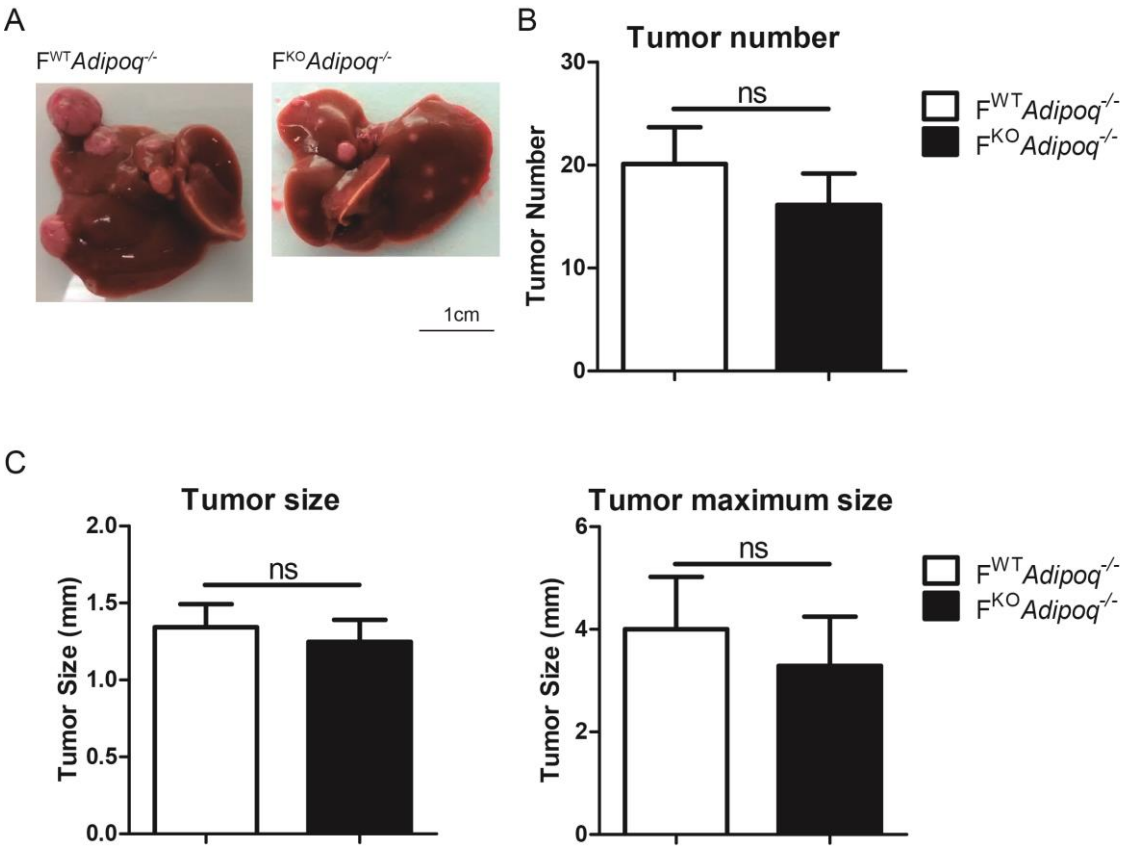

Figure R11. HCC development in F^{WT}*Adipoq*$^{-/-}$ and F^{KO}*Adipoq*$^{-/-}$.
Adiponectin knock out mice were crossed with adipose tissue JNK1 deficient mice and control mice to obtain F^{WT}*Adipoq*$^{-/-}$ and F^{KO}*Adipoq*$^{-/-}$ mice. F^{WT}*Adipoq*$^{-/-}$ and F^{KO}*Adipoq*$^{-/-}$ mice were injected i.p. with diethylnitrosamine (DEN; 50 mg/kg) on postnatal day 14 and sacrificed 8 months later. A) DEN-induced HCC in and mice at 8.5 months of age. B, C) Quantification of tumor number (B) and size (C). C) The maximum diameter of individual tumor nodules (right panel) and the mean width of tumor nodules (left panel) are presented. Data are shown as means ± SEM; ns= No statistically significant difference; Student's *t*-test; n=10-15

1.9 Adiponectin signaling is induced in livers from F^{KO} mice

Adiponectin receptor 1 and 2 (AdipoR1, AdipoR2) transduce adiponectin signaling into a cellular response (Yamauchi et al., 2007). In fact, once

adiponectin binds to AdipoR1 and AdipoR2, they induce 5' AMP-activated protein kinase α (AMPKα) phosphorylation and activation (Yamauchi et al., 2002). In order to study the molecular mechanism by which adiponectin controls tumor progression, 14-days-old F^{WT} and F^{KO} mice were injected with DEN and sacrificed 15 days later. As 8 months DEN-treated mice (Figure R7A), no differences between genotypes were observed in body weight 15 days DEN post-injection (Figure R12A).

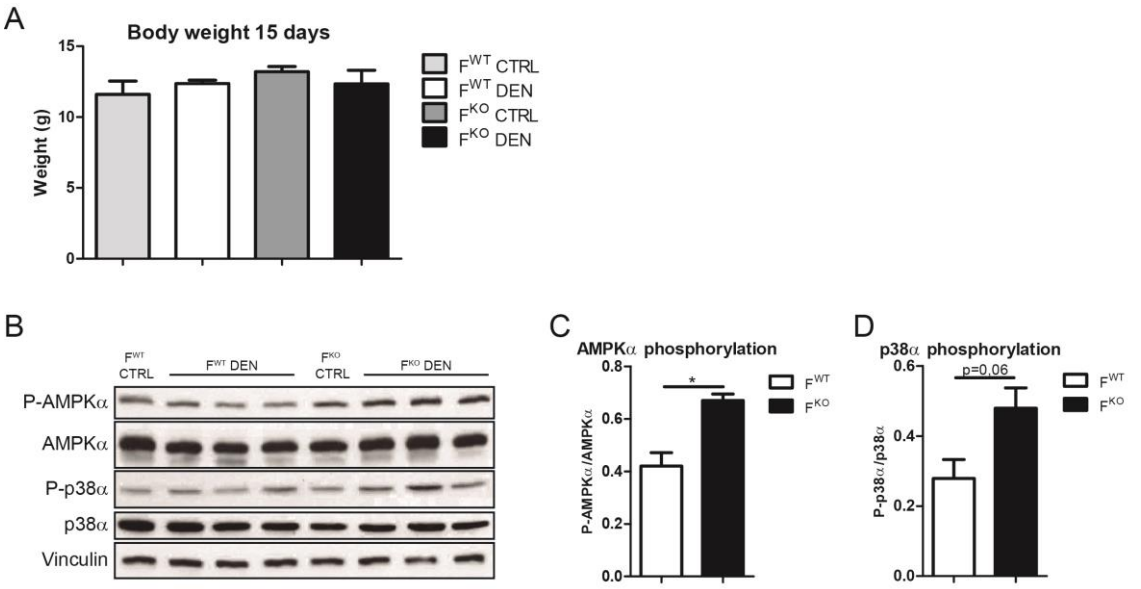

Figure R12. Adiponectin signaling in liver from F^{WT} and F^{KO} after DEN treatment

ND-fed control and adipose tissue JNK1 knock out mice were i.p. injected with diethylnitrosamine (DEN; 50 mg/kg) at postnatal day 14 and sacrificed 15 days later. A) Body weight analysis of DEN treated (DEN) or not treated (CTRL) F^{WT} and F^{KO} mice. B) Immunoblot analysis of adiponectin signaling pathway in liver samples from ND-fed F^{WT} and F^{KO} mice. Membranes were probed against P-AMPKα, AMPKα, P-p38α and p38α. Vinculin protein expression was monitored as loading control. C, D) Quantification of p38α (C) and AMPKα (D) phosphorylation in DEN treated animals. Data are shown as means ±SEM; * $p<0.05$. Student's *t*-test; n=3.

To check adiponectin-signaling activation in hepatocytes, we homogenized whole liver samples from F^{WT} and F^{KO} mice and tested them for AMPKα phosphorylation. We observed a stronger phosphorylation of AMPKα in livers from F^{KO} mice compared with F^{WT} counterparts (Figure R12B, C). It has been shown that activation of AMPKα is able to promote p38α phosphorylation (Mao et al., 2006, Li et al., 2005), and p38α activation is known to suppress cancer

cells proliferation (Hui et al., 2007, Iyoda et al., 2003). Thus, we analyze p38α activation in liver lysates. An increase in the level of phosphorylated p38α was observed in livers from F^{KO} mice compared with F^{WT} mice (Figure R12B, D). Together, these data indicate that adiponectin signaling is indeed enhanced in F^{KO} livers.

1.10 AMPKα activation inhibits tumor growth

To assess the role of AMPKα activation in F^{KO} mice phenotype, C57BL/6J wild type mice were treated with an AMPK activator, metformin (Hawley et al., 2002), in drinking water (300 mg/day/kg of body weight) starting one week before the subcutaneous injection of 5 x 10^4 cells of Hep53.4 cell line. Treatment with metformin was maintained during all the experiment. Measurement of tumors volume at sacrifice showed that metformin treatment reduced tumor growth compared with control drinking water (Figure R13). This result indicates that AMPKα activation is sufficient to decrease tumor growth and that protects against tumor development.

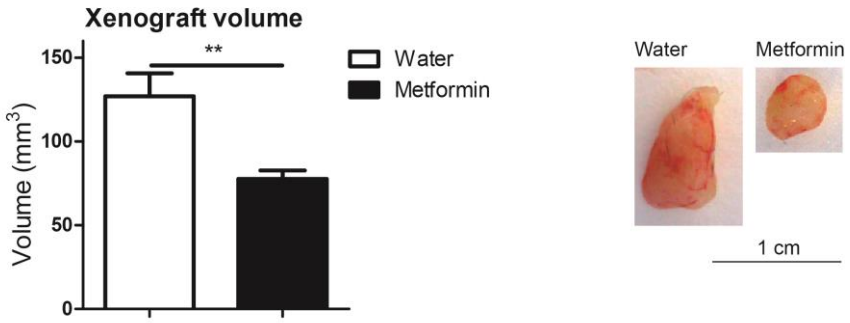

Figure R13. Hep53.4 cells xenograft in water or metformin treated C57BL/6J mice.
C57BL/6J mice were treated with metformin in drinking water (300 mg/day per kilogram of body weight) and subcutaneously injected with 5 x 10^4 Hep53.4 cells in each flank. Mice were sacrificed 3 weeks after inoculation and xenograft volume was calculated for each tumor. Control mice were given normal water. Mean of tumor volumes at sacrifice are represented. Data are shown as means ± SEM; ** $p<0.01$; Student's *t*-test; n=20 tumors (10 mice for each genotype).

1.11 Constitutive active p38α blocks tumor growth

To evaluate the role of p38α activation in HCC development, and whether the activation of p38α by adiponectin could be responsible of the F^{KO} phenotype,

C57BL/6J wild type mice were subcutaneously injected with 5 x 10^4 cells of Hep53.4 cell line. Nine days later, retroviruses expressing a constitutive active form of p38α or a control virus were injected directly in the tumor. A second virus dose was delivered 14 days after. Measurement of tumors volume at sacrifice showed that virus expressing the active p38α significantly reduced tumor growth compared with control virus (Figure R14). This result indicates that p38α activation is sufficient to decrease tumor growth and protects against tumor development.

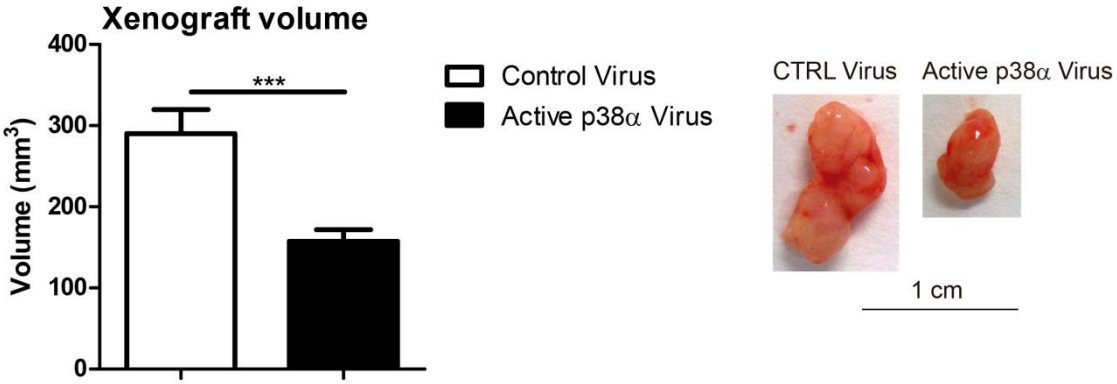

Figure R14. Hep53.4 cells xenograft treated with retrovirus expressing p38α constitutively active form.
C57BL/6J mice were treated subcutaneously injected with 5 x 10^4 Hep53.4 cells in each flank. Tumors were treated with a retrovirus expressing constitutively active p38α or an empty vector, as a control, 9 and 22 days after inoculation. Mice were sacrificed 1 week after the second virus treatment and xenograft volume was calculated for each tumor. Mean of tumor volumes at sacrifice are represented. Data are shown as means ± SEM; *** $p<0.001$; Student's *t*-test; n=20 tumors (10 mice for each genotype).

1.12 RNA-sequencing reveals TRAIL as another possible mediator of tumor protection

JNK1 phosphorylates a wide variety of protein targets, including numerous transcription factors, to mediate the appropriate cell response to the external *stimulus* (Davis, 2000, Chang and Karin, 2001). Thus, we asked whether other molecules regulated by JNK1 in adipose tissue could also being affecting tumor development. Changes in the gene expression pattern in adipose tissue from F^{KO} and F^{WT} chronically-treated with DEN (8 months after carcinogen injection) were assessed by RNA-sequencing. Surprisingly, despite the RNA-sequencing

was performed in adipose tissue, gene ontology analyses indicated that genes related with liver diseases and malignancies were downregulated in F^{KO} adipose tissue in comparison with F^{WT} (Figure R15).

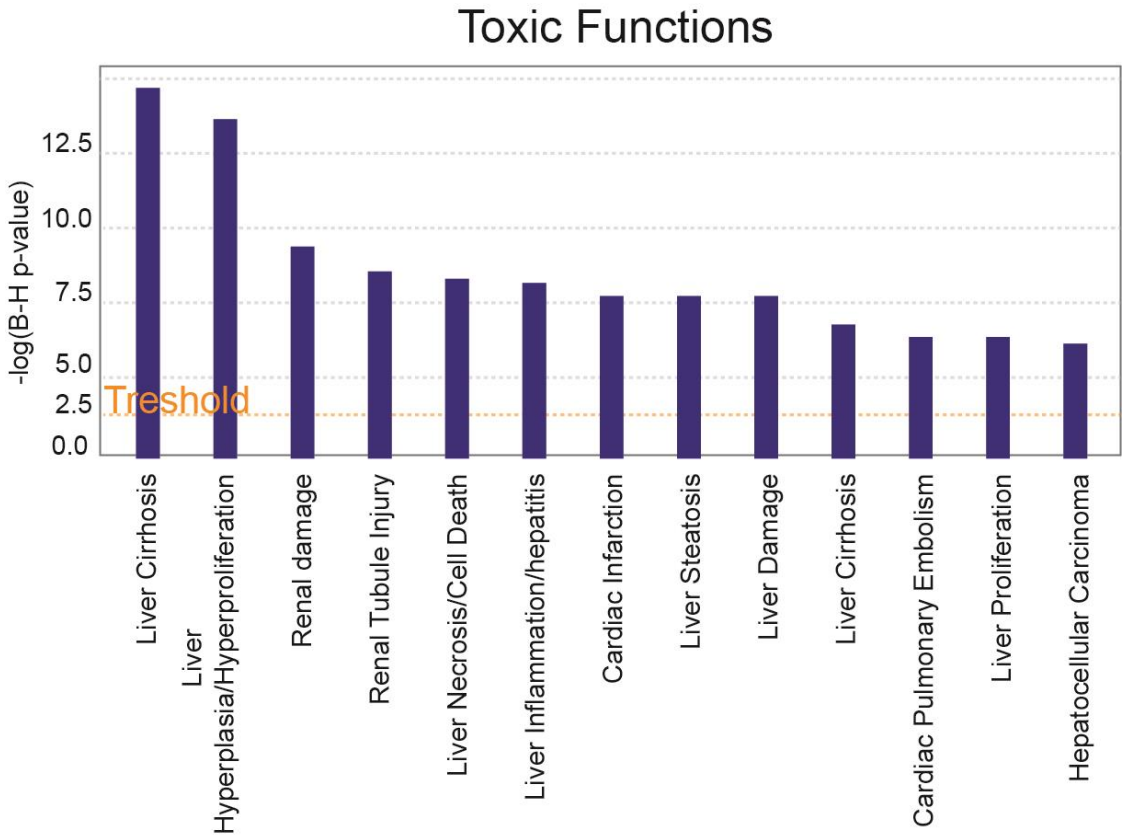

Figure R15. Adipose tissue RNA-sequencing from ND-fed F^{WT} and F^{KO} mice.
Gene expression of adipose tissue from ND-fed control (F^{WT}) and adipose tissue JNK1 deficient (F^{KO}) mice 8 months after diethylnitrosamine treatment (50 mg/kg) was assessed by RNA-sequencing and results analyzed by Ingenuity® Pathway Analysis. Graphical representation of signaling pathways by their participation in diseases.

Among the overexpressed genes we focused in those coding for secreted proteins with a potential anti-tumor effect. We found three genes that were slightly overexpressed in F^{KO} adipose tissue compared with controls and that encode for bloodstream secreted proteins: *Rasal2*, *SerpinE1* and *Tnfsf10*. These results were validated by qRT-PCR. We observed a significant increase of *Tnfsf10* and *Serpine1* expression in F^{KO} adipose tissue by qRT-PCR, while no differences were found in *Rasal2* expression (Figure R16).

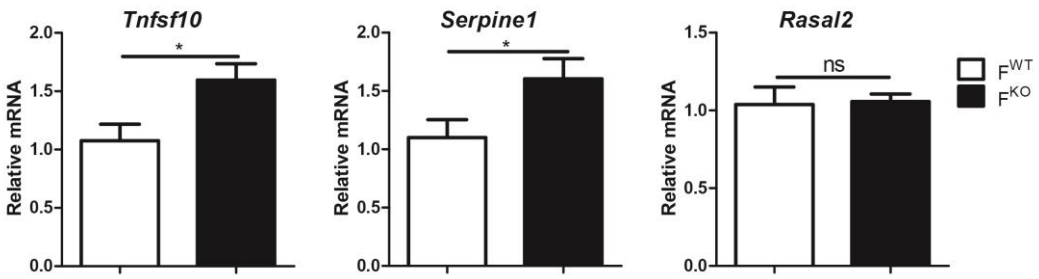

Figure R16. qRT-PCR RNA-seq validation of *Tnfsf10, Serpine1* and *Rasal2* in adipose tissue from ND-fed F^{WT} and F^{KO}.

Control (F^{WT}) and adipose tissue JNK1 deficient (F^{KO}) mice were injected with diethylnitrosamine (DEN; 50 mg/kg) at postnatal day 14 and sacrificed 8 months later. Gene expression of adipose tissue from ND-fed F^{WT} and F^{KO} mice 8 months after DEN treatment was assessed by RNA-sequencing. *Tnfsf10, Serpine1* and *Rasal2* expression were assessed by qRT-PCR. mRNA expression was normalized to *Gapdh*. Data are shown as means ±SEM; * $p<0.05$, ns= No statistically significant difference; Student's t-test; n=8

Tnfsf10 gene encodes for TNF-related apoptosis inducing ligand (TRAIL). TRAIL is a type II membrane protein belonging to TNF superfamily (Wiley et al., 1995, Pitti et al., 1996, Marsters et al., 1996). It is present as a cell surface protein or as a soluble molecule released to bloodstream (Wiley et al., 1995). TRAIL is able to induce apoptosis specifically in cancer cells but not in normal cells (Ashkenazi et al., 1999). Next, we asked if TRAIL could also have a role in F^{KO} mice protection against HCC development. It has been shown that TRAIL-induced apoptosis in cancer cells is mediated, at least partially, by RIP1 (receptor interacting protein 1) activation, followed by p38α phosphorylation (Azijli et al., 2013). As previously showed, we observed an increase in p38α activation in livers from F^{KO} mice 15 days after DEN injection (Figure R12B, C). A group of F^{WT} and F^{KO} mice were DEN-injected and sacrificed 1 month later. Livers from F^{KO} mice after DEN-treatment showed increased p38α activation compared with F^{WT} counterparts (Figure R17A, B).

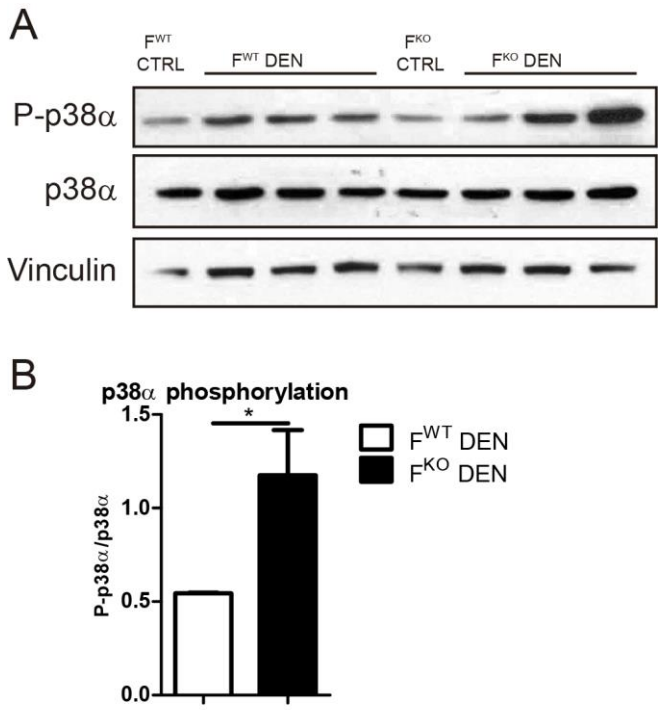

Figure R17. TRAIL signaling analysis in livers from ND-fed F^{WT} and F^{KO} mice.
Control (F^{WT}) and adipose tissue JNK1 deficient (F^{KO}) mice were injected with diethylnitrosamine (DEN; 50 mg/kg) at postnatal day 14 and sacrificed 1 month later. A) Immunoblot analysis of p38α phosphorylation in liver from ND-fed F^{WT} and F^{KO} mice. Blots were probed with P-p38α and p38α antibodies. Vinculin protein expression was monitored as loading control. B) Quantification of p38α phosphorylation. Data are shown as means ±SEM; * $p<0.05$. Student's *t*-test.

However, it has been shown that cancer cells can avoid TRAIL-induced apoptosis through FLICE-inhibitory protein (FLIP), which inhibits caspase-8 activity (Irmler et al., 1997, Zhang and Fang, 2005). We tested the levels of FLIP in tumors from F^{KO} and F^{WT} control mice. We observed a reduction in FLIP protein in F^{KO} mice compared with F^{WT} (Figure R18A, B). These results indicate that tumors raised in F^{KO} mice might be more prone to undergo to TRAIL-mediated apoptosis compared with F^{WT} ones.

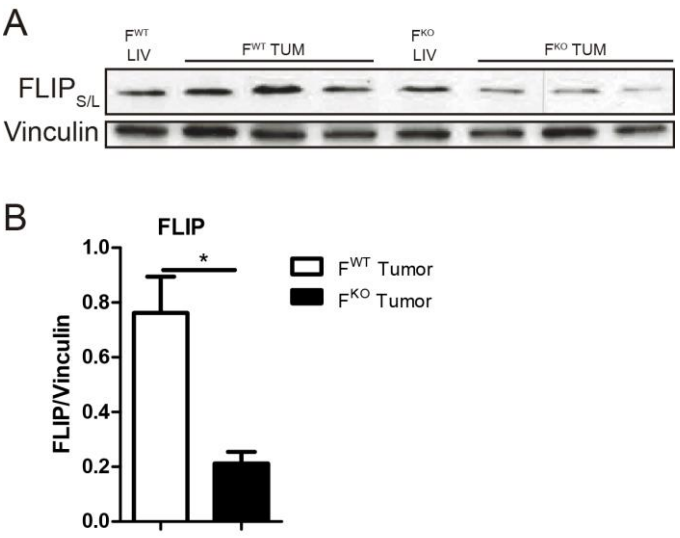

Figure R18. FLIP expression analysis in tumors from ND-fed F^{WT} and F^{KO} mice.
Control (FWT) and adipose tissue JNK1 deficient (FKO) mice were injected with diethylnitrosamine (DEN; 50 mg/kg) at postnatal day 14 and sacrificed 8 months later. A) Immunoblot analysis of FLIP expression in tumors from ND-fed F^{WT} and F^{KO} mice. Vinculin protein expression was monitored as loading. B) Quantification of FLIP expression. Data are shown as means ±SEM; * $p<0.05$. Student's *t*-test.

2. ROLE OF PPARα ACTIVATION IN LIVER CANCER

Obesity has been linked with increased incidence of liver cancer (Klein et al., 2014, Calle et al., 2003). However, little is known about how obesity reshapes liver metabolism during tumor development. High fat diet (HFD) consumption changes hepatic gene expression through activation of the transcription factor peroxisome proliferator-activated receptor α (PPARα) (Memon et al., 2000). Thus, we investigated the role of PPARα during hepatocellular carcinoma (HCC) development. We used full-body knock out *Ppara* mice (*Ppara*$^{-/-}$) and we compared them with wild type C57BL/6 mice (WT).

2.1 PPARα deficiency protects against DEN-induced HCC development in HFD-fed mice

To study the role of PPARα in DEN-induced HCC in the context of obesity, we administered diethylnitrosamine (DEN) to WT and *Ppara*$^{-/-}$ mice on postnatal day 14, and 6 weeks later we placed the animals on either a normal chow diet (ND) or a high-fat diet (HFD), in which 60% of calories are fat-derived. HCC insurgence was monitored 8 months after DEN injection (Figure R19A). On the normal chow diet, the two genotypes showed no statistically significant differences in body weight (Figure R19B) and in tumor number or size (Figure R19C, D). In contrast, HFD-fed *Ppara*$^{-/-}$ mice were protected against HFD-induced obesity (Figure R20A). Moreover, they showed a strong protection against HCC development (Figure R20B); in fact, the mean number of tumors per animal was lower in *Ppara*$^{-/-}$ mice compared with WT counterparts (Figure R20C). Additionally, tumors were smaller in *Ppara*$^{-/-}$ mice than in WT mice (Figure R20D). Such protection against HCC development in HFD-fed *Ppara*$^{-/-}$ mice also correlated with better survival (Figure R20E). Collectively, these data indicate that absence of PPARα protects against DEN-induced HCC in HFD-fed mice, but not during normal diet.

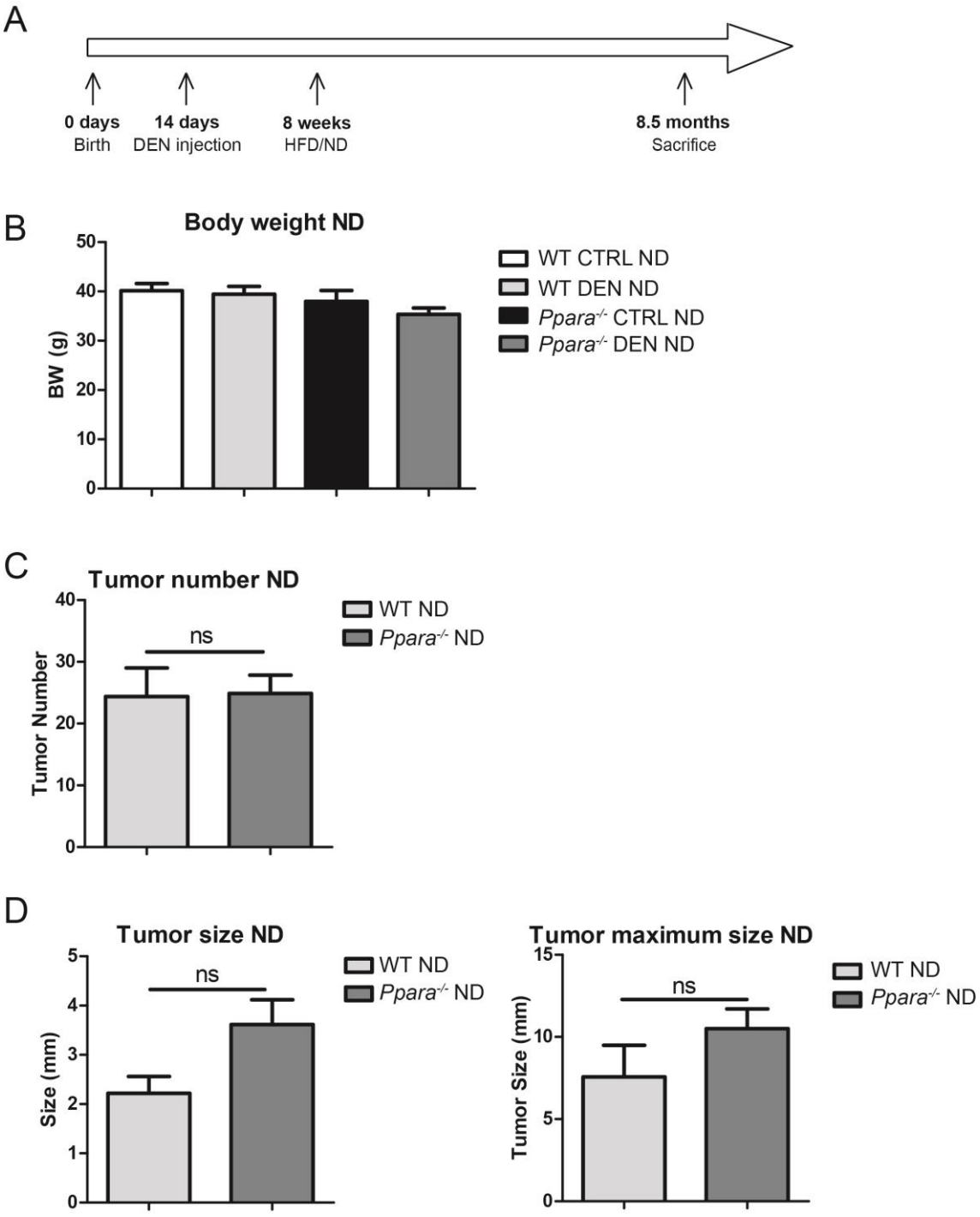

Figure R19. Effect of PPARα deficiency on HCC in ND-fed animals

A) WT and *Ppara*$^{-/-}$ mice were i.p. injected on postnatal day 14 with diethylnitrosamine (DEN; 50 mg/kg) and put on a high-fat diet (HFD) or normal chow diet (ND) 6 weeks later. Mice were sacrificed 8 months after DEN injection. B) Body weight (BW) of ND-fed WT and *Ppara*$^{-/-}$ mice 13 months after DEN injection. C, D) Quantification of tumor number and size in ND-fed DEN-injected WT and *Ppara*$^{-/-}$ mice. The maximum diameter of individual tumor nodules (right panel) and the mean width of tumor nodules (left panel) are presented. Data are shown as means ± SEM; ns=No statistically significant difference (Student's *t*-test; n=8-14).

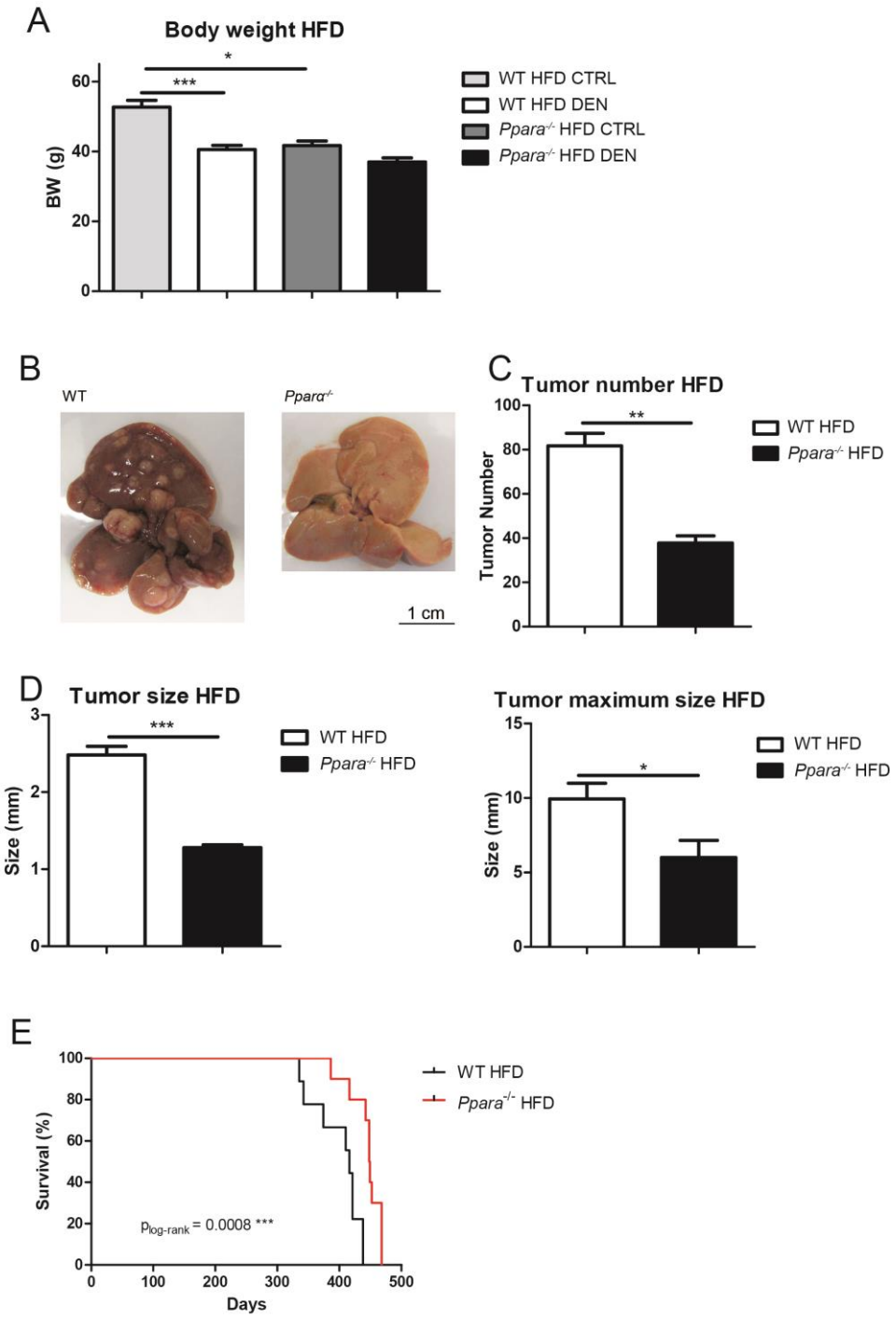

Figure R20. Effect of PPARα deficiency on HCC in HFD-fed animals

WT and Ppara-/- mice were i.p. injected on postnatal day 14 with diethylnitrosamine (DEN; 50 mg/kg) and put on a high-fat diet (HFD) 6 weeks later. Mice were sacrificed 8 months after DEN injection. A) Body weight (BW) of HFD-fed WT and Ppara-/- mice 8 months after DEN injection. B) DEN-induced HCC in HFD-fed WT and Ppara-/- mice at 8.5 months of age. C, D) Quantification of tumor number and size in HFD-fed DEN-injected WT and Ppara-/- mice. The maximum diameter of individual tumor nodules (right panel) and the mean width of tumor nodules (left panel) are presented. Data are shown as means ± SEM; ** p<0.005, *** p<0.001 (Student's *t*-test; n=25). E) Kaplan-Meier analysis of the survival of HFD-fed DEN-injected WT and *Ppara*$^{-/-}$ mice; ***p<0.001 (Mantel-Cox log-rank test; n=9-10).

2.2 Lack of PPARα does not influence liver regeneration

A well-studied model to assess liver proliferation avoiding hepatocyte cell death is two-thirds partial hepatectomy. After partial liver resection, mature hepatocytes are able to enter cell cycle and regenerate the loss tissue (Michalopoulos, 2007). Therefore we checked the capacity of HFD-fed *Ppara*$^{-/-}$ liver to regenerate after partial hepatectomy (PHx). Six-week-old WT and *Ppara*$^{-/-}$ mice were fed with HFD during six weeks before surgery (Figure R21A). No differences were observed between *Ppara*$^{-/-}$ and WT liver mass, nor 48 hours (Figure R21B) neither 15 days after PHx (Figure R21C). However, *Ppara*$^{-/-}$ mice showed increased mortality after PHx compared with WT counterparts (Figure R20D). It has been showed that PPARα is necessary in the inflammatory phase of wound healing and its absence causes a delay in the healing that could explain the increased mortality after surgery (Michalik et al., 2001). Despite *Ppara*$^{-/-}$ mice were adversely affected by PHx their livers were able to regenerate. These results suggest that lack of PPARα does not influence mature hepatocytes capability to enter cell cycle.

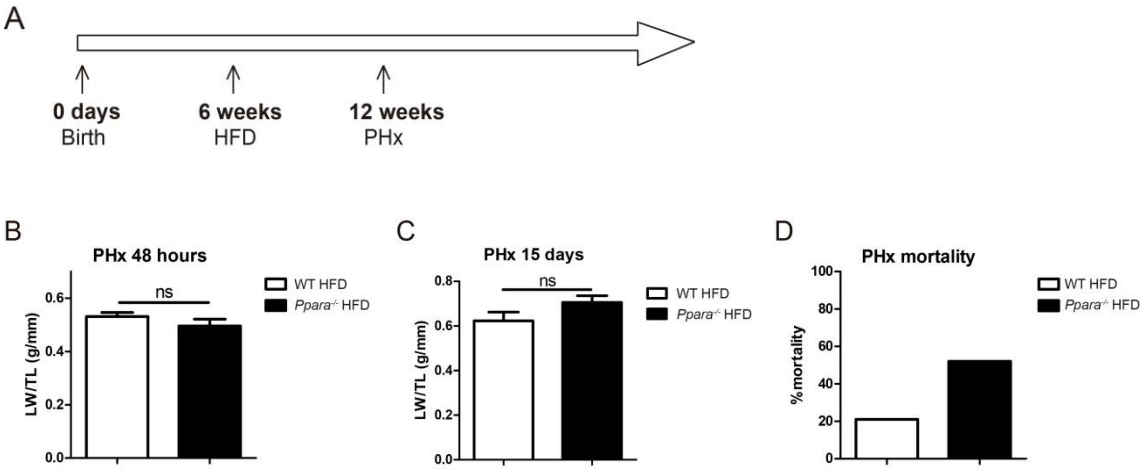

Figure R21. Liver regeneration after partial hepatectomy in HFD-fed WT and *Ppara*$^{-/-}$ mice.

A) Six-week-old WT and *Ppara*$^{-/-}$ mice were fed a high-fat diet (HFD) during 6 weeks before partial hepatectomy (PHx). B, C) Liver mass was analyzed 48 hours (B) and 15 days (C) after PHx in HFD-fed WT and *Ppara*$^{-/-}$ mice. Ratio between liver weight (LW) and tibia length (TL) is represented. Data are shown as means ± SEM; ns= No statistically significant difference; Student's *t*-test; n=15-8 (B); n=9-6 (C). D) Representation of mortality percentage after PHx of HFD-fed WT and *Ppara*$^{-/-}$ mice.

2.3 *Ppara* deletion protects from liver damage on HFD

Contrary to partial hepatectomy, DEN treatment induces hepatocyte death associated with enhanced compensatory proliferation and augmented HCC development (Maeda et al., 2005, Hui et al., 2007, Das et al., 2011). To assay whether lack of PPARα on HFD could affect hepatocyte cell death we evaluated liver damage after acute DEN injection in HFD-fed animals (Figure R22A). Measurement of blood levels ALT and AST revealed less liver damage in *Ppara*$^{-/-}$ mice than in WT counterparts (Figure R22B).

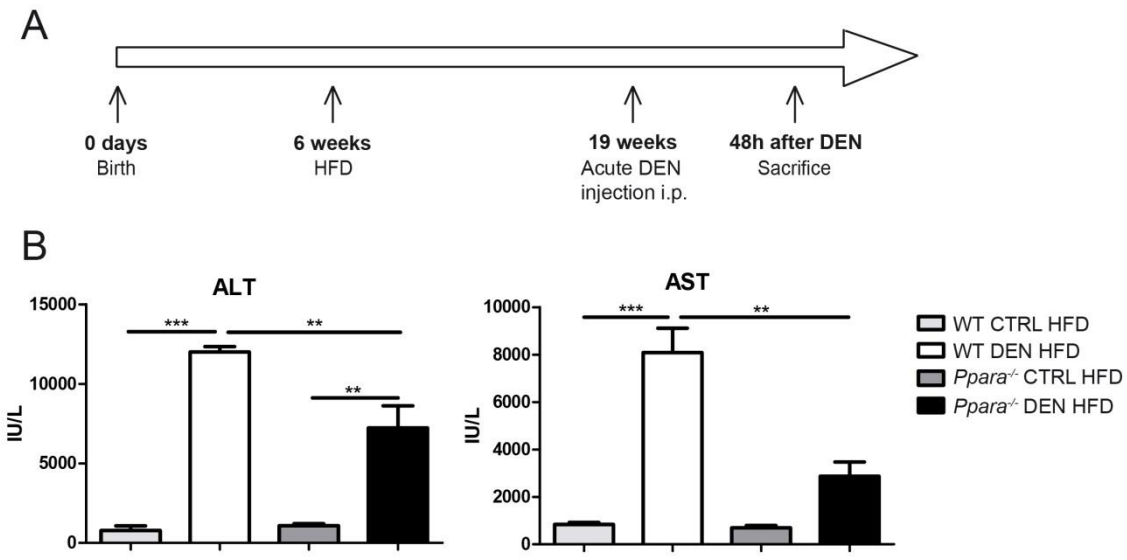

Figure R22. Liver damage analysis after acute DEN treatment on HFD-fed WT and *Ppara*$^{-/-}$ mice.

A) WT and *Ppara*$^{-/-}$ mice were fed a high-fat diet (HFD) from 6 weeks of age. At 19 weeks, mice were injected i.p. with diethylnitrosamine (DEN; 100 mg/kg) and sacrificed 48 hours later. B) Liver damage was assessed from serum measurements of ALT and AST; n=3-7 (3 non-injected mice and 7 injected mice per genotype). Data are shown as means ± SEM; ** $p<0.005$; *** $p<0.001$ (one-way ANOVA coupled to Bonferroni's post-test).

Moreover, DEN-induced apoptosis in liver tissue was reduced in HFD-fed *Ppara*$^{-/-}$ mice as indicated by caspase-3 cleavage (Figure R23A). Different types of cell signaling pathways can modulate tumor development. Among them Ras/Raf/MEK/ERK and STAT3 pathways have a major role in HCC development (Huynh et al., 2003, He et al., 2010), promoting tumor growth and inhibiting apoptosis. Thus we checked by western blot ERK and STAT3 activation. We found both proteins to be less activated in livers from *Ppara*$^{-/-}$ mice (Figure R23B), correlating with reduced proliferation and higher apoptosis

(Figure R23A). We next examined activation of JNK, a kinase affected by inflammation and obesity and known to modulate HCC development (Hui et al., 2008, Maeda et al., 2005, Das et al., 2011, Sabio et al., 2009, Han et al., 2016). Interestingly, HFD-fed *Ppara*$^{-/-}$ mice exhibited reduced JNK activity in liver after DEN injection.

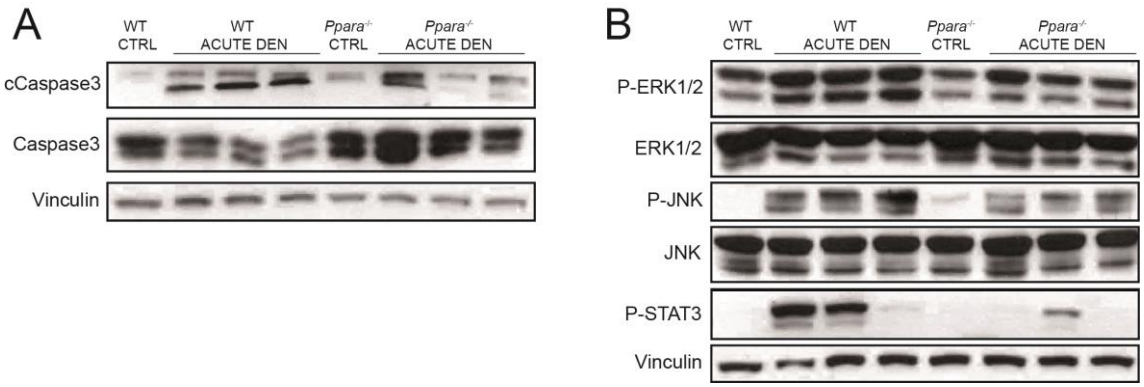

Figure R23. Signaling analysis in acute DEN-treated HFD-fed in WT and *Ppara*$^{-/-}$ mice.
WT and *Ppara*$^{-/-}$ mice were fed a high-fat diet (HFD) from 6 weeks of age. At 19 weeks, mice were injected i.p. with diethylnitrosamine (DEN; 100 mg/kg) and sacrificed 48 hours later. A) Immunoblot analysis of caspase3 and cleaved caspase3 in liver samples from untreated (CTRL) and acutely DEN-treated (ACUTE DEN) HFD-fed WT and *Ppara*$^{-/-}$ mice. Vinculin protein expression was monitored as a loading control. B) Immunoblot analysis of signaling pathways in liver samples from untreated and acutely DEN-treated WT and *Ppara*$^{-/-}$ mice; blots were probed with antibodies to p-ERK, ERK, p-JNK, JNK, and p-STAT3. Vinculin protein expression was monitored as a loading control.

Inflammation plays a central role in cancer development. In particular, it has been shown that HCC is a typical inflammation-driven malignancy (Maeda et al., 2005). To address the role of inflammation in *Ppara*$^{-/-}$ mice protection from liver damage, we checked circulating levels of different pro-inflammatory cytokines. Surprisingly, no significant reduction in serum levels of the cytokines IL-6, TNFα, IL-1β, CCL2, and IFNγ in HFD-fed *Ppara*$^{-/-}$ mice were observed, suggesting that HFD-fed *Ppara*$^{-/-}$ protection against acute DEN-induced liver damage was not associated with lower inflammation (Figure R24). In contrast, after acute DEN injection, HFD-fed *Ppara*$^{-/-}$ mice showed higher levels of pro-inflammatory chemokines CXCL2 and CCL3 than WT counterparts (Figure R24), correlating with the higher levels of markers of immune cells infiltration in tumors 8 months after DEN injection (Figure R25).

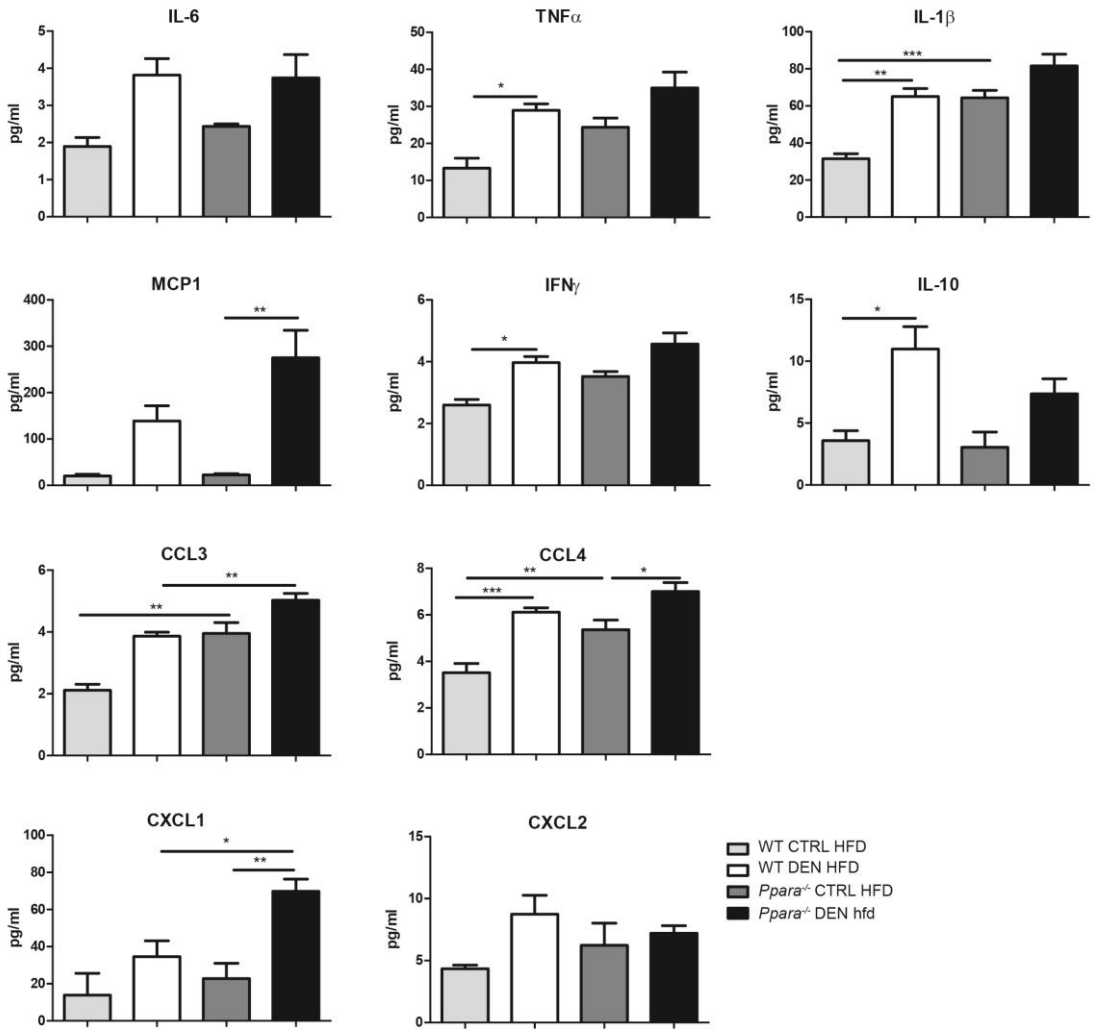

Figure R24. Circulating cytokines after acute DEN treatment of HFD-fed WT and *Ppara*$^{-/-}$ mice.

WT and *Ppara*$^{-/-}$ mice were fed a high-fat diet (HFD) from 6 weeks of age. At 19 weeks, mice were injected i.p. with diethylnitrosamine (DEN; 100 mg/kg) and sacrificed 48 hours later. Luminex analysis of cytokines and chemokines in blood. Data are shown as means ± SEM; * $p<0.05$, ** $p<0.005$, *** $p<0.001$. One-way ANOVA coupled with Bonferroni's post-test statistical analysis was performed (n=4-7).

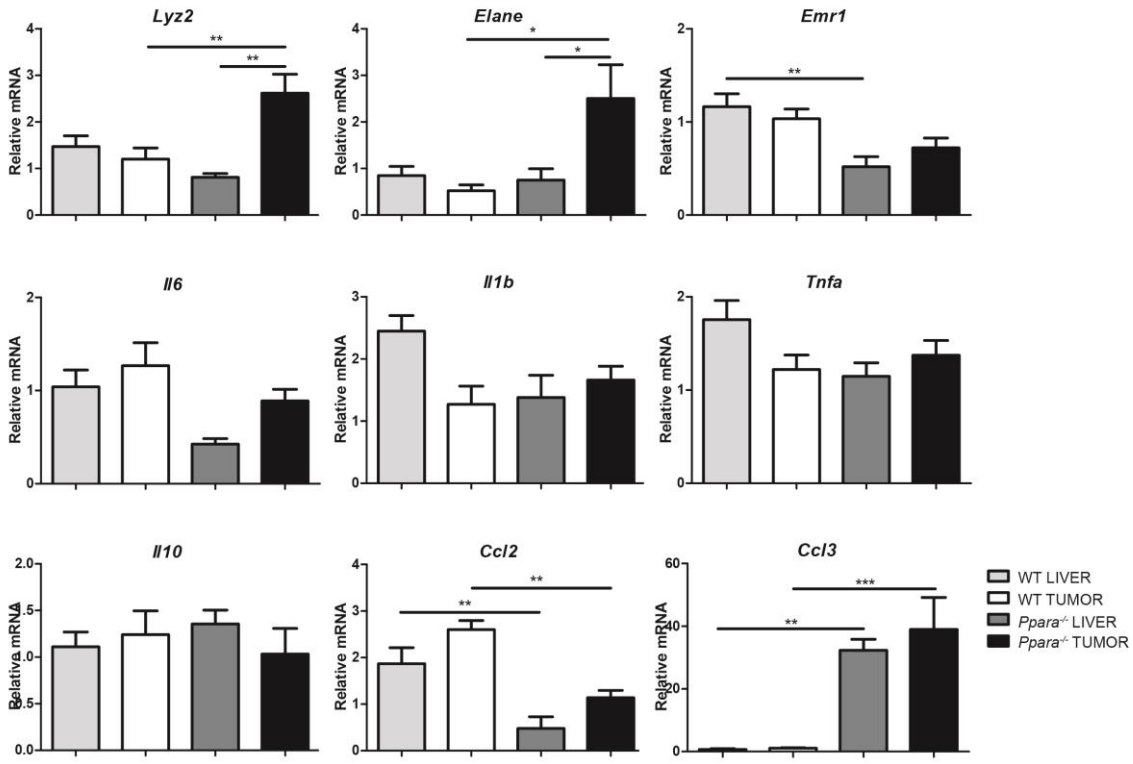

Figure R25. Liver and tumor infiltration and cytokines production in chronic-DEN treated HFD-fed WT and *Ppara*$^{-/-}$ mice.

WT and *Ppara*$^{-/-}$ mice were i.p. injected on postnatal day 14 with diethylnitrosamine (DEN; 50 mg/kg) and put on a high-fat diet (HFD) 6 weeks later. They were sacrificed 8 months after DEN injection. qRT-PCR analysis of liver and hepatic tumor cytokine and chemokine expression in WT and PPARα$^{-/-}$ mice. mRNA expression was normalized to *Gapdh* and to WT liver. Data are shown as means ± SEM; * $p<0.05$, ** $p<0.005$, *** $p<0.001$ (One-way ANOVA coupled to Bonferroni's post-test; n=6).

Obesity is linked to increased incidence of non-alcoholic fatty liver disease (NAFLD), which can degenerate in cirrhosis and, subsequently, HCC. Lipid peroxidation is an important feature of NAFLD and generates reactive oxygen species (ROS) that can induce DNA mutations (Caldwell et al., 2004). Analysis of thiobarbituric acid reactive substances (T-BARS), a by-product of lipid peroxidation, revealed lower oxidized lipid content in the livers of HFD-fed *Ppara*$^{-/-}$ mice (Figure R26). These results suggest that PPARα in the liver, but not in hematopoietic cells, promotes HCC development in HFD-fed WT animals.

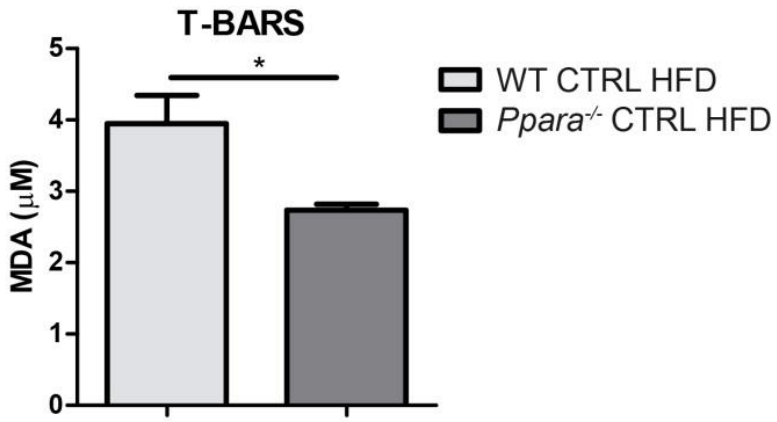

Figure R26. Lipid peroxidation analysis in livers from HFD-fed WT and *Ppara*$^{-/-}$ mice.
WT and *Ppara*$^{-/-}$ mice were fed a high-fat diet (HFD) from 6 weeks of age. At 19 weeks, mice were sacrificed. Lipid peroxidation was analyzed by T-BARS assay in livers from WT and *Ppara*$^{-/-}$ mice. Data are shown as means ± SEM *** $p<0.001$ (Student's *t*-test; n=3).

2.4 Lack of PPARα protects against HCC independently of bone marrow.

PPARα is a transcription factor that is highly expressed in liver, controlling its metabolism. It has a central role in the regulation of genes involved in fatty acids transport and degradation in mitochondria and peroxisome (Gulick et al., 1994, Evans et al., 2004). Moreover, PPARα is expressed in immune cells where has an anti-inflammatory activity in both mice and humans (Devchand et al., 1996, Staels et al., 1998, Clark, 2002). In order to verify in which compartment PPARα expression plays a role in HFD-fed *Ppara*$^{-/-}$ mice protection against HCC development, we generated chimera mice transplanting WT or *Ppara*$^{-/-}$ bone marrow (BM) into lethally irradiated WT or *Ppara*$^{-/-}$ recipients (Figure R27A). Chronic-DEN-induced HCC development was strongly suppressed in reconstituted *Ppara*$^{-/-}$ mice compared with reconstituted WT mice, irrespective of donor BM genotype (Figure R27B). On the HFD, reconstituted *Ppara*$^{-/-}$ mice also developed significantly smaller tumors than their WT counterparts, again irrespective of donor BM genotype (Figure R27C). These results indicate that bone-marrow-derived cells do not primarily mediate the protection against HCC in HFD-fed *Ppara*$^{-/-}$ mice, suggesting the involvement of a cell-autonomous mechanism

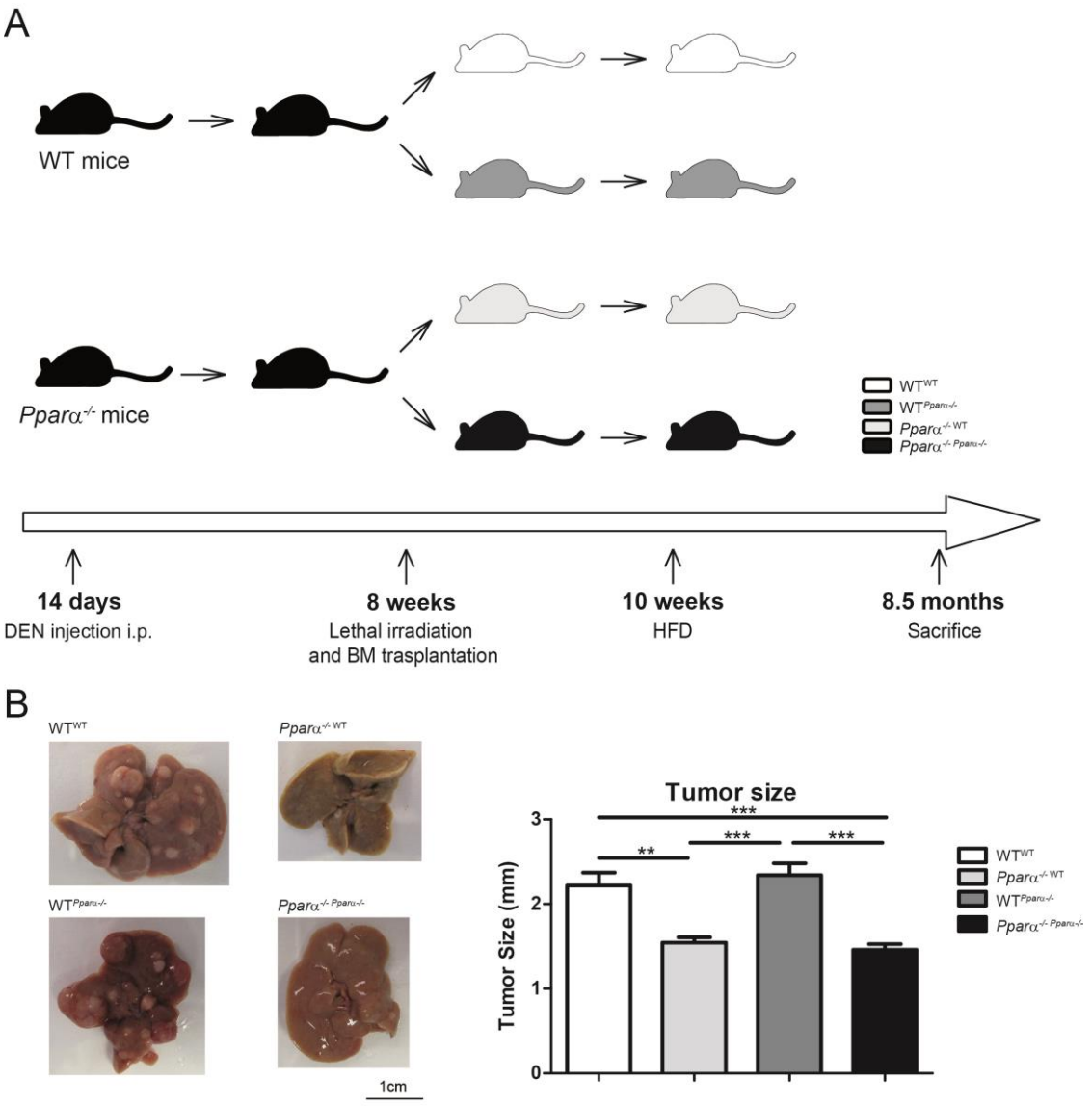

Figure R27. HCC development in HFD-fed chimera mice.
A) WT and *Ppara*$^{-/-}$ mice were injected i.p. on postnatal day 14 with diethylnitrosamine (DEN; 50 mg/kg). At 8 weeks of age mice were lethally irradiated and inoculated i.v. with bone marrow cells from WT or *Ppara*$^{-/-}$ mice. Bone marrow donor genotype is indicated as superscript. After 2 weeks, mice were placed on high-fat diet (HFD) and sacrificed at 8.5 months of age. B) DEN-induced liver cancers in WT and *Ppara*$^{-/-}$ mice transplanted with WT or *Pparα*$^{-/-}$ bone marrow (bone marrow donor genotype is indicated as superscript). The bar chart shows mean tumor size, and photographs show representative images of livers from each condition. Data are shown as means ± SEM; ** p<0.005, *** p<0.001 (one-way ANOVA coupled to Bonferroni's post-test; n=12-22).

2.5 PPARα deficiency inhibits hepatocyte proliferation

To define the molecular mechanism underlying HCC protection in HFD-fed *Ppara*$^{-/-}$ mice we examined multiple signaling pathway involved in liver

proliferation and cell death in liver and tumor homogenates from chronic DEN-treated HFD-fed WT and *Ppara*$^{-/-}$ mice. To identify signaling pathways responsible for the reduced liver damage in HFD-fed *Ppara*$^{-/-}$ mice, we examined liver and tumor samples for the activation of protein kinases known to be affected by metabolic state. AKT/mTOR signaling pathway is known to be sensor of metabolic state of the cell and its activation can induce cell proliferation (Deberardinis et al., 2008, Manning and Cantley, 2007). ERK is the effector of Ras/Raf/MEK pathway and induces cell proliferation and response to oxidative stress (Huynh et al., 2003, He et al., 2010). HFD-fed *Ppara*$^{-/-}$ mice exhibited reduced activation of ERK and AKT, as we observed lower phosphorylation levels of both kinases in healthy liver and hepatic tumors from HFD-fed *Ppara*$^{-/-}$ mice (Figure R28). The tumor suppressor p53 coordinates anti-proliferative responses that restrict malignant-cell expansion. Lack of p53 facilitates de-differentiation of mature hepatocytes and correlates with HCC (Tschaharganeh et al., 2014). We found that chronic DEN treatment induced p53 loss in tumor and liver tissue from HFD-fed WT mice, whereas p53 levels in HFD-fed *Ppara*$^{-/-}$ mice were maintained (Figure R28).

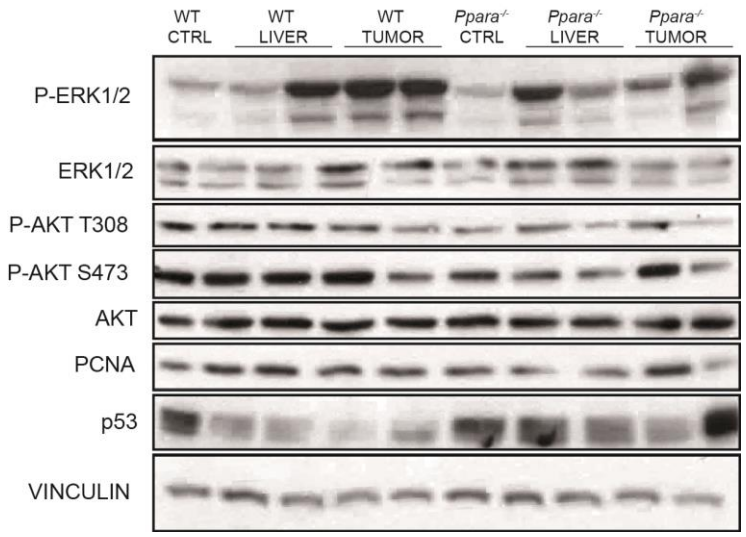

Figure R28. Cell signaling analysis of livers and tumors from chronic-DEN treated HFD-fed WT and *Ppara*$^{-/-}$ mice.

WT and *Ppara*$^{-/-}$ mice were i.p. injected on postnatal day 14 with diethylnitrosamine (DEN; 50 mg/kg) and put on a high-fat diet (HFD) 6 weeks later. They were sacrificed 8 months after DEN injection. Immunoblot analysis of ERK, JNK, AKT, their phosphorylated forms, PCNA, and p53 in tumors isolated from WT mice and *Ppara*$^{-/-}$ mice after chronic DEN (liver and tumor samples) and not injected controls (CTRL). Vinculin protein expression was monitored as a loading control.

qRT-PCR analyses of tumor and non-tumor tissues from WT and *Ppara*$^{-/-}$ mice revealed reduced expression of the cell-cycle regulators *Cdk2*, *CcnA1*, *Foxm1*, and *Cdc25c* in non-tumor samples from *Ppara*$^{-/-}$ mice (Figure R29A) and enhanced expression of the cell-cycle regulatory genes *p21*, *Trp53*, *p19* and *p57* in *Ppara*$^{-/-}$ tumor tissue (Figure R29B). This finding strongly suggests lower hepatocyte proliferation in *Ppara*$^{-/-}$ livers.

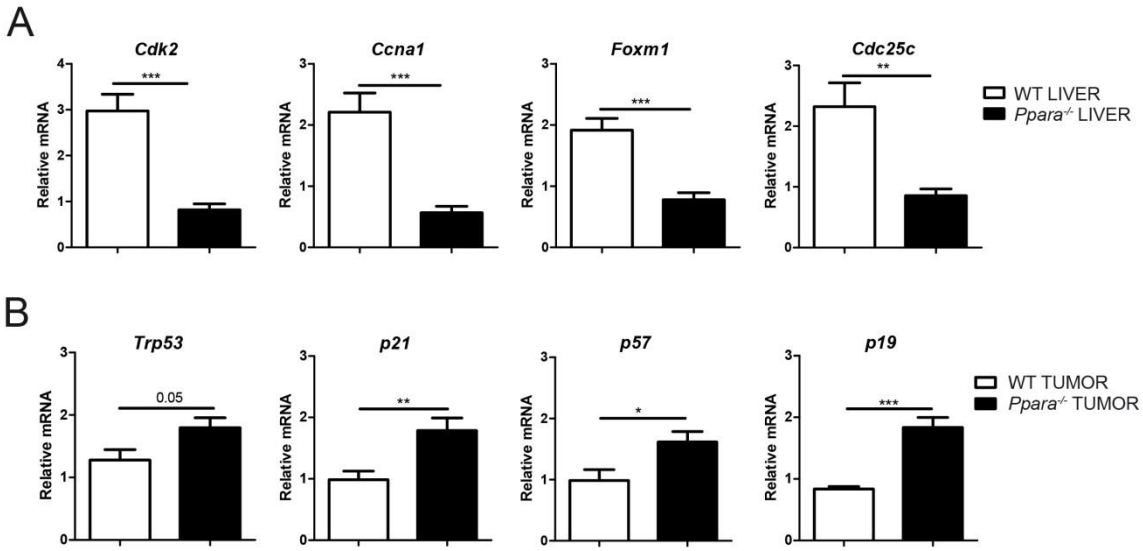

Figure R29. Cell cycle regulators analysis in livers and tumors from chronic-DEN treated HFD-fed WT and *Ppara*$^{-/-}$ mice.

WT and *Ppara*$^{-/-}$ mice were i.p. injected on postnatal day 14 with diethylnitrosamine (DEN; 50 mg/kg) and put on a high-fat diet (HFD) 6 weeks later. They were sacrificed 8 months after DEN injection. A) qRT-PCR analysis of cyclin and cell cycle regulator expression in liver samples from WT and *Ppara*$^{-/-}$ mice. mRNA expression was normalized to *Gapdh* and WT liver expression. Data are shown as means ± SEM; **p<0.005, *** p<0.001 (Student's *t*-test; n=6). B) qRT-PCR analysis of cyclin and cell cycle regulator expression in hepatic tumors from WT and *Ppara*$^{-/-}$ mice. mRNA expression was normalized to *Gapdh* and WT liver expression. Data are shown as means ± SEM; **p<0.005, *** p<0.001 (Student's *t*-test; n=6).

2.6 PPARα hyperactivation in hepatocytes promotes liver cancer

JNK suppresses PPARα activity and mice lacking hepatocyte JNK1/2 expression show elevated PPARα activity and fatty acid oxidation (Vernia et al., 2014). To determine whether PPARα activation was sufficient to promote liver cancer, we examined adult liver from *Alb-Cre* control (LWT) mice and mice with compound JNK1/2 deficiency in hepatocytes (LDKO). At 10 months of age, LWT mice showed no evidence of hepatic pathology; in contrast, 82% of LDKO

mice displayed multifocal bile duct hyperplasia associated with fibrosis and inflammatory cell infiltration (Figure R30). Bile duct epithelial cells from these LDKO mice stained positive for the proliferation marker PCNA. The remaining LDKO mice exhibited cholangiocarcinoma (6%) or appeared to be healthy (12%).

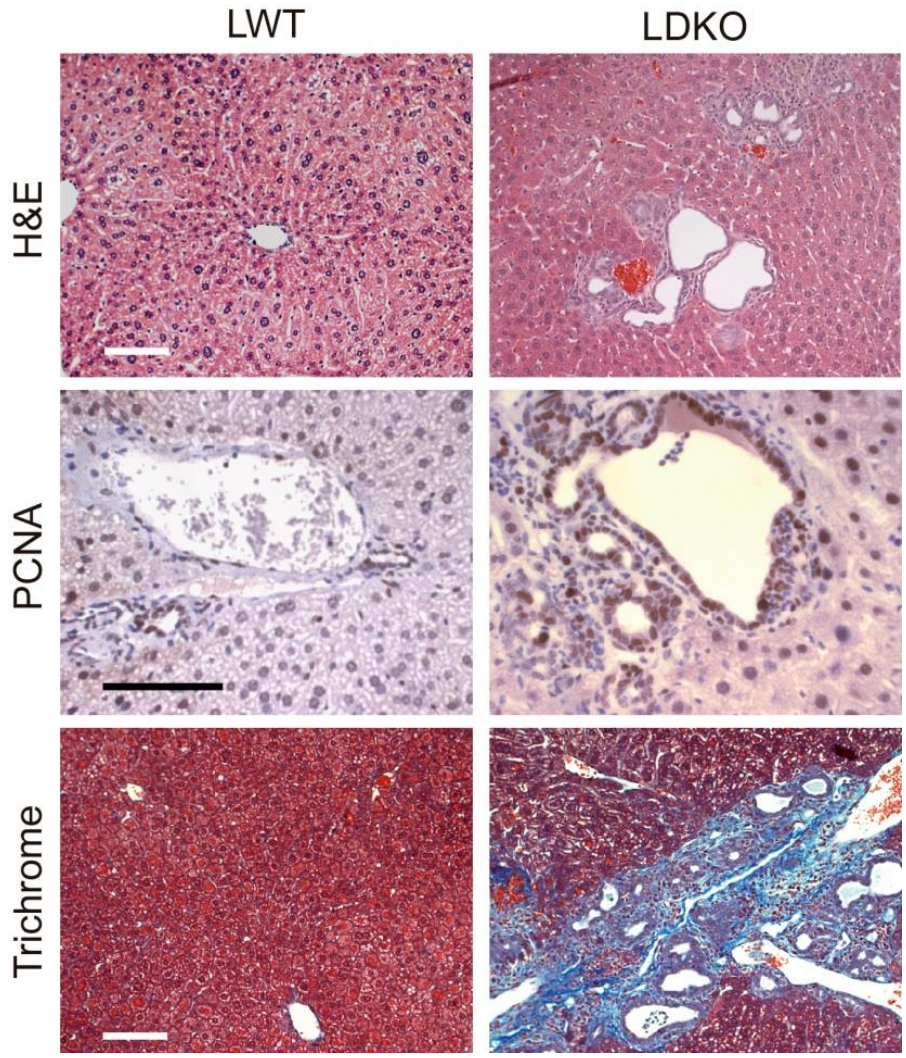

Figure R30. Histological analysis of 10-month-old ND-fed LWT and LDKO mice.
Histochemical analysis of liver from LWT (Alb-cre control) and LDKO (liver-specific JNK1/2 deficient) mice fed standard chow diet (ND) for 10 months. Panels show representative liver sections stained with hematoxylin and eosin (H&E), antibody to PCNA and Masson's trichrome. Scale bar = 100 μm.

At 14 months of age, 94% of LDKO mice displayed cholangiocarcinoma associated with fibrosis (Figure R31A, D) and increased liver mass (Figure R31B), and the remaining LDKO mice (6%) had cystic livers with bile duct hyperplasia. Moreover, LDKO mice showed elevated serum ALT levels,

indicating liver damage (Figure R31C). Together, these data confirm that mature mice with compound deficiency of JNK1 and JNK2 in hepatocytes progressively develop cholangiocarcinoma.

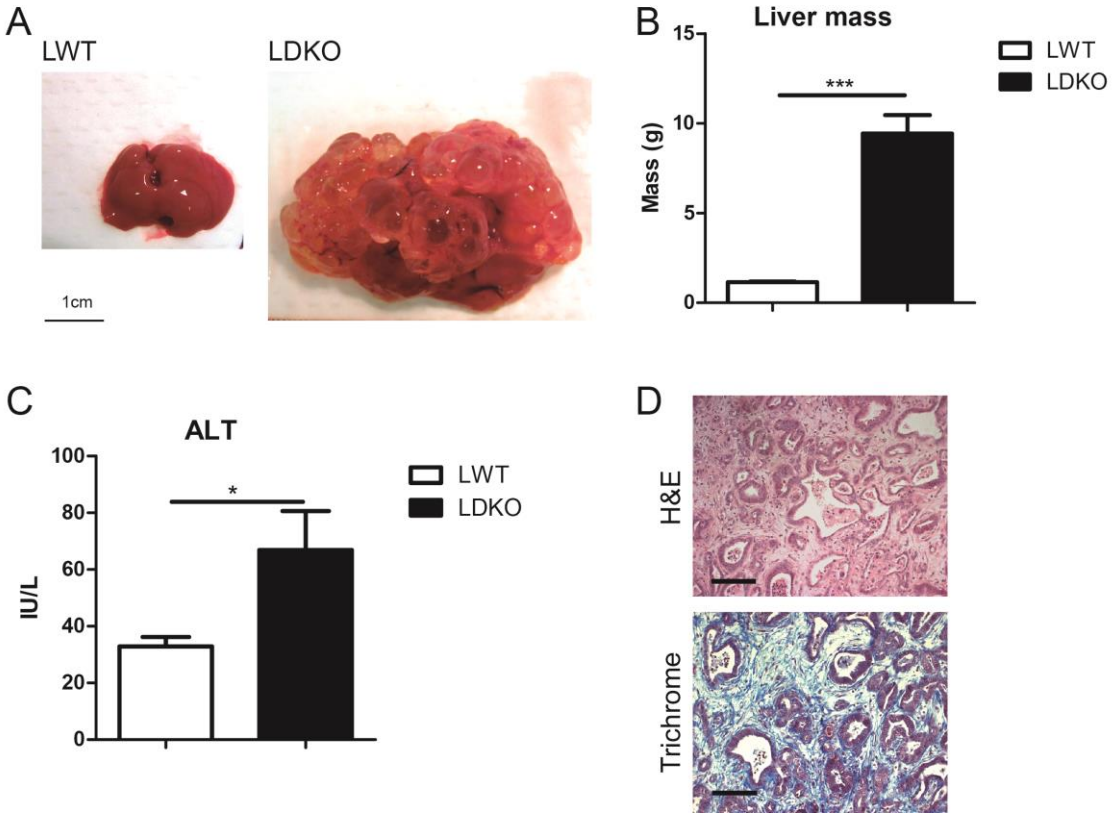

Figure R31. Analysis of 14-month-old ND-fed LWT and LDKO mice.
LWT (Alb-cre control) and LDKO (liver-specific JNK1/2 deficient) mice fed standard chow diet (ND) for 14 months. A) Representative livers from chow-fed 14-month-old LWT and LDKO mice. B) Liver mass (g) in 14-month-old chow-fed LWT and LDKO mice. Data are shown as means ± SEM; *** $p<0.001$ (Student's *t*-test; n=15). C) Liver damage measured by ALT in 14-month-old chow-fed LWT and LDKO mice. Data are shown as means ± SEM; *$p<0.05$ (Student's *t*-test; n=11). D) Representative H&E and Masson's trichrome staining on liver sections from14-month-old chow-fed LDKO mice. Scale bar = 100 µm.

DISCUSSION

Cancer is a leading cause of death in many high-income countries; moreover its incidence is growing in low and middle-income nations (Bray et al., 2012), leading to the worldwide increase of morbidity and mortality of this non-communicable disease. Nowadays therapy options exist for several types of malignancies, thanks to early diagnosis and effective treatments (for example estrogen responsive breast cancers, melanoma and prostate cancers). Nevertheless, other types of malignancies does not benefit of the same situations: diagnosis occurs in late-stages and no curative treatments are available for pancreatic cancer, hepatocellular carcinoma, nodular melanoma and triple-negative breast cancer, to mention some. Therefore, there is a growing attention to newly recognized risk factors for cancer and the molecular mechanisms that link them to malignancies. In this scenario, obesity and metabolic disorders are becoming major risk factors for different types of cancer (hepatocellular carcinoma, gynecological cancers, stomach and colon cancer) (Calle et al., 2003, Font-Burgada et al., 2016). Altered metabolism can lead to low-grade chronic inflammation, hyperinsulinemia and hyperglycemia that together create a favorable environment for cancer development (Font-Burgada et al., 2016). In particular, a strong causal connection between metabolic disorders and hepatocellular carcinoma has been discovered (Calle et al., 2003, Baffy et al., 2012). The main purpose of this Thesis was to further dissect the connection between metabolism and HCC and unravel the contribution of organs crosstalk in HCC development. For this reason, we studied the role of two genes involved in metabolism, *Jnk1* and *Ppara,* in liver tumorigenesis.

1. ROLE OF JNK1 IN ADIPOSE TISSUE-LIVER CROSSTALK IN HCC DEVELOPMENT

1.1 IL-6 produced by adipose tissue is not relevant for DEN-induced HCC

IL-6 is a pro-inflammatory cytokine that plays a pivotal role in hepatic steatosis and HCC development (Sabio et al., 2008, Park et al., 2010). Liver steatosis is a common consequence of obesity and it triggers activation of residential Kupffer cells increasing pro-inflammatory cytokines production (Park et al., 2010). It has been described that JNK1 expression in adipose tissue during

obesity leads to an increase in IL-6 production and secretion from adipose tissue (Sabio et al., 2008). In fact, mice lacking JNK1 in adipose tissue are protected against HFD-induced liver steatosis due to a reduction of IL-6 levels (Sabio et al., 2008). These results suggest that lack of JNK1 in adipose tissue might protect animals against obesity-increased HCC development. However, our results show that lack of JNK1 in the adipose tissue does not protect against DEN-induced HCC in HFD (Figure R2); in fact, the same number and size of tumors were observed in F^{KO} (*Fab-Cre*$^{+}$*Jnk1*$^{f/-}$) and F^{WT} (*Fab-Cre*$^{+}$*Jnk1*$^{+/}$) mice under HFD conditions (Figure R2). A possible explanation of these results is that Kupffer cells are the main producers of IL-6 and TNFα in this mouse model. In fact, it has been shown that JNK1 regulates TNFα and IL-6 expression in Kupffer cells, thus controlling hepatocyte cell death (Das et al., 2009). In F^{KO} mice Kupffer cells have normal levels of JNK1. Thus we can hypothesize that the reduction of IL-6 production from adipose tissue of HFD-F^{KO} mice does not have a strong influence on chemical-induced HCC development. Taking into account that both stimuli, HFD and DEN, strongly induce a pro-inflammatory environment, it is possible that the decrease of IL-6 production from adipose tissue might result imperceptible. However, understand the role of IL-6 produced by adipose tissue during obesity in HCC would be appealing, as it could be a new therapeutic target. For this purpose, it would be necessary to use a different experimental model, different from the one we used, based on chemical-induced inflammation to provoke cancer development. One possibility would be to apply, for example, a genetic model of HCC. In fact, mutations in *Tpr53* gene are highly frequent in human HCC (Fujimoto et al., 2012) and hepatocyte-specific *Tpr53* deletion induces HCC in 5 months with 80% of incidence in mice (Katz et al., 2012). This genetic model can be obtained using the CRISPR/Cas9 technology (Seruggia and Montoliu, 2014). F^{KO} and F^{WT} mice, or alternatively adipose tissue-specific *Il6* knock out mice, could be crossed with *Rosa26-Cas9* knock-in mice (Platt et al., 2014), to obtain whole body constitutive expression of Cas9. To obtain liver-specific deletion of *Trp53* gene, mice can be intravenously injected with hepatocyte-specific adeno-associated virus (AAV8 or AAV9) carrying the CRISPR guide RNA targeting *Tpr53* (*Trp53* sgRNA). Alternatively, hepatocyte-specific delivery of *Tpr53* sgRNA can be obtained through hydrodynamic tail vein

injection (Zhang et al., 1999). However, both ways of delivery are also associated with low grade liver inflammation. It would be opportune to monitor the level of inflammation induced. Another alternative experiment to study the role of adipose tissue IL-6 in HCC development in the absence of chemical-induced inflammation consists in the long term feeding of F^{WT} and F^{KO} mice with choline-deficient high fat diet (CD-HFD) (Wolf et al., 2014). Wolf and colleagues demonstrated that feeding mice with a CD-HFD during 12 months induces HCC development with incidence around 25% in C57BL/6 mice. Despite the low HCC incidence, this method could be useful to avoid experimental-derived inflammation and to study the contribution of adipose tissue IL-6 in HCC development during obesity.

1.2 ND-F^{KO} mice are protected against HCC development and have normal liver regeneration after partial hepatectomy

In contrast with the results obtained with HFD-fed F^{KO} mice, ND-fed F^{KO} mice are protected against DEN-induced HCC development; in fact, they showed a decrease in both number and size of tumors (Figure R3). These data were also confirmed in a xenograft model: F^{KO} mice showed protection against tumor growth when injected with Hep53.4 cells, a HCC cell line isolated from tumors DEN-induced in C57BL/6J mice (Figure R5). Taken together, these data show that JNK1 in adipose tissue promotes liver tumor development, indicating a crosstalk between adipocytes and hepatocytes, in which JNK1 plays an important role. A well-known model to assess hepatocytes proliferation is partial hepatectomy (Michalopoulos, 2007). However, we did not observe any differences in liver regeneration (Figure R6A, B). These results suggest that JNK1 in the adipose tissue does control HCC development but does not influence liver regeneration. Together with liver transplantation, partial hepatectomy is the most curative therapy for HCC (Llovet et al., 2003). However, nearly 80% of patients suffer HCC recurrence in 5 years after partial hepatectomy (Yamamoto et al., 1996). Partial liver resection induces differentiated hepatocytes to entrance in cell cycle, triggering their proliferation until the liver mass is reestablished. On the other hand, it is clear that liver regeneration after partial hepatectomy enhances HCC recurrence (Man et al., 2007, Picardo et al., 1998). Therefore, it is fundamental to balance the protection against HCC recurrence and liver

regeneration ability. In this context, our model suggests that reducing the activity of JNK1 in the adipose tissue could favor such balance. However, further experiments are necessary in order to confirm this point. For example a study of liver regeneration after tumor resection or, alternatively, intra-hepatic injection of HCC cells just before partial hepatectomy in F^{KO} and F^{WT} mice. Notably, the latter experiment would also mimic the presence of not detectable tumor cells in the liver, a possible cause of HCC recurrence in patients (Picardo et al., 1998).

1.3 Different metabolic profile in F^{WT} and F^{KO} mice

To further dissect the metabolic difference between F^{KO} and F^{WT} mice, we analyzed circulating metabolites by serum mass spectrometry (MS). Each of the analyzed genotypes showed a unique metabolic signature (Figure R4), indicating important differences between F^{WT} and F^{KO} mice. In fact, tumor growth induces changes in cell metabolism that are reflected in the metabolites produced and secreted in the bloodstream (Holmes et al., 2008, Odunsi et al., 2005, Asiago et al., 2010). These results might be relevant in the framework of cancer diagnostics. In fact early analytical biomarkers for HCC are needed, especially because late diagnosis is responsible of the high mortality rate of HCC. For this reason, in the last years, more efforts have been made to improve the early diagnosis of this malignancy (Tsuchiya et al., 2015, Zeng et al., 2015). In this scenario, metabolomics studies of early-detected HCC represent a valuable resource to the diagnosis of liver cancer. However, the main weakness of this analysis is that we cannot discriminate between markers of HCC and metabolites differentially produced by F^{KO} and F^{WT} mice. It would be useful to examine serum from control F^{KO} and F^{WT} mice at the same age. This more extended analysis would also indicate whether lack of JNK1 in adipose tissue could affect serum metabolic profile and whether any of these metabolites that are differentially expressed could be exploited as a potential target of therapy.

1.4 Adipose tissue from F^{KO} mice is functional

We observed no differences in body weight of F^{KO} and F^{WT} mice (Figure R7A), indicating that the protection against HCC is not caused by a reduction in weight gain. Moreover, adipose tissue from both genotypes presented a

completely normal structure and functionality (Figure R7B, C), and no differences in infiltration were observed (Figure R8A). JNK1 activation in adipose tissue has been described to promote pro-inflammatory cytokines production during HFD (Sabio et al., 2008, Sun et al., 2011). Thus, we analyzed IL-6, TNFα and IL-1β production in adipose tissue. Despite we observed a decrease in the expression of TNFα and IL-1β in adipose tissue from F^{KO} mice (Figure R8B), these results were not reflected in circulating levels of these cytokines (Figure R8C), indicating that cytokines levels are not the driving cause of the observed phenotype.

1.5 Adiponectin protects against HCC development

Adipose tissue is involved in the production of several molecules, commonly referred to as adipokines (Gavrilova et al., 2000). These molecules regulate appetite and metabolism. In addition, adipokines are also involved in inflammation, cell growth and differentiation. Among them, *adiponectin* is one of the most expressed and most representing (Maeda et al., 1996). Moreover, it has been described that JNK1 full knock out mice show an increase in adiponectin levels (Hirosumi et al., 2002). Interestingly, adiponectin circulating levels are decreased in both HCC and obese state (Kelesidis et al., 2006, Arita et al., 1999). We found that adiponectin circulating levels are increased in F^{KO} mice compared with F^{WT} counterparts, suggesting a role of adiponectin in the observed protection of F^{KO} mice against HCC development (Figure R9A, B). Moreover, genetic depletion of adiponectin in F^{KO} and F^{WT} mice using adiponectin knock out mice completely reverted F^{KO} protection against HCC development, confirming the importance of adiponectin in this model (Figure R10A, B and R11). One of the proposed mechanisms in adiponectin-induced protection against malignancies is the inhibition of cancer cells proliferation through the activation of AMPKα signaling (Mao et al., 2006). Moreover, it has been showed that transforming growth factor-β-activated protein kinase 1-binding protein-1 (TAB1)-AMPKα complex can recruit p38α MAPK inducing its auto-phosphorylation (Li et al., 2005). We observed that both AMPKα and p38α were more phosphorylated in F^{KO} livers 15 days after DEN injection (Figure R12B, C, D). Moreover, metformin-induced AMPKα activation (Figure R13) and intra-tumor injection of active p38α retrovirus

inhibit tumor growth in xenograft model (Figure R14). This correlates with the observation that diabetic patients treated with metformin have less tumor incidence compared with insulin-treated patients (Bowker et al., 2006, Singh et al., 2013), and that metformin can inhibit hepatoma cells growth *in vitro* (Chen et al., 2013). In fact, currently there are several clinical trials in progress to assess the efficacy of metformin in cancer treatment and prevention. Additionally, p38α has a pivotal role in cancer development. In particular, deletion of p38α in hepatocytes enhances DEN-induced HCC development, underlying its protective role in liver tumorigenesis (Hui et al., 2007). Moreover, human HCC frequently shows reduced levels of phosphorylated p38α; also, expressing a constitutive active form of p38α in hepatoma cell lines induces apoptosis (Iyoda et al., 2003). In contrast, Rudalska *et al.* demonstrated that Sorafenib resistance in HCC could be reverted by p38α inhibition in Ras-induced tumors (Rudalska et al., 2014). The differences observed in the effect of p38α activation could be explained by differences in the experimental model used, genetic *versus* chemical-induced HCC, and that Sorafenib treatment itself could induce specific mutations that would in turn affect tumor behavior. Further analysis is necessary to verify if F^{KO} tumors are resistant to Sorafenib. In conclusion, we propose that adiponectin-mediated inhibition on HCC growth occurs through the activation of AMPKα, which in turn activates, directly or indirectly, p38α inducing tumor growth inhibition. It would be interesting to test whether adiponectin-induced AMPKα/p38α signaling would increase Sorafenib response of resistant HCC.

1.6 Adipose tissue RNAseq reveals TRAIL as another mediator in tumor protection

JNKs protein targets are multiple and mediate diverse functions (Davis, 2000). The first data that emerged from the analysis of adipose tissue RNA-seq performed using the Ingenuity® Pathway Analysis (IPA) platform was that the majority of the pathways down regulated in F^{KO} adipose tissue 8 months after DEN injection were related with liver diseases and malignancies (Figure R15). This result is partially biased by the analysis system itself; in fact, IPA is based on published data - independently of the tissue in which the study has been originally held. It is clear that adipose tissue has been less studied than liver and liver diseases. However, among the over-expressed molecules in F^{KO}

adipose tissue, we found three secreted proteins that have a known role in cancer protection (Figure R16). Among them, TRAIL particularly attracted our attention due to its ability to selectively recognize and induce apoptosis in cancer cells (Ashkenazi et al., 1999). Moreover, it has been described that TRAIL can promote apoptosis in cancer cells through p38α activation (Azijli et al., 2013). This correlated with the higher phosphorylation of p38α in livers from F^{KO} mice 15 days and 1 month after DEN injection (Figure R12B, C and Figure R17A, B). In addition, tumors from F^{KO} mice present lower levels of FLIP in comparison with tumors from F^{WT} mice (Figure R18A, B). Further analyses are needed to understand the role of TRAIL in this HCC model; however we can hypothesize that high levels of TRAIL can trigger apoptosis in F^{KO} tumors.

In conclusion, our data demonstrated that JNK1 in adipose tissue plays an important role in HCC development, controlling both adiponectin and TRAIL production (Figure D1). These results highlighted the importance of adipose tissue to liver crosstalk during HCC development. Finally, our results indicate that the signaling pathway adiponectin/AMPKα/p38α can inhibit HCC proliferation and, together with TRAIL-induction of apoptosis, results in reduced tumor development, suggesting this molecules in combination as a potential treatment for HCC.

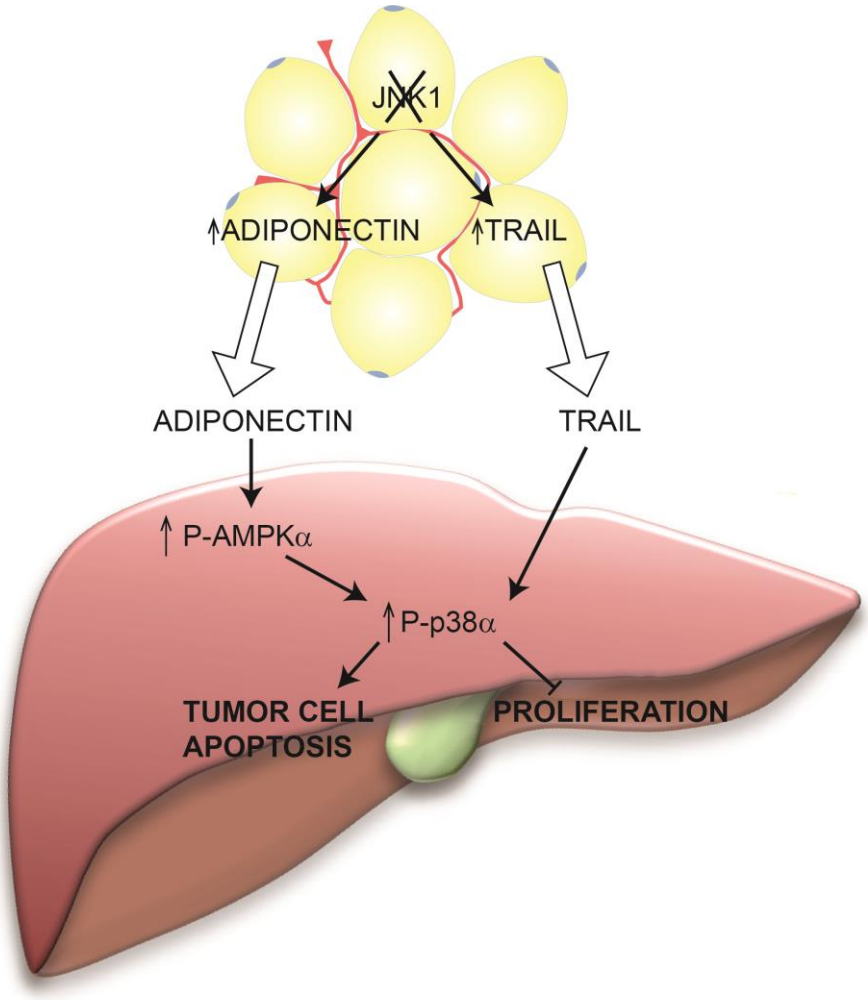

Figure D1. Schematic representation of the role of JNK1 in adipose tissue-liver crosstalk during HCC development.

JNK1 depletion in adipose tissue induces increase in circulating levels of adiponectin and TRAIL. Adiponectin and TRAIL promotes p38α activation in liver, avoiding hepatocytes proliferation and triggering tumor cells apoptosis.

2. ROLE OF PPARα ACTIVATION IN LIVER CANCER

2.1 PPARα activation is necessary for HCC development during obesity

PPARα is a transcription factor that plays a pivotal role in sensing metabolic changes and inducing fatty acids transport and oxidation (Pawlak et al., 2015). It has been shown that PPARα activation protects against steatosis and obesity-induced liver inflammation (Stienstra et al., 2007, Ip et al., 2003). However, its role in HCC development is controversial (Zhang et al., 2014, Peters et al., 1997). We did not find any significant difference either in body weight or in DEN-induced HCC development under normal chow diet condition between *Ppara*$^{-/-}$ and WT mice (Figure R19). However, HFD-fed *Ppara*$^{-/-}$ mice were protected against both HFD-induced obesity and DEN-induced hepatocarcinogenesis compared with WT mice (Figure R20), underlying a role of PPARα in HCC development. Last year, Gao *et al.* described the impact of PPARα in genetic-induced obesity (Gao et al., 2015). These authors described that *Ppara*$^{-/-}$*ob/ob* mice become more obese than *ob/ob* mice. Additionally, *Ppara*$^{-/-}$*ob/ob* treated with Wy-14643, a PPARα agonist, show the same hepatic tumor incidence as *ob/ob* control mice, but less than Wy-14643 treated *ob/ob* mice (Gao et al., 2015). However, Wy-14643 induces the same tumor development in WT as in *ob/ob* mice, indicating that in this model, tumor development depends on response to peroxisome proliferator Wy-14643 and is independent of obesity. Using a different model we were able to show that PPARα contributes to obesity-induction in mice fed a HFD and in this scenario, PPARα promotes DEN-induced HCC development. Moreover, DEN-treated HFD-fed *Ppara*$^{-/-}$ displayed a significant increase in survival (Figure R20E) and no differences in body weight compared with no DEN-treated HFD-fed *Ppara*$^{-/-}$ (Figure R20B), indicating less physical distress and cachexia, probably linked with a decrease in HCC development (Figure R20B, C). However, upon partial hepatectomy, we did not observe differences in liver regeneration between HFD-fed *Ppara*$^{-/-}$ and WT mice (Figure R21B, C) indicating that these mice have no defects in proliferation induced by liver resection. Nevertheless, HFD-fed *Ppara*$^{-/-}$ mice showed an increase in mortality after partial hepatectomy (Figure R21C), probably due to PPARα role in the inflammatory phase of wound healing

(Michalik et al., 2001) after surgery. Taken together, these results indicate a role for PPARα activation in HCC development, strictly during obesity and not in normal diet. Moreover, the mechanism involved in PPARα-induced HCC does not affect liver regeneration, indicating that lack of PPARα does not influence cell cycle entrance and progression in hepatocytes.

2.2 *Ppara*$^{-/-}$ mice are protected against DEN-induced liver damage

Compensatory proliferation after hepatocytes death is the most important mechanism that triggers liver cancer development (Baffy et al., 2012). After an acute dose of DEN, we observed enhanced cellular damage in livers from HFD-fed WT mice, but not in HFD-fed *Ppara*$^{-/-}$ mice, as indicated by AST and ALT circulating levels (Figure R22B, C). Moreover, *Ppara*$^{-/-}$ livers showed less apoptosis (Figure R23A) and less activation of signaling molecules involved in proliferative response (Figure R23B). However, livers from HFD-fed *Ppara*$^{-/-}$ mice did not produce less pro-inflammatory cytokines; on the contrary, they presented more circulating levels of chemokines (CCL3, CCL4 and MCP1) (Figure R24), which correlates with higher tumor infiltration (Figure R25). HCC is a classic model of inflammation-linked malignancy, however in HFD-fed *Ppara*$^{-/-}$ mice higher levels of inflammation and infiltration are associated with less liver damage and less HCC development; furthermore, lipid peroxidation is reduced in livers from HFD-fed *Ppara*$^{-/-}$ mice (Figure R26). In the obese state, the levels of circulating FFA are increased. FFA stimulates PPARα activation (Memon et al., 2000), inducing lipid peroxidation and consequently ROS formation, increasing DNA damage in DEN-stimulated hepatocytes (Caldwell et al., 2004). Together, these results suggest a cell-autonomous role of PPARα in HCC development during obesity.

2.3 PPARα induces HCC development in HFD in a cell-autonomous way

A part from its role in hepatic metabolism, PPARα exerts an important anti-inflammatory function, controlling the production of pro-inflammatory cytokines and repressing NF-κB signaling (Poynter and Daynes, 1998, Staels et al., 1998). However, the results obtained in bone marrow transplantation experiments confirm that PPARα activation in hepatocytes, but not in immune cells, triggers HCC development in HFD-fed mice. In fact, our results showed

that, independently from the donor bone marrow genotype, HFD-fed *Ppara*$^{-/-}$ recipient mice were protected against hepatocarcinogenesis (Figure R27B). These data further demonstrate the cell-autonomous role of PPARα in hepatocytes during HCC development.

2.4 PPARα activation induces uncontrolled proliferation

To elucidate the molecular mechanism underlies the phenotype observed in HFD-fed *Ppara*$^{-/-}$ mice, we analyzed signaling pathways involved in tumorigenesis. We observed a reduction in ERK and AKT activation in *Ppara*$^{-/-}$ liver and tumor tissues, which are important for proliferative and pro-survival response (Figure R28). Moreover, chronic DEN treatment induced p53 loss in tumor and liver tissues from HFD-fed WT mice, whereas in *Ppara*$^{-/-}$ mice its expression was maintained (Figure R28). p53 is an important tumor suppressor and it is frequently lost or mutated in the first stages of tumor development, inducing cell dedifferentiation and uncontrolled proliferation (Tschaharganeh et al., 2014). Additionally, the expression of other cell-cycle regulatory genes was increased in *Ppara*$^{-/-}$ tumors compared with WT, whereas mRNA levels of genes important in cell-cycle progression were reduced in livers from *Ppara*$^{-/-}$ mice treated with DEN (Figure R29). These results indicate a reduction in proliferative signaling not only in tumors from *Ppara*$^{-/-}$ but also in surrounding liver, which is the tissue that can generate more tumors. Moreover, loss of p53 expression in both, livers and tumors, in DEN-treated WT mice but not in *Ppara*$^{-/-}$ ones points out that activation of PPARα primes hepatocytes to increased proliferation. We hypothesized that increased PPARα activation due to obesity induces lipid peroxidation and ROS production. The mutational ratio is enhanced by ROS, causing p53 loss or mutation and dysregulation of cell-cycle regulators. Together these events provoke uncontrolled proliferation and activation of pro-survival signaling pathway. These data are consistent with a recently published work that recognized PPARδ, another nuclear receptor, as the link between obesity and colon cancer (Beyaz et al., 2016).

2.5 PPARα hyperactivation promotes liver cancer

It has been described that JNK1 and JNK2 suppress PPARα activation in hepatocytes (Vernia et al., 2014) and lack of both JNKs results in constitutively active PPARα. To further confirm the major role of PPARα activation in liver

cancer development, we used hepatocytes-specific *Jnk1* and *Jnk2* knock out mice. These mice spontaneously developed cholangiocarcinoma at 14 months of age, with an incidence of 94% (Figure R31A, B). They showed enhanced liver damage, as demonstrated by ALT levels (Figure R31C). The differences observed in the type of liver cancer in the two models might be a consequence of the tumorigenic stimuli. In fact, DEN induces hepatocytes compensatory proliferation in response to massive hepatocytes death. However, in absence of a damaging *stimulus* the most proliferative cells in the liver are bile duct cells.

Taken together our results demonstrate that PPARα activation plays an important role in liver cancer development and that its influence is cell-autonomous. In fact it triggers hepatic lipid storage and peroxidation, inducing ROS production, loss of p53 expression and enhancing uncontrolled proliferation (Figure D2). Additionally, we demonstrated that PPARα activation together with liver damage enhanced hepatocytes compensatory proliferation inducing HCC development, while in absence of a damaging *stimulus* it increases proliferative rate of bile duct cells resulting in cholangiocarcinoma formation. PPARα activators, as fibrates, have been introduced as therapy for obesity and NAFLD. Our results pointed out that these therapies could be dangerous for patients, and further studies would be necessary to assess their safety.

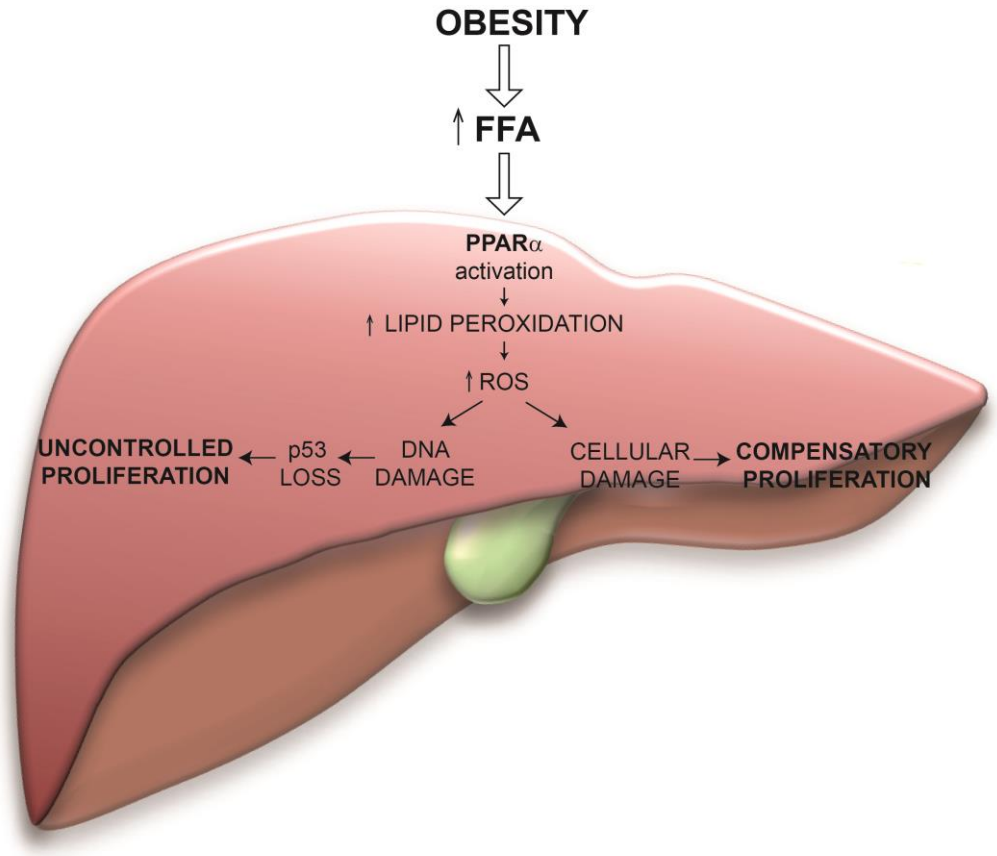

Figure D2. Schematic representation of the role of PPARα activation in liver cancer.
Obesity increases circulating free fatty acids inducing PPARα activation in hepatocytes. PPARα promotes lipid peroxidation, which in turn increases ROS production. On one hand ROS induces DNA damage and uncontrolled proliferation due to loss or mutation of p53 and other cell cycle regulators. On the other hand, ROS provokes cellular damage that triggers compensatory proliferation.

CONCLUSIONS

1. ND-fed F^{KO} mice are protected against hepatocellular carcinoma development

2. JNK1 in adipose tissue does not affect liver regeneration after partial hepatectomy

3. ND-fed F^{KO} mice present no changes in functionality or infiltration in adipose tissue

4. JNK1 in adipose tissue controls adiponectin circulating levels, which in turn inhibits liver cancer development through AMPKα and p38α activation

5. TRAIL expression in the adipose tissue is controlled by JNK1 and could be a good candidate for hepatocellular carcinoma treatment

6. Activation of PPARα by high fat diet triggers hepatocellular carcinoma development

7. Lack of PPARα reduces hepatectomy-survival rate but does not affect liver regeneration on high fat diet fed mice

8. PPARα activation during obesity increases chemical-induced liver damage and compensatory proliferation

9. PPARα activation in hepatocytes but not in immune cells promotes hepatocellular carcinoma development

10. PPARα activation through *Jnk1* and *Jnk2* deletion in hepatocytes triggers liver cancer development

CONCLUSIONES

1. JNK1 en el tejido adiposo induce el desarrollo del carcinoma hepatocelular en ratones alimentados con dieta normal pero no en ratones alimentado con dieta grasa

2. JNK1 en tejido adiposo no tiene efectos sobre la regeneración hepática tras la hepatectomía parcial

3. La expresión de JNK1 en el tejido adiposo en dieta normal no influye en la funcionalidad ni en la infiltración del tejido adiposo

4. JNK1 controla los niveles circulantes de adiponectina, que a su vez inhibe el desarrollo del carcinoma hepático a través de la activación de AMPKα y de p38α

5. La expresión de TRAIL en el tejido adiposo es controlada por JNK1. TRAIL podría ser una buena diana terapéutica en el tratamiento del carcinoma hepático

6. La activación de PPARα en la obesidad induce el desarrollo del carcinoma hepático

7. La carencia de PPARα no afecta a la regeneración hepática, pero reduce el ratio de supervivencia en animales alimentados con dieta grasa

8. La activación de PPARα en la obesidad aumenta el daño hepático y la subsecuente proliferación compensatoria

9. La activación de PPARα en los hepatocitos y no en el sistema inmune incrementa el desarrollo del carcinoma hepatocelular

10. La activación de PPARα eliminando *Jnk1* y *Jnk2* en los hepatocitos induce el desarrollo de colangiosarcoma

REFERENCES

A, I. J., JEANNIN, E., WAHLI, W. & DESVERGNE, B. 1997. Polarity and specific sequence requirements of peroxisome proliferator-activated receptor (PPAR)/retinoid X receptor heterodimer binding to DNA. A functional analysis of the malic enzyme gene PPAR response element. *J Biol Chem,* 272**,** 20108-17.

ABDELMALEK, M. F. & DIEHL, A. M. 2007. Nonalcoholic fatty liver disease as a complication of insulin resistance. *Med Clin North Am,* 91**,** 1125-49, ix.

AGUIRRE, V., WERNER, E. D., GIRAUD, J., LEE, Y. H., SHOELSON, S. E. & WHITE, M. F. 2002. Phosphorylation of Ser307 in insulin receptor substrate-1 blocks interactions with the insulin receptor and inhibits insulin action. *J Biol Chem,* 277**,** 1531-7.

ANTUNA-PUENTE, B., FEVE, B., FELLAHI, S. & BASTARD, J. P. 2008. Adipokines: the missing link between insulin resistance and obesity. *Diabetes Metab,* 34**,** 2-11.

AOYAMA, T., PETERS, J. M., IRITANI, N., NAKAJIMA, T., FURIHATA, K., HASHIMOTO, T. & GONZALEZ, F. J. 1998. Altered constitutive expression of fatty acid-metabolizing enzymes in mice lacking the peroxisome proliferator-activated receptor alpha (PPARalpha). *J Biol Chem,* 273**,** 5678-84.

ARITA, Y., KIHARA, S., OUCHI, N., TAKAHASHI, M., MAEDA, K., MIYAGAWA, J., HOTTA, K., SHIMOMURA, I., NAKAMURA, T., MIYAOKA, K., KURIYAMA, H., NISHIDA, M., YAMASHITA, S., OKUBO, K., MATSUBARA, K., MURAGUCHI, M., OHMOTO, Y., FUNAHASHI, T. & MATSUZAWA, Y. 1999. Paradoxical decrease of an adipose-specific protein, adiponectin, in obesity. *Biochem Biophys Res Commun,* 257**,** 79-83.

ASAYAMA, K., HAYASHIBE, H., DOBASHI, K., UCHIDA, N., NAKANE, T., KODERA, K., SHIRAHATA, A. & TANIYAMA, M. 2003. Decrease in serum adiponectin level due to obesity and visceral fat accumulation in children. *Obes Res,* 11**,** 1072-9.

ASHKENAZI, A., PAI, R. C., FONG, S., LEUNG, S., LAWRENCE, D. A., MARSTERS, S. A., BLACKIE, C., CHANG, L., MCMURTREY, A. E., HEBERT, A., DEFORGE, L., KOUMENIS, I. L., LEWIS, D., HARRIS, L., BUSSIERE, J., KOEPPEN, H., SHAHROKH, Z. & SCHWALL, R. H. 1999. Safety and antitumor activity of recombinant soluble Apo2 ligand. *J Clin Invest,* 104**,** 155-62.

ASIAGO, V. M., ALVARADO, L. Z., SHANAIAH, N., GOWDA, G. A., OWUSU-SARFO, K., BALLAS, R. A. & RAFTERY, D. 2010. Early detection of recurrent breast cancer using metabolite profiling. *Cancer Res,* 70**,** 8309-18.

AZIJLI, K., YUVARAJ, S., VAN ROOSMALEN, I., FLACH, K., GIOVANNETTI, E., PETERS, G. J., DE JONG, S. & KRUYT, F. A. 2013. MAPK p38 and JNK have opposing activities on TRAIL-induced apoptosis activation in NSCLC H460 cells that involves RIP1 and caspase-8 and is mediated by Mcl-1. *Apoptosis,* 18**,** 851-60.

BADMAN, M. K., PISSIOS, P., KENNEDY, A. R., KOUKOS, G., FLIER, J. S. & MARATOS-FLIER, E. 2007. Hepatic fibroblast growth factor 21 is regulated by PPARalpha and is a key mediator of hepatic lipid metabolism in ketotic states. *Cell Metab,* 5**,** 426-37.

BAFFY, G., BRUNT, E. M. & CALDWELL, S. H. 2012. Hepatocellular carcinoma in non-alcoholic fatty liver disease: an emerging menace. *J Hepatol,* 56**,** 1384-91.

BAKIRI, L. & WAGNER, E. F. 2013. Mouse models for liver cancer. *Mol Oncol,* 7**,** 206-23.

BALKWILL, F. & MANTOVANI, A. 2001. Inflammation and cancer: back to Virchow? *Lancet,* 357**,** 539-45.

BEYAZ, S., MANA, M. D., ROPER, J., KEDRIN, D., SAADATPOUR, A., HONG, S. J., BAUER-ROWE, K. E., XIFARAS, M. E., AKKAD, A., ARIAS, E., PINELLO, L., KATZ, Y., SHINAGARE, S., ABU-REMAILEH, M., MIHAYLOVA, M. M., LAMMING, D. W., DOGUM, R., GUO, G., BELL, G. W., SELIG, M., NIELSEN, G. P., GUPTA, N., FERRONE, C. R., DESHPANDE, V., YUAN, G. C., ORKIN, S. H., SABATINI, D. M. & YILMAZ, O. H. 2016. High-fat diet enhances stemness and tumorigenicity of intestinal progenitors. *Nature,* 531**,** 53-8.

BOLLRATH, J., PHESSE, T. J., VON BURSTIN, V. A., PUTOCZKI, T., BENNECKE, M., BATEMAN, T., NEBELSIEK, T., LUNDGREN-MAY, T., CANLI, O., SCHWITALLA, S., MATTHEWS, V., SCHMID, R. M., KIRCHNER, T., ARKAN, M. C., ERNST, M. & GRETEN, F. R. 2009. gp130-

mediated Stat3 activation in enterocytes regulates cell survival and cell-cycle progression during colitis-associated tumorigenesis. *Cancer Cell,* 15**,** 91-102.

BOWKER, S. L., MAJUMDAR, S. R., VEUGELERS, P. & JOHNSON, J. A. 2006. Increased cancer-related mortality for patients with type 2 diabetes who use sulfonylureas or insulin: Response to Farooki and Schneider. *Diabetes Care,* 29**,** 1990-1.

BRAY, F., JEMAL, A., GREY, N., FERLAY, J. & FORMAN, D. 2012. Global cancer transitions according to the Human Development Index (2008-2030): a population-based study. *Lancet Oncol,* 13**,** 790-801.

BRIGUGLIO, E., DI PAOLA, R., PATERNITI, I., MAZZON, E., OTERI, G., CORDASCO, G. & CUZZOCREA, S. 2010. WY-14643, a Potent Peroxisome Proliferator Activator Receptor-alpha PPAR-alpha Agonist Ameliorates the Inflammatory Process Associated to Experimental Periodontitis. *PPAR Res,* 2010**,** 193019.

CALDWELL, S. H., CRESPO, D. M., KANG, H. S. & AL-OSAIMI, A. M. 2004. Obesity and hepatocellular carcinoma. *Gastroenterology,* 127**,** S97-103.

CALLE, E. E., RODRIGUEZ, C., WALKER-THURMOND, K. & THUN, M. J. 2003. Overweight, obesity, and mortality from cancer in a prospectively studied cohort of U.S. adults. *N Engl J Med,* 348**,** 1625-38.

CATLETT-FALCONE, R., LANDOWSKI, T. H., OSHIRO, M. M., TURKSON, J., LEVITZKI, A., SAVINO, R., CILIBERTO, G., MOSCINSKI, L., FERNANDEZ-LUNA, J. L., NUNEZ, G., DALTON, W. S. & JOVE, R. 1999. Constitutive activation of Stat3 signaling confers resistance to apoptosis in human U266 myeloma cells. *Immunity,* 10**,** 105-15.

CATRINA, S. B., OKAMOTO, K., PEREIRA, T., BRISMAR, K. & POELLINGER, L. 2004. Hyperglycemia regulates hypoxia-inducible factor-1alpha protein stability and function. *Diabetes,* 53**,** 3226-32.

CHANG, L. & KARIN, M. 2001. Mammalian MAP kinase signalling cascades. *Nature,* 410**,** 37-40.

CHEN, H. P., SHIEH, J. J., CHANG, C. C., CHEN, T. T., LIN, J. T., WU, M. S., LIN, J. H. & WU, C. Y. 2013. Metformin decreases hepatocellular carcinoma risk in a dose-dependent manner: population-based and in vitro studies. *Gut,* 62**,** 606-15.

CLARK, R. B. 2002. The role of PPARs in inflammation and immunity. *J Leukoc Biol,* 71**,** 388-400.

CONSIDINE, R. V., SINHA, M. K., HEIMAN, M. L., KRIAUCIUNAS, A., STEPHENS, T. W., NYCE, M. R., OHANNESIAN, J. P., MARCO, C. C., MCKEE, L. J., BAUER, T. L. & ET AL. 1996. Serum immunoreactive-leptin concentrations in normal-weight and obese humans. *N Engl J Med,* 334**,** 292-5.

CORDA, S., LAPLACE, C., VICAUT, E. & DURANTEAU, J. 2001. Rapid reactive oxygen species production by mitochondria in endothelial cells exposed to tumor necrosis factor-alpha is mediated by ceramide. *Am J Respir Cell Mol Biol,* 24**,** 762-8.

DALAMAGA, M., DIAKOPOULOS, K. N. & MANTZOROS, C. S. 2012. The role of adiponectin in cancer: a review of current evidence. *Endocr Rev,* 33**,** 547-94.

DAS, M., GARLICK, D. S., GREINER, D. L. & DAVIS, R. J. 2011. The role of JNK in the development of hepatocellular carcinoma. *Genes Dev,* 25**,** 634-45.

DAS, M., SABIO, G., JIANG, F., RINCON, M., FLAVELL, R. A. & DAVIS, R. J. 2009. Induction of hepatitis by JNK-mediated expression of TNF-alpha. *Cell,* 136**,** 249-60.

DAVIS, R. J. 2000. Signal transduction by the JNK group of MAP kinases. *Cell,* 103**,** 239-52.

DAYNES, R. A. & JONES, D. C. 2002. Emerging roles of PPARs in inflammation and immunity. *Nat Rev Immunol,* 2**,** 748-59.

DEBERARDINIS, R. J., SAYED, N., DITSWORTH, D. & THOMPSON, C. B. 2008. Brick by brick: metabolism and tumor cell growth. *Curr Opin Genet Dev,* 18**,** 54-61.

DEVCHAND, P. R., KELLER, H., PETERS, J. M., VAZQUEZ, M., GONZALEZ, F. J. & WAHLI, W. 1996. The PPARalpha-leukotriene B4 pathway to inflammation control. *Nature,* 384**,** 39-43.

DREYER, C., KREY, G., KELLER, H., GIVEL, F., HELFTENBEIN, G. & WAHLI, W. 1992. Control of the peroxisomal beta-oxidation pathway by a novel family of nuclear hormone receptors. *Cell,* 68**,** 879-87.

EFERL, R., RICCI, R., KENNER, L., ZENZ, R., DAVID, J. P., RATH, M. & WAGNER, E. F. 2003. Liver tumor development. c-Jun antagonizes the proapoptotic activity of p53. *Cell,* 112**,** 181-92.

EL-HASCHIMI, K., PIERROZ, D. D., HILEMAN, S. M., BJORBAEK, C. & FLIER, J. S. 2000. Two defects contribute to hypothalamic leptin resistance in mice with diet-induced obesity. *J Clin Invest,* 105**,** 1827-32.

EL-SERAG, H. B. 2011. Hepatocellular carcinoma. *N Engl J Med,* 365**,** 1118-27.

EL-SERAG, H. B. & RUDOLPH, K. L. 2007. Hepatocellular carcinoma: epidemiology and molecular carcinogenesis. *Gastroenterology,* 132**,** 2557-76.

EVANS, R. M., BARISH, G. D. & WANG, Y. X. 2004. PPARs and the complex journey to obesity. *Nat Med,* 10**,** 355-61.

FAJAS, L., AUBOEUF, D., RASPE, E., SCHOONJANS, K., LEFEBVRE, A. M., SALADIN, R., NAJIB, J., LAVILLE, M., FRUCHART, J. C., DEEB, S., VIDAL-PUIG, A., FLIER, J., BRIGGS, M. R., STAELS, B., VIDAL, H. & AUWERX, J. 1997. The organization, promoter analysis, and expression of the human PPARgamma gene. *J Biol Chem,* 272**,** 18779-89.

FERNANDEZ-ALVAREZ, A., ALVAREZ, M. S., GONZALEZ, R., CUCARELLA, C., MUNTANE, J. & CASADO, M. 2011. Human SREBP1c expression in liver is directly regulated by peroxisome proliferator-activated receptor alpha (PPARalpha). *J Biol Chem,* 286**,** 21466-77.

FONT-BURGADA, J., SUN, B. & KARIN, M. 2016. Obesity and Cancer: The Oil that Feeds the Flame. *Cell Metab,* 23**,** 48-62.

FORMAN, B. M., CHEN, J. & EVANS, R. M. 1997. Hypolipidemic drugs, polyunsaturated fatty acids, and eicosanoids are ligands for peroxisome proliferator-activated receptors alpha and delta. *Proc Natl Acad Sci U S A,* 94**,** 4312-7.

FREEMAN, A. J., DORE, G. J., LAW, M. G., THORPE, M., VON OVERBECK, J., LLOYD, A. R., MARINOS, G. & KALDOR, J. M. 2001. Estimating progression to cirrhosis in chronic hepatitis C virus infection. *Hepatology,* 34**,** 809-16.

FRIED, S. K., BUNKIN, D. A. & GREENBERG, A. S. 1998. Omental and subcutaneous adipose tissues of obese subjects release interleukin-6: depot difference and regulation by glucocorticoid. *J Clin Endocrinol Metab,* 83**,** 847-50.

FUJIMOTO, A., FURUTA, M., TOTOKI, Y., TSUNODA, T., KATO, M., SHIRAISHI, Y., TANAKA, H., TANIGUCHI, H., KAWAKAMI, Y., UENO, M., GOTOH, K., ARIIZUMI, S., WARDELL, C. P., HAYAMI, S., NAKAMURA, T., AIKATA, H., ARIHIRO, K., BOROEVICH, K. A., ABE, T., NAKANO, K., MAEJIMA, K., SASAKI-OKU, A., OHSAWA, A., SHIBUYA, T., NAKAMURA, H., HAMA, N., HOSODA, F., ARAI, Y., OHASHI, S., URUSHIDATE, T., NAGAE, G., YAMAMOTO, S., UEDA, H., TATSUNO, K., OJIMA, H., HIRAOKA, N., OKUSAKA, T., KUBO, M., MARUBASHI, S., YAMADA, T., HIRANO, S., YAMAMOTO, M., OHDAN, H., SHIMADA, K., ISHIKAWA, O., YAMAUE, H., CHAYAMA, K., MIYANO, S., ABURATANI, H., SHIBATA, T. & NAKAGAWA, H. 2016. Whole-genome mutational landscape and characterization of noncoding and structural mutations in liver cancer. *Nat Genet,* 48**,** 500-9.

FUJIMOTO, A., TOTOKI, Y., ABE, T., BOROEVICH, K. A., HOSODA, F., NGUYEN, H. H., AOKI, M., HOSONO, N., KUBO, M., MIYA, F., ARAI, Y., TAKAHASHI, H., SHIRAKIHARA, T., NAGASAKI, M., SHIBUYA, T., NAKANO, K., WATANABE-MAKINO, K., TANAKA, H., NAKAMURA, H., KUSUDA, J., OJIMA, H., SHIMADA, K., OKUSAKA, T., UENO, M., SHIGEKAWA, Y., KAWAKAMI, Y., ARIHIRO, K., OHDAN, H., GOTOH, K., ISHIKAWA, O., ARIIZUMI, S., YAMAMOTO, M., YAMADA, T., CHAYAMA, K., KOSUGE, T., YAMAUE, H., KAMATANI, N., MIYANO, S., NAKAGAMA, H., NAKAMURA, Y., TSUNODA, T., SHIBATA, T. & NAKAGAWA, H. 2012. Whole-genome sequencing of liver cancers identifies etiological influences on mutation patterns and recurrent mutations in chromatin regulators. *Nat Genet,* 44**,** 760-4.

GAO, Q., JIA, Y., YANG, G., ZHANG, X., BODDU, P. C., PETERSEN, B., NARSINGAM, S., ZHU, Y. J., THIMMAPAYA, B., KANWAR, Y. S. & REDDY, J. K. 2015. PPARalpha-Deficient ob/ob

Obese Mice Become More Obese and Manifest Severe Hepatic Steatosis Due to Decreased Fatty Acid Oxidation. *Am J Pathol,* 185**,** 1396-408.

GARCIA, A. & BARBAS, C. 2011. Gas chromatography-mass spectrometry (GC-MS)-based metabolomics. *Methods Mol Biol,* 708**,** 191-204.

GAVRILOVA, O., MARCUS-SAMUELS, B., GRAHAM, D., KIM, J. K., SHULMAN, G. I., CASTLE, A. L., VINSON, C., ECKHAUS, M. & REITMAN, M. L. 2000. Surgical implantation of adipose tissue reverses diabetes in lipoatrophic mice. *J Clin Invest,* 105**,** 271-8.

GIRROIR, E. E., HOLLINGSHEAD, H. E., HE, P., ZHU, B., PERDEW, G. H. & PETERS, J. M. 2008. Quantitative expression patterns of peroxisome proliferator-activated receptor-beta/delta (PPARbeta/delta) protein in mice. *Biochem Biophys Res Commun,* 371**,** 456-61.

GREEN, S. & WAHLI, W. 1994. Peroxisome proliferator-activated receptors: finding the orphan a home. *Mol Cell Endocrinol,* 100**,** 149-53.

GREENMAN, C., STEPHENS, P., SMITH, R., DALGLIESH, G. L., HUNTER, C., BIGNELL, G., DAVIES, H., TEAGUE, J., BUTLER, A., STEVENS, C., EDKINS, S., O'MEARA, S., VASTRIK, I., SCHMIDT, E. E., AVIS, T., BARTHORPE, S., BHAMRA, G., BUCK, G., CHOUDHURY, B., CLEMENTS, J., COLE, J., DICKS, E., FORBES, S., GRAY, K., HALLIDAY, K., HARRISON, R., HILLS, K., HINTON, J., JENKINSON, A., JONES, D., MENZIES, A., MIRONENKO, T., PERRY, J., RAINE, K., RICHARDSON, D., SHEPHERD, R., SMALL, A., TOFTS, C., VARIAN, J., WEBB, T., WEST, S., WIDAA, S., YATES, A., CAHILL, D. P., LOUIS, D. N., GOLDSTRAW, P., NICHOLSON, A. G., BRASSEUR, F., LOOIJENGA, L., WEBER, B. L., CHIEW, Y. E., DEFAZIO, A., GREAVES, M. F., GREEN, A. R., CAMPBELL, P., BIRNEY, E., EASTON, D. F., CHENEVIX-TRENCH, G., TAN, M. H., KHOO, S. K., TEH, B. T., YUEN, S. T., LEUNG, S. Y., WOOSTER, R., FUTREAL, P. A. & STRATTON, M. R. 2007. Patterns of somatic mutation in human cancer genomes. *Nature,* 446**,** 153-8.

GRIVENNIKOV, S., KARIN, E., TERZIC, J., MUCIDA, D., YU, G. Y., VALLABHAPURAPU, S., SCHELLER, J., ROSE-JOHN, S., CHEROUTRE, H., ECKMANN, L. & KARIN, M. 2009. IL-6 and Stat3 are required for survival of intestinal epithelial cells and development of colitis-associated cancer. *Cancer Cell,* 15**,** 103-13.

GRIVENNIKOV, S. I., GRETEN, F. R. & KARIN, M. 2010. Immunity, inflammation, and cancer. *Cell,* 140**,** 883-99.

GULICK, T., CRESCI, S., CAIRA, T., MOORE, D. D. & KELLY, D. P. 1994. The peroxisome proliferator-activated receptor regulates mitochondrial fatty acid oxidative enzyme gene expression. *Proc Natl Acad Sci U S A,* 91**,** 11012-6.

GUPTA, S., BARRETT, T., WHITMARSH, A. J., CAVANAGH, J., SLUSS, H. K., DERIJARD, B. & DAVIS, R. J. 1996. Selective interaction of JNK protein kinase isoforms with transcription factors. *EMBO J,* 15**,** 2760-70.

HAN, J., LI, E., CHEN, L., ZHANG, Y., WEI, F., LIU, J., DENG, H. & WANG, Y. 2015. The CREB coactivator CRTC2 controls hepatic lipid metabolism by regulating SREBP1. *Nature,* 524**,** 243-6.

HAN, M. S., BARRETT, T., BREHM, M. A. & DAVIS, R. J. 2016. Inflammation Mediated by JNK in Myeloid Cells Promotes the Development of Hepatitis and Hepatocellular Carcinoma. *Cell Rep,* 15**,** 19-26.

HAN, M. S., JUNG, D. Y., MOREL, C., LAKHANI, S. A., KIM, J. K., FLAVELL, R. A. & DAVIS, R. J. 2013. JNK expression by macrophages promotes obesity-induced insulin resistance and inflammation. *Science,* 339**,** 218-22.

HANAHAN, D. & WEINBERG, R. A. 2011. Hallmarks of cancer: the next generation. *Cell,* 144**,** 646-74.

HASLAM, D. W. & JAMES, W. P. 2005. Obesity. *Lancet,* 366**,** 1197-209.

HAWLEY, S. A., GADALLA, A. E., OLSEN, G. S. & HARDIE, D. G. 2002. The antidiabetic drug metformin activates the AMP-activated protein kinase cascade via an adenine nucleotide-independent mechanism. *Diabetes,* 51**,** 2420-5.

HE, G., YU, G. Y., TEMKIN, V., OGATA, H., KUNTZEN, C., SAKURAI, T., SIEGHART, W., PECK-RADOSAVLJEVIC, M., LEFFERT, H. L. & KARIN, M. 2010. Hepatocyte IKKbeta/NF-kappaB inhibits tumor promotion and progression by preventing oxidative stress-driven STAT3 activation. *Cancer Cell,* 17**,** 286-97.

HE, W., BARAK, Y., HEVENER, A., OLSON, P., LIAO, D., LE, J., NELSON, M., ONG, E., OLEFSKY, J. M. & EVANS, R. M. 2003. Adipose-specific peroxisome proliferator-activated receptor gamma knockout causes insulin resistance in fat and liver but not in muscle. *Proc Natl Acad Sci U S A,* 100**,** 15712-7.

HELLEDIE, T., GRONTVED, L., JENSEN, S. S., KIILERICH, P., RIETVELD, L., ALBREKTSEN, T., BOYSEN, M. S., NOHR, J., LARSEN, L. K., FLECKNER, J., STUNNENBERG, H. G., KRISTIANSEN, K. & MANDRUP, S. 2002. The gene encoding the Acyl-CoA-binding protein is activated by peroxisome proliferator-activated receptor gamma through an intronic response element functionally conserved between humans and rodents. *J Biol Chem,* 277**,** 26821-30.

HERTZ, R., BISHARA-SHIEBAN, J. & BAR-TANA, J. 1995. Mode of action of peroxisome proliferators as hypolipidemic drugs. Suppression of apolipoprotein C-III. *J Biol Chem,* 270**,** 13470-5.

HILL, D. J. & MILNER, R. D. 1985. Insulin as a growth factor. *Pediatr Res,* 19**,** 879-86.

HIROSUMI, J., TUNCMAN, G., CHANG, L., GORGUN, C. Z., UYSAL, K. T., MAEDA, K., KARIN, M. & HOTAMISLIGIL, G. S. 2002. A central role for JNK in obesity and insulin resistance. *Nature,* 420**,** 333-6.

HOLMES, E., WILSON, I. D. & NICHOLSON, J. K. 2008. Metabolic phenotyping in health and disease. *Cell,* 134**,** 714-7.

HOTAMISLIGIL, G. S., JOHNSON, R. S., DISTEL, R. J., ELLIS, R., PAPAIOANNOU, V. E. & SPIEGELMAN, B. M. 1996. Uncoupling of obesity from insulin resistance through a targeted mutation in aP2, the adipocyte fatty acid binding protein. *Science,* 274**,** 1377-9.

HOTAMISLIGIL, G. S., SHARGILL, N. S. & SPIEGELMAN, B. M. 1993. Adipose expression of tumor necrosis factor-alpha: direct role in obesity-linked insulin resistance. *Science,* 259**,** 87-91.

HUI, L., BAKIRI, L., MAIRHORFER, A., SCHWEIFER, N., HASLINGER, C., KENNER, L., KOMNENOVIC, V., SCHEUCH, H., BEUG, H. & WAGNER, E. F. 2007. p38alpha suppresses normal and cancer cell proliferation by antagonizing the JNK-c-Jun pathway. *Nat Genet,* 39**,** 741-9.

HUI, L., ZATLOUKAL, K., SCHEUCH, H., STEPNIAK, E. & WAGNER, E. F. 2008. Proliferation of human HCC cells and chemically induced mouse liver cancers requires JNK1-dependent p21 downregulation. *J Clin Invest,* 118**,** 3943-53.

HUSSAIN, S. P., HOFSETH, L. J. & HARRIS, C. C. 2003. Radical causes of cancer. *Nat Rev Cancer,* 3**,** 276-85.

HUYNH, H., NGUYEN, T. T., CHOW, K. H., TAN, P. H., SOO, K. C. & TRAN, E. 2003. Over-expression of the mitogen-activated protein kinase (MAPK) kinase (MEK)-MAPK in hepatocellular carcinoma: its role in tumor progression and apoptosis. *BMC Gastroenterol,* 3**,** 19.

IP, E., FARRELL, G. C., ROBERTSON, G., HALL, P., KIRSCH, R. & LECLERCQ, I. 2003. Central role of PPARalpha-dependent hepatic lipid turnover in dietary steatohepatitis in mice. *Hepatology,* 38**,** 123-32.

IRMLER, M., THOME, M., HAHNE, M., SCHNEIDER, P., HOFMANN, K., STEINER, V., BODMER, J. L., SCHROTER, M., BURNS, K., MATTMANN, C., RIMOLDI, D., FRENCH, L. E. & TSCHOPP, J. 1997. Inhibition of death receptor signals by cellular FLIP. *Nature,* 388**,** 190-5.

ISSEMANN, I. & GREEN, S. 1990. Activation of a member of the steroid hormone receptor superfamily by peroxisome proliferators. *Nature,* 347**,** 645-50.

IYODA, K., SASAKI, Y., HORIMOTO, M., TOYAMA, T., YAKUSHIJIN, T., SAKAKIBARA, M., TAKEHARA, T., FUJIMOTO, J., HORI, M., WANDS, J. R. & HAYASHI, N. 2003. Involvement of the p38 mitogen-activated protein kinase cascade in hepatocellular carcinoma. *Cancer,* 97**,** 3017-26.

JONES, S., ZHANG, X., PARSONS, D. W., LIN, J. C., LEARY, R. J., ANGENENDT, P., MANKOO, P., CARTER, H., KAMIYAMA, H., JIMENO, A., HONG, S. M., FU, B., LIN, M. T., CALHOUN, E. S., KAMIYAMA, M., WALTER, K., NIKOLSKAYA, T., NIKOLSKY, Y., HARTIGAN, J., SMITH, D. R., HIDALGO, M., LEACH, S. D., KLEIN, A. P., JAFFEE, E. M., GOGGINS, M., MAITRA, A., IACOBUZIO-DONAHUE, C., ESHLEMAN, J. R., KERN, S. E., HRUBAN, R. H., KARCHIN, R., PAPADOPOULOS, N., PARMIGIANI, G., VOGELSTEIN, B., VELCULESCU, V. E. & KINZLER, K. W. 2008. Core signaling pathways in human pancreatic cancers revealed by global genomic analyses. *Science,* 321**,** 1801-6.

KATZ, S. F., LECHEL, A., OBENAUF, A. C., BEGUS-NAHRMANN, Y., KRAUS, J. M., HOFFMANN, E. M., DUDA, J., ESHRAGHI, P., HARTMANN, D., LISS, B., SCHIRMACHER, P., KESTLER, H. A., SPEICHER, M. R. & RUDOLPH, K. L. 2012. Disruption of Trp53 in livers of mice induces formation of carcinomas with bilineal differentiation. *Gastroenterology,* 142**,** 1229-1239 e3.

KEATING, G. M. & SANTORO, A. 2009. Sorafenib: a review of its use in advanced hepatocellular carcinoma. *Drugs,* 69**,** 223-40.

KELESIDIS, I., KELESIDIS, T. & MANTZOROS, C. S. 2006. Adiponectin and cancer: a systematic review. *Br J Cancer,* 94**,** 1221-5.

KESSENBROCK, K., PLAKS, V. & WERB, Z. 2010. Matrix metalloproteinases: regulators of the tumor microenvironment. *Cell,* 141**,** 52-67.

KIM, J., KUNDU, M., VIOLLET, B. & GUAN, K. L. 2011. AMPK and mTOR regulate autophagy through direct phosphorylation of Ulk1. *Nat Cell Biol,* 13**,** 132-41.

KLEIN, J., DAWSON, L. A., TRAN, T. H., ADEYI, O., PURDIE, T., SHERMAN, M. & BRADE, A. 2014. Metabolic syndrome-related hepatocellular carcinoma treated by volumetric modulated arc therapy. *Curr Oncol,* 21**,** e340-4.

KLIEWER, S. A., FORMAN, B. M., BLUMBERG, B., ONG, E. S., BORGMEYER, U., MANGELSDORF, D. J., UMESONO, K. & EVANS, R. M. 1994. Differential expression and activation of a family of murine peroxisome proliferator-activated receptors. *Proc Natl Acad Sci U S A,* 91**,** 7355-9.

KRESS, S., KONIG, J., SCHWEIZER, J., LOHRKE, H., BAUER-HOFMANN, R. & SCHWARZ, M. 1992. p53 mutations are absent from carcinogen-induced mouse liver tumors but occur in cell lines established from these tumors. *Mol Carcinog,* 6**,** 148-58.

KREY, G., BRAISSANT, O., L'HORSET, F., KALKHOVEN, E., PERROUD, M., PARKER, M. G. & WAHLI, W. 1997. Fatty acids, eicosanoids, and hypolipidemic agents identified as ligands of peroxisome proliferator-activated receptors by coactivator-dependent receptor ligand assay. *Mol Endocrinol,* 11**,** 779-91.

LEE, J. S., CHU, I. S., MIKAELYAN, A., CALVISI, D. F., HEO, J., REDDY, J. K. & THORGEIRSSON, S. S. 2004. Application of comparative functional genomics to identify best-fit mouse models to study human cancer. *Nat Genet,* 36**,** 1306-11.

LEE, Y. H., GIRAUD, J., DAVIS, R. J. & WHITE, M. F. 2003. c-Jun N-terminal kinase (JNK) mediates feedback inhibition of the insulin signaling cascade. *J Biol Chem,* 278**,** 2896-902.

LI, J., MILLER, E. J., NINOMIYA-TSUJI, J., RUSSELL, R. R., 3RD & YOUNG, L. H. 2005. AMP-activated protein kinase activates p38 mitogen-activated protein kinase by increasing recruitment of p38 MAPK to TAB1 in the ischemic heart. *Circ Res,* 97**,** 872-9.

LLOVET, J. M., BURROUGHS, A. & BRUIX, J. 2003. Hepatocellular carcinoma. *Lancet,* 362**,** 1907-17.

LLOVET, J. M., RICCI, S., MAZZAFERRO, V., HILGARD, P., GANE, E., BLANC, J. F., DE OLIVEIRA, A. C., SANTORO, A., RAOUL, J. L., FORNER, A., SCHWARTZ, M., PORTA, C., ZEUZEM, S., BOLONDI, L., GRETEN, T. F., GALLE, P. R., SEITZ, J. F., BORBATH, I., HAUSSINGER, D.,

GIANNARIS, T., SHAN, M., MOSCOVICI, M., VOLIOTIS, D. & BRUIX, J. 2008. Sorafenib in advanced hepatocellular carcinoma. *N Engl J Med,* 359**,** 378-90.

LUMENG, C. N., BODZIN, J. L. & SALTIEL, A. R. 2007. Obesity induces a phenotypic switch in adipose tissue macrophage polarization. *J Clin Invest,* 117**,** 175-84.

MAEDA, K., OKUBO, K., SHIMOMURA, I., FUNAHASHI, T., MATSUZAWA, Y. & MATSUBARA, K. 1996. cDNA cloning and expression of a novel adipose specific collagen-like factor, apM1 (AdiPose Most abundant Gene transcript 1). *Biochem Biophys Res Commun,* 221**,** 286-9.

MAEDA, S., KAMATA, H., LUO, J. L., LEFFERT, H. & KARIN, M. 2005. IKKbeta couples hepatocyte death to cytokine-driven compensatory proliferation that promotes chemical hepatocarcinogenesis. *Cell,* 121**,** 977-90.

MAGGIORA, M., ORALDI, M., MUZIO, G. & CANUTO, R. A. 2010. Involvement of PPARalpha and PPARgamma in apoptosis and proliferation of human hepatocarcinoma HepG2 cells. *Cell Biochem Funct,* 28**,** 571-7.

MAN, K., NG, K. T., LO, C. M., HO, J. W., SUN, B. S., SUN, C. K., LEE, T. K., POON, R. T. & FAN, S. T. 2007. Ischemia-reperfusion of small liver remnant promotes liver tumor growth and metastases--activation of cell invasion and migration pathways. *Liver Transpl,* 13**,** 1669-77.

MANDARD, S., MULLER, M. & KERSTEN, S. 2004. Peroxisome proliferator-activated receptor alpha target genes. *Cell Mol Life Sci,* 61**,** 393-416.

MANIERI, E. & SABIO, G. 2015. Stress kinases in the modulation of metabolism and energy balance. *J Mol Endocrinol,* 55**,** R11-22.

MANNING, B. D. & CANTLEY, L. C. 2007. AKT/PKB signaling: navigating downstream. *Cell,* 129**,** 1261-74.

MANTOVANI, A., SICA, A., SOZZANI, S., ALLAVENA, P., VECCHI, A. & LOCATI, M. 2004. The chemokine system in diverse forms of macrophage activation and polarization. *Trends Immunol,* 25**,** 677-86.

MAO, X., KIKANI, C. K., RIOJAS, R. A., LANGLAIS, P., WANG, L., RAMOS, F. J., FANG, Q., CHRIST-ROBERTS, C. Y., HONG, J. Y., KIM, R. Y., LIU, F. & DONG, L. Q. 2006. APPL1 binds to adiponectin receptors and mediates adiponectin signalling and function. *Nat Cell Biol,* 8**,** 516-23.

MARSTERS, S. A., PITTI, R. M., DONAHUE, C. J., RUPPERT, S., BAUER, K. D. & ASHKENAZI, A. 1996. Activation of apoptosis by Apo-2 ligand is independent of FADD but blocked by CrmA. *Curr Biol,* 6**,** 750-2.

MARTIN, G., SCHOONJANS, K., LEFEBVRE, A. M., STAELS, B. & AUWERX, J. 1997. Coordinate regulation of the expression of the fatty acid transport protein and acyl-CoA synthetase genes by PPARalpha and PPARgamma activators. *J Biol Chem,* 272**,** 28210-7.

MASCARO, C., ACOSTA, E., ORTIZ, J. A., MARRERO, P. F., HEGARDT, F. G. & HARO, D. 1998. Control of human muscle-type carnitine palmitoyltransferase I gene transcription by peroxisome proliferator-activated receptor. *J Biol Chem,* 273**,** 8560-3.

MASCARO, C., ACOSTA, E., ORTIZ, J. A., RODRIGUEZ, J. C., MARRERO, P. F., HEGARDT, F. G. & HARO, D. 1999. Characterization of a response element for peroxisomal proliferator activated receptor (PPRE) in human muscle-type carnitine palmitoyltransferase I. *Adv Exp Med Biol,* 466**,** 79-85.

MAYI, T. H., DAOUDI, M., DERUDAS, B., GROSS, B., BORIES, G., WOUTERS, K., BROZEK, J., CAIAZZO, R., RAVERDI, V., PIGEYRE, M., ALLAVENA, P., MANTOVANI, A., PATTOU, F., STAELS, B. & CHINETTI-GBAGUIDI, G. 2012. Human adipose tissue macrophages display activation of cancer-related pathways. *J Biol Chem,* 287**,** 21904-13.

MEIER, B., RADEKE, H. H., SELLE, S., YOUNES, M., SIES, H., RESCH, K. & HABERMEHL, G. G. 1989. Human fibroblasts release reactive oxygen species in response to interleukin-1 or tumour necrosis factor-alpha. *Biochem J,* 263**,** 539-45.

MEMON, R. A., TECOTT, L. H., NONOGAKI, K., BEIGNEUX, A., MOSER, A. H., GRUNFELD, C. & FEINGOLD, K. R. 2000. Up-regulation of peroxisome proliferator-activated receptors (PPAR-alpha) and PPAR-gamma messenger ribonucleic acid expression in the liver in murine obesity: troglitazone induces expression of PPAR-gamma-responsive adipose tissue-specific genes in the liver of obese diabetic mice. *Endocrinology,* 141**,** 4021-31.

MICHALIK, L., DESVERGNE, B., TAN, N. S., BASU-MODAK, S., ESCHER, P., RIEUSSET, J., PETERS, J. M., KAYA, G., GONZALEZ, F. J., ZAKANY, J., METZGER, D., CHAMBON, P., DUBOULE, D. & WAHLI, W. 2001. Impaired skin wound healing in peroxisome proliferator-activated receptor (PPAR)alpha and PPARbeta mutant mice. *J Cell Biol,* 154**,** 799-814.

MICHALOPOULOS, G. K. 2007. Liver regeneration. *J Cell Physiol,* 213**,** 286-300.

MITCHELL, C. & WILLENBRING, H. 2008. A reproducible and well-tolerated method for 2/3 partial hepatectomy in mice. *Nat Protoc,* 3**,** 1167-70.

NAUGLER, W. E., SAKURAI, T., KIM, S., MAEDA, S., KIM, K., ELSHARKAWY, A. M. & KARIN, M. 2007. Gender disparity in liver cancer due to sex differences in MyD88-dependent IL-6 production. *Science,* 317**,** 121-4.

ODUNSI, K., WOLLMAN, R. M., AMBROSONE, C. B., HUTSON, A., MCCANN, S. E., TAMMELA, J., GEISLER, J. P., MILLER, G., SELLERS, T., CLIBY, W., QIAN, F., KEITZ, B., INTENGAN, M., LELE, S. & ALDERFER, J. L. 2005. Detection of epithelial ovarian cancer using 1H-NMR-based metabonomics. *Int J Cancer,* 113**,** 782-8.

PANIGRAHY, D., KAIPAINEN, A., HUANG, S., BUTTERFIELD, C. E., BARNES, C. M., FANNON, M., LAFORME, A. M., CHAPONIS, D. M., FOLKMAN, J. & KIERAN, M. W. 2008. PPARalpha agonist fenofibrate suppresses tumor growth through direct and indirect angiogenesis inhibition. *Proc Natl Acad Sci U S A,* 105**,** 985-90.

PARK, E. J., LEE, J. H., YU, G. Y., HE, G., ALI, S. R., HOLZER, R. G., OSTERREICHER, C. H., TAKAHASHI, H. & KARIN, M. 2010. Dietary and genetic obesity promote liver inflammation and tumorigenesis by enhancing IL-6 and TNF expression. *Cell,* 140**,** 197-208.

PATEL, D. D., KNIGHT, B. L., WIGGINS, D., HUMPHREYS, S. M. & GIBBONS, G. F. 2001. Disturbances in the normal regulation of SREBP-sensitive genes in PPAR alpha-deficient mice. *J Lipid Res,* 42**,** 328-37.

PAUL, A., WILSON, S., BELHAM, C. M., ROBINSON, C. J., SCOTT, P. H., GOULD, G. W. & PLEVIN, R. 1997. Stress-activated protein kinases: activation, regulation and function. *Cell Signal,* 9**,** 403-10.

PAWLAK, M., LEFEBVRE, P. & STAELS, B. 2015. Molecular mechanism of PPARalpha action and its impact on lipid metabolism, inflammation and fibrosis in non-alcoholic fatty liver disease. *J Hepatol,* 62**,** 720-33.

PETERS, J. M., CATTLEY, R. C. & GONZALEZ, F. J. 1997. Role of PPAR alpha in the mechanism of action of the nongenotoxic carcinogen and peroxisome proliferator Wy-14,643. *Carcinogenesis,* 18**,** 2029-33.

PICARDO, A., KARPOFF, H. M., NG, B., LEE, J., BRENNAN, M. F. & FONG, Y. 1998. Partial hepatectomy accelerates local tumor growth: potential roles of local cytokine activation. *Surgery,* 124**,** 57-64.

PIKARSKY, E., PORAT, R. M., STEIN, I., ABRAMOVITCH, R., AMIT, S., KASEM, S., GUTKOVICH-PYEST, E., URIELI-SHOVAL, S., GALUN, E. & BEN-NERIAH, Y. 2004. NF-kappaB functions as a tumour promoter in inflammation-associated cancer. *Nature,* 431**,** 461-6.

PITTI, R. M., MARSTERS, S. A., RUPPERT, S., DONAHUE, C. J., MOORE, A. & ASHKENAZI, A. 1996. Induction of apoptosis by Apo-2 ligand, a new member of the tumor necrosis factor cytokine family. *J Biol Chem,* 271**,** 12687-90.

PLATT, R. J., CHEN, S., ZHOU, Y., YIM, M. J., SWIECH, L., KEMPTON, H. R., DAHLMAN, J. E., PARNAS, O., EISENHAURE, T. M., JOVANOVIC, M., GRAHAM, D. B., JHUNJHUNWALA, S., HEIDENREICH, M., XAVIER, R. J., LANGER, R., ANDERSON, D. G., HACOHEN, N., REGEV,

A., FENG, G., SHARP, P. A. & ZHANG, F. 2014. CRISPR-Cas9 knockin mice for genome editing and cancer modeling. *Cell,* 159**,** 440-55.

POYNTER, M. E. & DAYNES, R. A. 1998. Peroxisome proliferator-activated receptor alpha activation modulates cellular redox status, represses nuclear factor-kappaB signaling, and reduces inflammatory cytokine production in aging. *J Biol Chem,* 273**,** 32833-41.

RENEHAN, A. G., TYSON, M., EGGER, M., HELLER, R. F. & ZWAHLEN, M. 2008. Body-mass index and incidence of cancer: a systematic review and meta-analysis of prospective observational studies. *Lancet,* 371**,** 569-78.

RUDALSKA, R., DAUCH, D., LONGERICH, T., MCJUNKIN, K., WUESTEFELD, T., KANG, T. W., HOHMEYER, A., PESIC, M., LEIBOLD, J., VON THUN, A., SCHIRMACHER, P., ZUBER, J., WEISS, K. H., POWERS, S., MALEK, N. P., EILERS, M., SIPOS, B., LOWE, S. W., GEFFERS, R., LAUFER, S. & ZENDER, L. 2014. In vivo RNAi screening identifies a mechanism of sorafenib resistance in liver cancer. *Nat Med,* 20**,** 1138-46.

SABIO, G., CAVANAGH-KYROS, J., KO, H. J., JUNG, D. Y., GRAY, S., JUN, J. Y., BARRETT, T., MORA, A., KIM, J. K. & DAVIS, R. J. 2009. Prevention of steatosis by hepatic JNK1. *Cell Metab,* 10**,** 491-8.

SABIO, G., DAS, M., MORA, A., ZHANG, Z., JUN, J. Y., KO, H. J., BARRETT, T., KIM, J. K. & DAVIS, R. J. 2008. A stress signaling pathway in adipose tissue regulates hepatic insulin resistance. *Science,* 322**,** 1539-43.

SABIO, G. & DAVIS, R. J. 2014. TNF and MAP kinase signalling pathways. *Semin Immunol,* 26**,** 237-45.

SABIO, G., KENNEDY, N. J., CAVANAGH-KYROS, J., JUNG, D. Y., KO, H. J., ONG, H., BARRETT, T., KIM, J. K. & DAVIS, R. J. 2010. Role of muscle c-Jun NH2-terminal kinase 1 in obesity-induced insulin resistance. *Mol Cell Biol,* 30**,** 106-15.

SCHAFFER, J. E. & LODISH, H. F. 1994. Expression cloning and characterization of a novel adipocyte long chain fatty acid transport protein. *Cell,* 79**,** 427-36.

SCHMIDT-SUPPRIAN, M. & RAJEWSKY, K. 2007. Vagaries of conditional gene targeting. *Nat Immunol,* 8**,** 665-8.

SCHOONJANS, K., PEINADO-ONSURBE, J., LEFEBVRE, A. M., HEYMAN, R. A., BRIGGS, M., DEEB, S., STAELS, B. & AUWERX, J. 1996a. PPARalpha and PPARgamma activators direct a distinct tissue-specific transcriptional response via a PPRE in the lipoprotein lipase gene. *EMBO J,* 15**,** 5336-48.

SCHOONJANS, K., STAELS, B. & AUWERX, J. 1996b. Role of the peroxisome proliferator-activated receptor (PPAR) in mediating the effects of fibrates and fatty acids on gene expression. *J Lipid Res,* 37**,** 907-25.

SERUGGIA, D. & MONTOLIU, L. 2014. The new CRISPR-Cas system: RNA-guided genome engineering to efficiently produce any desired genetic alteration in animals. *Transgenic Res,* 23**,** 707-16.

SINGH, R., WANG, Y., XIANG, Y., TANAKA, K. E., GAARDE, W. A. & CZAJA, M. J. 2009. Differential effects of JNK1 and JNK2 inhibition on murine steatohepatitis and insulin resistance. *Hepatology,* 49**,** 87-96.

SINGH, S., SINGH, P. P., SINGH, A. G., MURAD, M. H., MCWILLIAMS, R. R. & CHARI, S. T. 2013. Anti-diabetic medications and risk of pancreatic cancer in patients with diabetes mellitus: a systematic review and meta-analysis. *Am J Gastroenterol,* 108**,** 510-9; quiz 520.

SOLINAS, G., NAUGLER, W., GALIMI, F., LEE, M. S. & KARIN, M. 2006. Saturated fatty acids inhibit induction of insulin gene transcription by JNK-mediated phosphorylation of insulin-receptor substrates. *Proc Natl Acad Sci U S A,* 103**,** 16454-9.

SOLINAS, G., VILCU, C., NEELS, J. G., BANDYOPADHYAY, G. K., LUO, J. L., NAUGLER, W., GRIVENNIKOV, S., WYNSHAW-BORIS, A., SCADENG, M., OLEFSKY, J. M. & KARIN, M. 2007. JNK1 in hematopoietically derived cells contributes to diet-induced inflammation and insulin resistance without affecting obesity. *Cell Metab,* 6**,** 386-97.

STAELS, B., KOENIG, W., HABIB, A., MERVAL, R., LEBRET, M., TORRA, I. P., DELERIVE, P., FADEL, A., CHINETTI, G., FRUCHART, J. C., NAJIB, J., MACLOUF, J. & TEDGUI, A. 1998. Activation of human aortic smooth-muscle cells is inhibited by PPARalpha but not by PPARgamma activators. *Nature,* 393**,** 790-3.

STARLEY, B. Q., CALCAGNO, C. J. & HARRISON, S. A. 2010. Nonalcoholic fatty liver disease and hepatocellular carcinoma: a weighty connection. *Hepatology,* 51**,** 1820-32.

STIENSTRA, R., MANDARD, S., PATSOURIS, D., MAASS, C., KERSTEN, S. & MULLER, M. 2007. Peroxisome proliferator-activated receptor alpha protects against obesity-induced hepatic inflammation. *Endocrinology,* 148**,** 2753-63.

STOTZ, M., GERGER, A., HAYBAECK, J., KIESSLICH, T., BULLOCK, M. D. & PICHLER, M. 2015. Molecular Targeted Therapies in Hepatocellular Carcinoma: Past, Present and Future. *Anticancer Res,* 35**,** 5737-44.

SUN, K., KUSMINSKI, C. M. & SCHERER, P. E. 2011. Adipose tissue remodeling and obesity. *J Clin Invest,* 121**,** 2094-101.

TAKAMURA, A., KOMATSU, M., HARA, T., SAKAMOTO, A., KISHI, C., WAGURI, S., EISHI, Y., HINO, O., TANAKA, K. & MIZUSHIMA, N. 2011. Autophagy-deficient mice develop multiple liver tumors. *Genes Dev,* 25**,** 795-800.

TANAKA, N., MORIYA, K., KIYOSAWA, K., KOIKE, K., GONZALEZ, F. J. & AOYAMA, T. 2008. PPARalpha activation is essential for HCV core protein-induced hepatic steatosis and hepatocellular carcinoma in mice. *J Clin Invest,* 118**,** 683-94.

TANSEY, J. T., SZTALRYD, C., GRUIA-GRAY, J., ROUSH, D. L., ZEE, J. V., GAVRILOVA, O., REITMAN, M. L., DENG, C. X., LI, C., KIMMEL, A. R. & LONDOS, C. 2001. Perilipin ablation results in a lean mouse with aberrant adipocyte lipolysis, enhanced leptin production, and resistance to diet-induced obesity. *Proc Natl Acad Sci U S A,* 98**,** 6494-9.

TSCHAHARGANEH, D. F., XUE, W., CALVISI, D. F., EVERT, M., MICHURINA, T. V., DOW, L. E., BANITO, A., KATZ, S. F., KASTENHUBER, E. R., WEISSMUELLER, S., HUANG, C. H., LECHEL, A., ANDERSEN, J. B., CAPPER, D., ZENDER, L., LONGERICH, T., ENIKOLOPOV, G. & LOWE, S. W. 2014. p53-dependent Nestin regulation links tumor suppression to cellular plasticity in liver cancer. *Cell,* 158**,** 579-92.

TSUCHIYA, N., SAWADA, Y., ENDO, I., SAITO, K., UEMURA, Y. & NAKATSURA, T. 2015. Biomarkers for the early diagnosis of hepatocellular carcinoma. *World J Gastroenterol,* 21**,** 10573-83.

TUGWOOD, J. D., ISSEMANN, I., ANDERSON, R. G., BUNDELL, K. R., MCPHEAT, W. L. & GREEN, S. 1992. The mouse peroxisome proliferator activated receptor recognizes a response element in the 5' flanking sequence of the rat acyl CoA oxidase gene. *EMBO J,* 11**,** 433-9.

TUNCMAN, G., HIROSUMI, J., SOLINAS, G., CHANG, L., KARIN, M. & HOTAMISLIGIL, G. S. 2006. Functional in vivo interactions between JNK1 and JNK2 isoforms in obesity and insulin resistance. *Proc Natl Acad Sci U S A,* 103**,** 10741-6.

UDDIN, S., HUSSAIN, A. R., SIRAJ, A. K., KHAN, O. S., BAVI, P. P. & AL-KURAYA, K. S. 2011. Role of leptin and its receptors in the pathogenesis of thyroid cancer. *Int J Clin Exp Pathol,* 4**,** 637-43.

VERNIA, S., CAVANAGH-KYROS, J., GARCIA-HARO, L., SABIO, G., BARRETT, T., JUNG, D. Y., KIM, J. K., XU, J., SHULHA, H. P., GARBER, M., GAO, G. & DAVIS, R. J. 2014. The PPARalpha-FGF21 hormone axis contributes to metabolic regulation by the hepatic JNK signaling pathway. *Cell Metab,* 20**,** 512-25.

VERNIA, S., MOREL, C., MADARA, J. C., CAVANAGH-KYROS, J., BARRETT, T., CHASE, K., KENNEDY, N. J., JUNG, D. Y., KIM, J. K., ARONIN, N., FLAVELL, R. A., LOWELL, B. B. & DAVIS, R. J. 2016. Excitatory transmission onto AgRP neurons is regulated by cJun NH2-terminal kinase 3 in response to metabolic stress. *Elife,* 5.

WAGNER, E. F. & NEBREDA, A. R. 2009. Signal integration by JNK and p38 MAPK pathways in cancer development. *Nat Rev Cancer,* 9**,** 537-49.

WAGNER, M., BJERKVIG, R., WIIG, H., MELERO-MARTIN, J. M., LIN, R. Z., KLAGSBRUN, M. & DUDLEY, A. C. 2012. Inflamed tumor-associated adipose tissue is a depot for macrophages that stimulate tumor growth and angiogenesis. *Angiogenesis,* 15**,** 481-95.

WANG, D., WEI, Y. & PAGLIASSOTTI, M. J. 2006a. Saturated fatty acids promote endoplasmic reticulum stress and liver injury in rats with hepatic steatosis. *Endocrinology,* 147**,** 943-51.

WANG, Y., LAM, K. S., CHAN, L., CHAN, K. W., LAM, J. B., LAM, M. C., HOO, R. C., MAK, W. W., COOPER, G. J. & XU, A. 2006b. Post-translational modifications of the four conserved lysine residues within the collagenous domain of adiponectin are required for the formation of its high molecular weight oligomeric complex. *J Biol Chem,* 281**,** 16391-400.

WARBURG, O. 1956. On the origin of cancer cells. *Science,* 123**,** 309-14.

WILEY, S. R., SCHOOLEY, K., SMOLAK, P. J., DIN, W. S., HUANG, C. P., NICHOLL, J. K., SUTHERLAND, G. R., SMITH, T. D., RAUCH, C., SMITH, C. A. & ET AL. 1995. Identification and characterization of a new member of the TNF family that induces apoptosis. *Immunity,* 3**,** 673-82.

WOLF, M. J., ADILI, A., PIOTROWITZ, K., ABDULLAH, Z., BOEGE, Y., STEMMER, K., RINGELHAN, M., SIMONAVICIUS, N., EGGER, M., WOHLLEBER, D., LORENTZEN, A., EINER, C., SCHULZ, S., CLAVEL, T., PROTZER, U., THIELE, C., ZISCHKA, H., MOCH, H., TSCHOP, M., TUMANOV, A. V., HALLER, D., UNGER, K., KARIN, M., KOPF, M., KNOLLE, P., WEBER, A. & HEIKENWALDER, M. 2014. Metabolic activation of intrahepatic CD8+ T cells and NKT cells causes nonalcoholic steatohepatitis and liver cancer via cross-talk with hepatocytes. *Cancer Cell,* 26**,** 549-64.

YAMAMOTO, J., KOSUGE, T., TAKAYAMA, T., SHIMADA, K., YAMASAKI, S., OZAKI, H., YAMAGUCHI, N. & MAKUUCHI, M. 1996. Recurrence of hepatocellular carcinoma after surgery. *Br J Surg,* 83**,** 1219-22.

YAMAUCHI, T., KAMON, J., MINOKOSHI, Y., ITO, Y., WAKI, H., UCHIDA, S., YAMASHITA, S., NODA, M., KITA, S., UEKI, K., ETO, K., AKANUMA, Y., FROGUEL, P., FOUFELLE, F., FERRE, P., CARLING, D., KIMURA, S., NAGAI, R., KAHN, B. B. & KADOWAKI, T. 2002. Adiponectin stimulates glucose utilization and fatty-acid oxidation by activating AMP-activated protein kinase. *Nat Med,* 8**,** 1288-95.

YAMAUCHI, T., NIO, Y., MAKI, T., KOBAYASHI, M., TAKAZAWA, T., IWABU, M., OKADA-IWABU, M., KAWAMOTO, S., KUBOTA, N., KUBOTA, T., ITO, Y., KAMON, J., TSUCHIDA, A., KUMAGAI, K., KOZONO, H., HADA, Y., OGATA, H., TOKUYAMA, K., TSUNODA, M., IDE, T., MURAKAMI, K., AWAZAWA, M., TAKAMOTO, I., FROGUEL, P., HARA, K., TOBE, K., NAGAI, R., UEKI, K. & KADOWAKI, T. 2007. Targeted disruption of AdipoR1 and AdipoR2 causes abrogation of adiponectin binding and metabolic actions. *Nat Med,* 13**,** 332-9.

YANG, J. D., KIM, W. R., COELHO, R., METTLER, T. A., BENSON, J. T., SANDERSON, S. O., THERNEAU, T. M., KIM, B. & ROBERTS, L. R. 2011. Cirrhosis is present in most patients with hepatitis B and hepatocellular carcinoma. *Clin Gastroenterol Hepatol,* 9**,** 64-70.

ZENG, J., HUANG, X., ZHOU, L., TAN, Y., HU, C., WANG, X., NIU, J., WANG, H., LIN, X. & YIN, P. 2015. Metabolomics Identifies Biomarker Pattern for Early Diagnosis of Hepatocellular Carcinoma: from Diethylnitrosamine Treated Rats to Patients. *Sci Rep,* 5**,** 16101.

ZHANG, G., BUDKER, V. & WOLFF, J. A. 1999. High levels of foreign gene expression in hepatocytes after tail vein injections of naked plasmid DNA. *Hum Gene Ther,* 10**,** 1735-7.

ZHANG, L. & FANG, B. 2005. Mechanisms of resistance to TRAIL-induced apoptosis in cancer. *Cancer Gene Ther,* 12**,** 228-37.

ZHANG, N., CHU, E. S., ZHANG, J., LI, X., LIANG, Q., CHEN, J., CHEN, M., TEOH, N., FARRELL, G., SUNG, J. J. & YU, J. 2014. Peroxisome proliferator activated receptor alpha inhibits

hepatocarcinogenesis through mediating NF-kappaB signaling pathway. *Oncotarget,* 5**,** 8330-40.

ZHONG, Z., WEN, Z. & DARNELL, J. E., JR. 1994. Stat3: a STAT family member activated by tyrosine phosphorylation in response to epidermal growth factor and interleukin-6. *Science,* 264**,** 95-8.